UNIVERSITÄTSKLINIKUM HAMBURG-EPPENDORF

Institut für Medizinische Mikrobiologie, Virologie und Hygiene

Prof. Dr. Martin Aepfelbacher

Modulation of gene expression and epigenetic modifications in human macrophages by *Yersinia enterocolitica*

Dissertation

Zur Erlangung des Doktorgrades für PhD Nicht-Medizin
an der Medizinischen Fakultät der Universität Hamburg.

vorgelegt von:

Indra Bekere
aus Riga, Lettland

Hamburg, 2021

(wird von der Medizinischen Fakultät ausgefüllt)

Angenommen von der Medizinischen Fakultät der Universität Hamburg am:
15.11.2021.

Veröffentlicht mit Genehmigung der Medizinischen Fakultät der Universität Hamburg.

Prüfungsausschuss, der/die Vorsitzende: **Prof. Dr. Martin Aepfelbacher**

Prüfungsausschuss, 2. Gutachter/in: **Prof. Dr. Adam Grundhoff**

Contents

1 Introduction

1.1 Pathogenic *Yersinia* spp.

The genus *Yersinia* contains Gram negative bacteria that belong to the family of Enterobacteriacea [1]. The genus contains a highly diverse group of 18 species which include both non-pathogenic and pathogenic species to animals and humans [1]. *Yersinia* spp. were first discovered by bacteriologist Alexandre Yersin in 1894 when he isolated *Yersinia pestis* and identified it as a causative agent of plague, also known as Black Death [2]. *Y. pestis* is transmitted to humans via bite of a flea which is carrying bacteria from infected rodents [3]. *Y. pestis* can be further transmitted through inhalation of respiratory droplets from persons with *Y. pestis* infected lungs [3]. Genus *Yersinia* contains two other human pathogenic species which cause a gastrointestinal disease: *Y. enterocolitica* and *Y. pseudotuberculosis* [4]. Enteropathogenic *Yersinia* spp. are found in the environment, such as water and soil, but also in contaminated food, such as raw pork meat and vegetables. *Yersinia* spp. are one of the main causes of bacterial gastroenteritis after *Salmonella* and *Campylobacter* infections [4]. In 2016 in the USA and Europe *Y. enterocolitica* accounted for about 117,000 and 7000 infections, respectively [4]. Despite the differences in the transmission mode and caused disease, all three pathogenic *Yersinia* spp. preferably colonize and replicate in the lymphatic tissues of the host, replicate extracellularly in micro abscesses and suppress the unspecific immune response of the host [5].

1.2 Characteristics of enteropathogenic *Yersinia* spp.

Enteropathogenic *Yersinia* spp. are rod-shaped facultative anaerobic bacteria with optimal growth temperature between 30-32 °C [6]. Important for the transmission is that they are psychrotrophic and thus able to replicate at 4 °C, however, most virulence factors are expressed at 37 °C [6]. Enteropathogenic *Yersinia* spp. express flagellar genes and are motile at 30 °C or lower but lose this ability at 37 °C [6].

In this work we used *Y. enterocolitica*, which is a very heterogeneous species and can be subdivided into six biotypes 1A, 1B, 2, 3, 4 and 5 based on biochemical properties [4]. The biotype 1A belongs to non-pathogenic environmental strains and does not possess the virulence plasmid and chromosomaly encoded virulence genes. In contrast, the biotype 1B has been characterized as highly pathogenic and belongs to a mice-lethal group [7, 8]. Biotypes 2-5 are weakly pathogenic and are unable to kill mice [7, 8]. Major difference between the highly pathogenic biotype 1B and lowly pathogenic biotypes 2-5 is that the biotype 1B

carries a chromosomal island termed high pathogenicity island (HPI) [7]. The island encodes for the siderophore yersiniabactin, which is a high-affinity iron chelating system [7]. Yersiniabactin enables yersiniae to capture iron molecules necessary for systemic spreading in the host, allows import of zinc in the bacteria and limits the respiratory burst of the host immune cells [1, 7]. Based on the structure of O-antigen of lipopolysaccharide, *Y. enterocolitica* can be further distinguished into more than 50 serotypes [9]. Distinct biotypes and serotypes dominate in various geographical locations. For instance, biotype 4, serotype O:3 causes the most infections in Europe, Canada and China while serotype O:8 biotype 1B is the most predominant in the USA [4, 9]. In this work the experiments were performed with *Y. enterocolitica* strain WA314 from the biotype 1B and serotype O:8 [10].

1.3 Clinical manifestations of yersiniosis

Yersiniosis is triggered when *Y. enterocolitica* or *Y. pseudotuberculosis* are taken up from contaminated water and food, where raw or undercooked pork is one of the main sources leading to infection in humans [11]. Infections usually occur as sporadic cases and mostly in infants and children of less than 10 years [11, 12].

After ingestion yersiniae reach the small intestine and penetrate the epithelial layer through the microfold (M) cells [12]. Yersiniae replicate in the lymphoid-associated follicles known as Peyer's patches from where bacteria can spread to mesenteric lymph nodes. Yersiniosis typically results in acute enteritis (mostly in young children), enterocolitis and mesenteric lymphadenitis [5]. Illness usually begins within 24-48 hours and persists for 3-14 days, although a chronic form might last for months [11]. Clinical symptoms of yersiniosis include abdominal pain, diarrhoea, vomiting, nausea and fever [11]. Mesenteric lymphadenitis in older children and adults can present as right-sided abdominal pain and fever which can be confused with appendicitis [4, 12]. Histological examination shows ulceration and necrosis of the tissue overlying lymphoid follicles [5]. Mesenteric lymph nodes are enlarged and there is presence of focal areas of necrosis and infiltration of leukocytes.

Yersiniosis is usually self-limiting [11], however severe infections can be caused in susceptible individuals, like people at very young or old age or with iron-overload and immunocompromised individuals [6]. In heavy cases yersiniae can spread systematically and cause formation of abscesses in deep organs [11]. Moreover, there can be post-infection development of secondary immunologically-induced diseases, such as reactive arthritis and glomerulonephritis [11].

1.4 *Yersinia* virulence factors

Upon invasion and crossing of the intestinal epithelium, enteropathogenic *Yersinia* spp. replicate extracellularly and are able to resist phagocytosis by macrophages and neutrophils, which are one of the primary yersiniae targets [5, 13]. These yersiniae activities are mediated by chromosomally- and virulence plasmid-encoded virulence factors. *Y. enterocolitica* carries a 70 kb virulence plasmid pYV (plasmid Yersinia Virulence) which encodes for the

Type Three Secretion System (T3SS), seven secreted effector proteins called Yops (Yersinia Outer Proteins) and adhesion factor Yersinia adhesin A (YadA) [9]. Chromosomally encoded virulence determinants include adhesins invasin and attachment and invasion locus (Ail) and factors specific to certain *Y. enterocolitica* subspecies, such as HPI and additional secretion systems [11]. Expression of the pYV T3SS, Yops, YadA and several chromosomally encoded factors is induced at 37 °C while invasin shows the highest expression at 26 °C, but expression is also increased at 37 °C under acidic conditions [2, 11, 14].

1.4.1 Adhesion factors

The most important adhesion factors in *Y. enterocolitica* are invasin and YadA, which mediate tight contact of bacteria to the host cells required for effector translocation through the T3SS [15]. YadA and invasin also induce activation of β1-integrin signalling [16] which triggers activation of small Ras homologous (Rho) GTPases, changes in actin cytoskeleton and bacterial uptake [16]. Invasin is essential for the first phase of the infection, where it binds to the β1-integrins on the M cells and triggers invasion and transcytosis of the epithelial layer [2]. YadA binds to epithelial cells, extracellular matrix, macrophages and neutrophils, mediates serum resistance, autoagglutination and resistance to phagocytosis [2]. YadA binds to β1-integrins indirectly via bridging with extracellular matrix [17].

1.4.2 Type three secretion system (T3SS)

Numerous Gram negative bacterial pathogens besides *Yersinia* spp. encode for the T3SS [18]. T3SS resembles a needle-like structure and consists of the basal body, the needle and the tip complex [18]. The basal body spans the inner and outer bacterial membranes, whereas needle forms a hollow channel, which extends from the basal body into the extracellular environment. The tip complex at the tip of the needle is composed of LcrV and pore complex made of YopB and YopD and is inserted into the host cell membrane forming a pore. T3SS provides a continuous channel across the bacterial membranes for protein transport from bacterial cytosol into the host target cells in a single step [15, 19]

Secretion and translocation of Yops through the T3SS depends on the surrounding conditions [14]. Building of injectisomes and expression of T3SS genes occur at low levels when bacteria are present at 37 °C and millimolar concentration of Ca^{2+} [15]. Upon Ca^{2+} chelation in vitro there is cessation of bacterial growth, strong upregulation of T3SS gene expression and secretion of effector proteins, known as low calcium response (LCR) [20]. In vivo, host cell contact triggers polarized translocation of effector proteins into target cells without cessation of bacterial growth [14, 15], which depends on activation of Ras-related C3 botulinum toxin substrate (Rac) 1 by YadA and invasin [19].

1.4.3 Effector proteins

Inside the host cells *Yersinia* effectors target the key pathways to suppress immune response (Figure 1.1). YopO/YpkA, YopT, YopE and YopH interfere with actin cytoskeleton dynamics thus inhibiting phagocytosis. YopP/J inhibits mitogen-activated protein kinase (MAPK) and

nuclear factor kappa-light-chain-enhancer of activated B cells (NF-κB) pathways, thus interfering with inflammatory gene expression and triggering cell death. YopM binds to several host proteins and translocates to the nucleus to regulate gene expression. YopT, YopE and pore proteins YopB and YopD trigger inflammasome activation which is suppressed by YopQ/K and YopM. YopP/J triggers pyroptosis and inflammasome activation due to caspase-8 activation but also inhibits it by blocking transcription of IL1β and IL18. Importantly, Yops suppress signalling which is induced by bacteria itself due to pathogen-associated molecular patterns (PAMPs) and activities of effectors sensed as danger-associated molecular patterns (DAMPs).

YopH

YopH is a protein tyrosine phosphatase [21] which mostly targets components of focal adhesion or focal-adhesion like complexes [22] and inhibits phagocytosis [23, 24]. YopH blocks phosphoinositide (PI) 3-kinase/ Akt pathway activation in J774 mouse macrophages resulting in dephosphorylation of Akt, glycogen synthase kinase 3 (GSK3) and forkhead homolog (rhabdomyosarcoma) like 1 (FKHRL1) and inhibited expression of macrophage chemotactic factor 1 (MCP-1) [25]. YopH also suppresses expression of interleukin (IL)-10 in neutrophils during mouse infection [26], inhibits oxidative burst in J774 mouse macrophages and neutrophils [24, 27, 28] and interferes with calcium signalling in neutrophils and T lymphocytes [26, 29, 30]. YopH appears to be the only effector specifically interfering with T and B cell lymphocyte activation by dephosphorylating signalling components associated with activated antigen receptors [31]. YopH is essential for infection in vivo, for instance, for colonization of mesenteric lymph nodes [32] and inhibition of neutrophil recruitment to Peyer's patches [33].

YopE

YopE is highly cytotoxic and induces rounding and detachment of target cells [34]. YopE possesses a GTPase-activating protein (GAP) activity, which promotes GTP hydrolysis of small Rho GTPases, thus causing their inactivation, actin cytoskeleton disruption and inhibition of phagocytosis [5, 16]. Suppression of Rac1 activity by YopE limits effector translocation and serves as a negative feedback mechanism [19, 35]. YopE also inhibits reactive oxygen species (ROS) production by inactivation of Rac2 in neutrophil-like HL-60 cells [36] and interferes with inflammatory response by inhibition of MAPK and NF-κB pathways [37]. YopE plays an unclear role regarding inflammasome activation [38–40]. In mouse Mf4/4 macrophages *Y. enterocolitica* YopE inhibited Rac1 dependent activation of caspase-1 and release of mature IL-1β [40]. In contrast, in bone marrow-derived macrophages (BMDMs) YopE induces pyrin inflammasome activation, due to the inactivation of small Rho GTPases, which is sensed as a danger signal by the host cell [38, 39]. YopE is essential for virulence in vivo as *Y. pseudotuberculosis* mutants unable to express YopE are avirulent after oral and intraperitoneal infections [34] and bacteria devoid of YopE GAP activity are unable to colonize spleen [41].

YopO/YpkA

YopO (Yersinia protein kinase A (YpkA) in *Y. pseudotuberculosis* and *Y. pestis*) is a kinase, which interferes with host actin cytoskeleton organization and causes cell rounding, disruption of stress fibers and inhibition of phagocytosis [42–46]. YopO/YpkA is translocated as an inactive kinase into target cells and gets activated upon binding of monomeric G-actin [44, 45, 47]. Moreover, actin serves as a bait to recruit actin binding proteins, several of which are phosphorylated by YopO/YpkA to misregulate their function [48]. YopO/YpkA also binds to and phosphorylates Gαq subunit of G protein-coupled receptors (GPCRs) to inhibit downstream signalling events induced upon GPCR activation, such as RhoA dependent stress fiber formation and nuclear translocation of TF tubby [49]. Additionally, YopO/YpkA possesses a GDP dissociation inhibitor (GDI)-like domain, which interacts with small Rho GTPases to interfere with GDP nucleotide exchange and inhibit phagocytosis [46, 50, 51]. Kinase activity and the ability to bind Rho GTPases by YopO/YpkA have been found to be essential for *Yersinia* virulence in in vivo mouse infection [42, 51, 52]. However, in other studies lack of YopO/YpkA resulted only in a minor attenuation of virulence [32, 53].

YopT

YopT is a cysteine protease which targets small Rho GTPases to disrupt actin cytoskeleton and inhibit phagocytosis [54–57]. YopT cleaves off the C-terminal isoprenylated cysteine from small Rho GTPases, which is important for Rho GTPase membrane localization and interaction with other proteins [58–60]. YopT did not to play a role for virulence in vivo [53] which could be due to YopT and YopE sharing overlapping functions [37]. However, in cells YopT seems to act towards RhoA while YopE is targeting Rac1 [16]. Additionally, YopT inhibits activation of MAPK and NF-κB pathways [37], whereas YopT inhibition of Rho GTPase signalling in macrophages is sensed as a danger signal, which triggers activation of pyrin inflammasome [38].

YopM

YopM is an acidic leucine rich repeat (LRR) protein which functions as a scaffold recruiting host proteins [5]. YopM structure resembles a “horseshoe”, which is built of two conserved N-terminal α-helices followed by species and strain specific number of 20-22 amino acid LRRs and conserved structurally disordered C-terminus [61–63]. YopM is highly essential for *Yersinia* virulence in vivo [53] and was first thought to function extracellularly by binding to thrombin [64]. However, YopM is also translocated into the host cells by T3SS where it enters the nucleus [65]. YopM interacts with isoforms of ribosomal S6 kinase (RSK) and protein kinase N (PKN), scaffold protein IQ motif containing GTPase activating protein 1 (IQGAP1), caspase-1 and DEAD box helicase 3 (DDX3) [66–70]. YopM forms a trimeric complex with RSK and PKN kinases, which do not interact under physiological conditions, and induce their activation [66, 67]. YopM binding to RSK induces immunosuppressive cytokine IL-10 expression in human macrophages [70]. Moreover, a prominent YopM function is inhibition of caspase-1 and inflammasome activation leading to blockage of IL-1β and IL-18 secretion

and pyroptosis [38, 39, 68, 69, 71, 72]. YopM hijacks active PKN to counteract pyrin inflammasome activation which is triggered due to the inactivation of Rho GTPases by YopT and YopE [38, 39].

YopP/J

YopP (YopJ in *Y. pseudotuberculosis* and *Y. pestis*) is a strong suppressor of pro-inflammatory signalling and cytokine expression and inducer of host cell death [5]. YopP/J possesses cysteine protease and deubiquitinase activity which promotes deubiquitination of immune signalling molecules to interfere with their activity [73–75]. Additionally, YopP/J is an acetylatransferase, which acetylates serine and threonine residues in the activation loop of kinases in MAPK and NF-κB pathways (MAPK kinases (MKKs), inhibitor of nuclear factor kappaB (IκB) kinase (IKK), transforming growth factor-beta-activated kinase 1 (TAK1)), thus inhibiting their phosphorylation and activation [76–80]. Moreover, YopM has been also shown to cooperate with YopP/J, which inhibits transcription of IL-1β and IL-18, to inhibit pyroptosis [71]. Cell death is induced due to simultaneous toll-like receptor (TLR) 4 stimulation by yersiniae LPS and inhibition of MAPK and NF-κB pathways by YopP/J, which reduces the synthesis of pro-survival factors and induces receptor-interacting serine/threonine-protein kinase 1 (RIPK1) mediated cleavage of caspase-8 [81]. Activated caspase-8 triggers apoptosis by cleavage of caspase-3/7/9 and pyroptosis due to the processing of caspase-1/11 and gasdermin (GSDM) D pore formation in the plasma membrane [81]. Pore formation also triggers K^+ efflux and inflammasome activation [82]. Interestingly, enhanced YopP/J cytotoxicity associates with higher attenuation of virulence in vivo [83–85]. Mice unable to undergo YopP/J induced cell death succumb to infection much earlier and show increased bacterial loads and dissemination than mice where cell death occurs during infection [86]. Therefore, inhibition of inflammatory signalling during TLR4 activation is sensed as a danger signal which triggers cell death as a protective response against bacteria.

YopQ/K

YopQ (YopK in *Y. pseudotuberculosis* and *Y. pestis*) regulates processes both in bacterial and host target cells. YopQ/K is thought to control the fidelity of Yop translocation from the bacterial side [15]. Additionally, YopQ/K interacts with T3SS pore proteins YopB and YopD on the cytoplasmic side of the host cell and limits the rate of Yop translocation including the pore proteins [15, 87]. Hypertranslocated YopB and YopD associate with lysosomal-associated membrane protein 1 (LAMP1) positive endosomal/ lysosomal membranes in the host cell cytosol [88]. The translocon induces membrane damage leading to recruitment of Galectin 3 and guanylate binding proteins (GBPs), which triggers inflammasome activation [88]. By limiting YopB and YopD hypertranslocation YopQ/K prevents recognition of T3SS pore by the host immune system [38, 39, 87–89]. Precise control of Yop translocation and inflammasome inhibition are essential for *Yersinia* virulence since YopQ/K mutants are highly attenuated in vivo [53, 89].

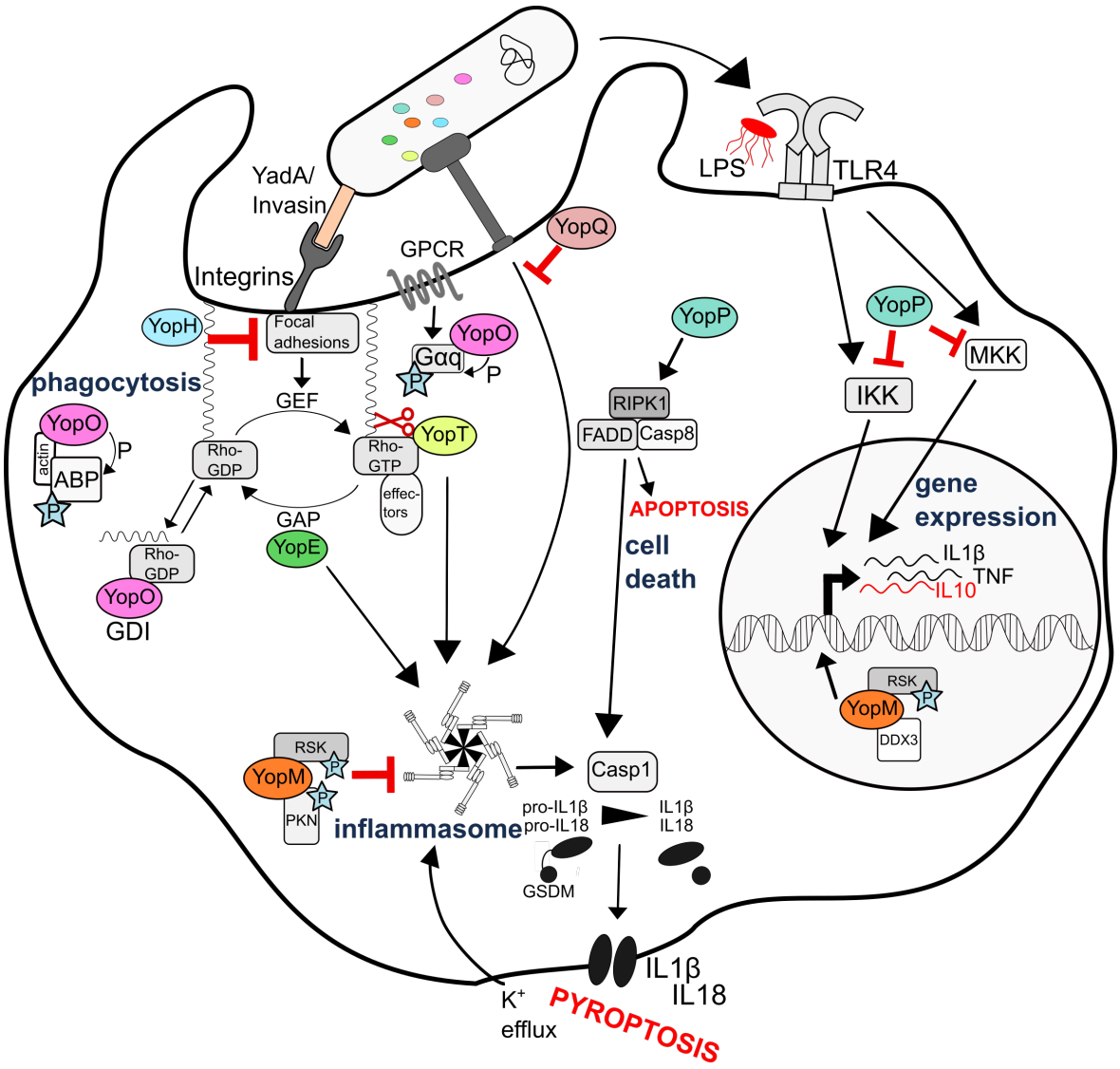

FIGURE 1.1: **Summary schematic of *Yersinia* virulence factor activities in the host cell.** *Yersinia* virulence factors modulate host signalling pathways to counteract immune response in macrophages which is induced by bacterial PAMPs and DAMPs. Activities of the effector proteins target phagocytosis, inflammatory gene expression, inflammasome activation and cell death.

1.5 *Yersinia* virulence factor modulation of gene expression

Modulation of host gene expression by *Yersinia* spp. is one of the main virulence strategies to suppress inflammatory response in macrophages. This modulation is mainly due to the activity of YopP/J, which efficiently inhibits NF-κB and MAPK pathways [22]. However, other effectors also interfere extensively with host cell signalling pathways and affect downstream gene expression programs. For instance, YopT induces expression of immunosuppressive proteins krueppel-like factor (KLF) 2 and glucocorticoid-induced leucine zipper (GILZ) [90, 91], YopH and YopE cooperates with YopP/J to suppress IL8 expression [92] and YopM upregulates immunosuppressive cytokine IL-10 [70]. Overall, Yops counteract expression of pro-inflammatory genes which are induced by factors from bacteria itself, such as LPS, YadA, invasin and T3SS pore upon TLR4 and small Rho GTPase activation [93–98].

Up to now, two studies have performed microarray analysis with *Y. enterocolitica* infected mouse macrophage cell lines to analyse the effect of virulence plasmid encoded factors on host gene expression [99, 100]. In PU5-1.8 cells 857 differentially expressed genes (DEGs) were found after infection for 2.5 h [99]. In contrast, in J774 cells only 50 DEGs were identified after infection for 2 h [100]. In both studies virulence plasmid encoded factors suppressed induction of pro-inflammatory genes by the plasmid-cured strain in a YopP dependent manner. However, YopP did not account for all wild type regulated gene expression changes, indicating the role also of other Yops. In PU5-1.8 cells YopM mediated expression of genes involved in cell cycle, cell growth and phagocytosis [99], whereas no effect on gene expression neither by YopM nor by YopH was observed in J774 cells [100].

Additional microarray and RNA-seq studies have been performed in BMDMs infected with wild type *Y. pseudotuberculosis* and YopJC172A strain, which is compromised in ability to induce apoptosis and inhibit NF-κB and MAPK pathways [101], NK cells stimulated with IL-12 and IL-18 and infected with wild type *Y. enterocolitica* [102], HeLa cells infected with wild type *Y. enterocolitica*, YopP mutant and virulence plasmid-cured strain with and without invasin [103], neutrophils infected with virulent *Y. pestis* KIM5 strain and avirulent KIM6 strain [104], Toll/IL-1R homology (TIR)-domain-containing adapter-inducing interferon-beta (Trif) $^{-/-}$ myeloid differentiation primary response 88 (MyD88)$^{-/-}$ BMDMs infected with *Y. pseudotuberculosis* lacking all translocated effectors with and without T3SS pore proteins [98], Peyer's patches from mice infected with wild type *Y. pseudotuberculosis* [105], ceca from mice infected with *Y. pseudotuberculosis* wild type strain and cytotoxic necrotizing factor (CNF) Y mutant [106] and primary human macrophages infected with wild type *Y. enterocolitica* and YopM mutant [70]. However, comprehensive analysis of the effect of virulence plasmid encoded factors on host gene expression in primary human macrophages with RNA-seq technology has not been performed until now.

1.6 Macrophages and recognition of pathogens

Macrophages are professional phagocytes which play an important role in tissue homeostasis, infection and various diseases, such as, atherosclerosis, cancer and type two diabetes [107]. Certain tissue-resident macrophage populations, such as microglia of the central nervous system and epidermal Langerhans cells, are seeded during waves of embryonic hematopoiesis from the yolk sac and/ or fetal liver and self-maintain independently of bone marrow contribution during adulthood [108, 109]. In contrast, in tissues, like intestine, dermis, heart and pancreas, macrophages are replenished from circulating blood monocytes [108]. Under physiological conditions macrophages ensure tissue homeostasis, however infectious agents or other stimuli trigger heterogeneous functional states adapted to the environmental input [107].

Classically, macrophages are defined by two phenotypic extremes of M1 and M2 macrophages [107]. M1 macrophages are induced after stimulation with pro-inflammatory signals such as LPS, interferon (IFN) γ and granulocyte-macrophage colony-stimulating

factor (GM-CSF). M1 macrophages show enhanced ability to kill microbes, present antigens, produce reactive oxygen or nitrogen species and produce pro-inflammatory cytokines [107]. In contrast, M2 macrophages are induced by IL-4, IL-13, transforming growth factor beta (TGF-β), IL-10, glucocorticoids and immune complexes. M2 macrophages downregulate inflammation by releasing anti-inflammatory cytokines and suppressors of inflammation and they are involved in tissue remodelling, wound healing, angiogenesis, anti-helminth responses, allergic reactions and tumour progression [107]. In reality, macrophage phenotypes range as a continuous spectrum of activation states between M1 and M2 states [110]. Macrophage phenotype is shaped by the local tissue environment and systemic signals and it can be altered during encounter with pathogens [107, 110]. Various signals induce specific signalling pathways that trigger alterations in metabolic state and chromatin modifications followed by associated gene expression changes to result in an adapted functional state [107, 111].

Conserved molecular motifs in pathogens known as PAMPs are recognized by pattern recognition receptors (PRRs), such as transmembrane proteins TLRs and C-type lectin receptors (CLRs) and cytoplasmic proteins retinoic acid-inducible gene (RIG)-I-like receptors (RLRs) and nucleotide-binding oligomerization domain (NOD)-like receptors (NLRs) [112]. Generally, recognition of PAMPs by PRRs regulates gene expression, immune cell migration, phagocytosis, cell differentiation, inflammasome activation and cell death [112–115]. Moreover, PRR activation induces profound metabolic reprogramming which is essential for modulation of effector functions and gene expression [111].

LPS is one of the main PAMPs and inducers of pro-inflammatory response in Gram negative bacteria through binding to TLR4 [116]. TLR4 binds to LPS in complex with myeloid differentiation factor 2 (MD-2) to initiate a signalling cascade which activates IKK complex and MAP kinases. IKK complex phosphorylates IκB, which undergoes proteosomal degradation and releases NF-κB for nuclear translocation and induction of pro-inflammatory cytokines. MAPK kinases phosphorylate and activate c-Jun NH2-terminal kinase (JNK), p38 and extracellular signal-regulated kinase (ERK) 1/2 kinases which activate TF activator protein 1 (AP-1) to induce inflammatory gene expression. TLR4 can be also endocytosed and signal from endosome to activate interferon regulatory factor (IRF) 3 for type I IFN production. LPS rapidly induces primary response genes (PRGs) which do not require new protein synthesis. PRGs encompass feedback regulators which fine tune inflammatory signalling and initiate production of late induced secondary response genes (SRGs), such as Interferon-stimulated genes (ISGs), which include antiviral proteins and TFs IRFs [117–119]. For instance, binding of type I IFNs to the IFN α receptor (IFNAR) activates janus kinase (JAK)/signal transducer and activator of transcription (STAT) signalling pathway to induce expression of ISGs containing DNA elements termed interferon-sensitive response elements (ISREs).

1.7 Epigenetics

Each cell in an eukaryotic organism possess the same genetic material in a form of DNA sequence, despite the presence of an immense phenotypic variability, which is maintained

from cell differentiation and across cell divisions [120]. This phenomena is explained by epigenetic changes which are inheritable changes that do not alter the DNA sequence but the properties of DNA and proteins or other molecules bound to it, thus regulating processes such as DNA replication, recombination, repair and transcription [121, 122].

In the nucleus 147 bp of DNA is wrapped around a histone protein octamer consisting of two copies of each histone (H) 2A, H2B, H3 and H4 to form a nucleosome, the basic repeating unit of chromatin [123] (Figure 1.2). Additionally, the linker histone H1 stabilizes the chromatin structure between nucleosomes. Chromatin is further organized into higher order structures to form chromosomes. Accessibility of the DNA in chromatin depends on epigenetic mechanisms, namely, post-translational modifications (PTMs) of histones, DNA methylation, ATP dependent nucleosome remodelling, non-coding RNAs and other epigenetic regulators [124]. Essentially, epigenetic mechanisms regulate contacts between the nucleosomes and DNA and modulate recruitment of regulatory proteins, thus promoting either euchromatin or heterochromatin state, which is open and closed chromatin conformation, respectively [122]. Deposition of different modifications and recruitment of proteins take place in an ordered manner at specific locations to carry out chromatin-associated processes accordingly. Gene transcriptional activation and repression are associated with certain combinations of histone modifications at cis-regulatory elements, like promoters and enhancers [125]. Promoters are located closely with the transcription start site (TSS) of the associated gene [126]. In contrast, enhancers are usually located far away from the TSS of the associated genes and they can be found upstream, downstream or within the target genes [127]. Enhancers form loops to the target genes within 3D genomic structures known as TADs (Topologically Associated Domains) to promote transcription.

Histones are post-translationally modified at various residues mostly at their flexible N-terminal tails with modifications such as methylation, acetylation, phosphorylation and ubiquitination to influence the chromatin state [122, 124]. For instance, histone acetylation promotes transcription by neutralizing the basic charge of modified lysine and therefore disrupting contacts with negatively charged DNA [122]. Histone methylation can be both activating and repressing. For instance, histone 3 lysine 4 trimethylation (H3K4me3) is a typical activating mark at gene promoters, whereas H3K27me3 and H3K9me3 are two repressive marks [128]. Deposition and removal of various histone marks are mediated by sequence specific TFs which bind certain DNA elements and recruit chromatin modifiers [120]. Histone modifications are deposited by enzymes termed “writers” such as methyltransferases, acetyltransferases and kinases [124]. Histone modifications are detected by “reader” proteins, which can additionally function as “writers”, transcriptional activators or repressors and recruit or displace other proteins to drive progression of specific chromatin function. Histone modifications are removed by “eraser” proteins, such as demethylases, deacetylases and phosphatases.

Overall, the “epigenetic landscape” of a cell, which is the sum of DNA methylation state, histone modifications and proteins and RNA bound to the chromatin, determines the accessibility to genomic regions and execution of chromatin associated processes [107]. It has become clear that the “epigenetic landscape” also plays a major role in rapid pathogen

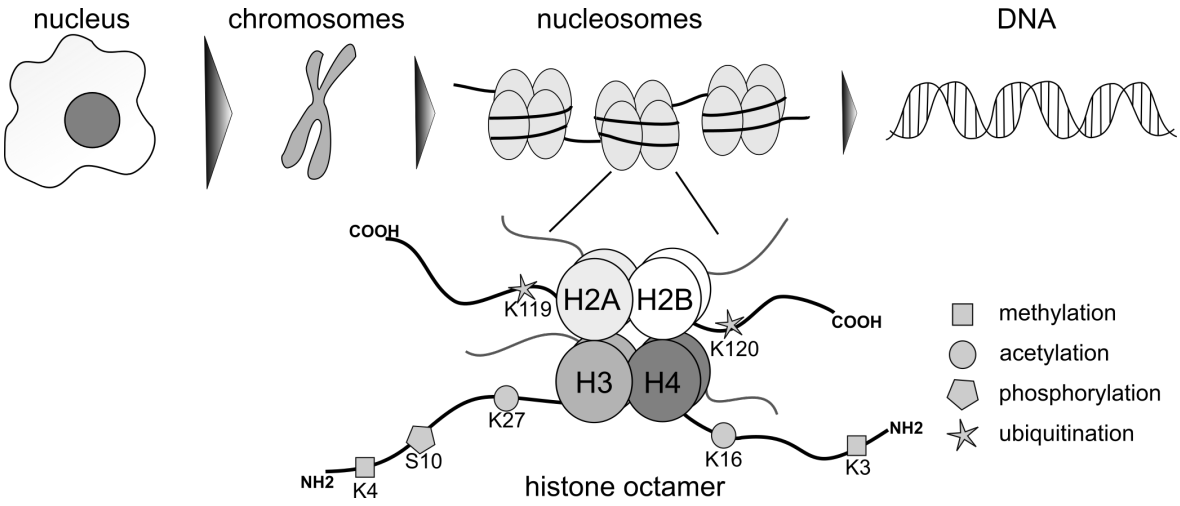

FIGURE 1.2: **Representation of the nuclear architecture.**In the nucleus, chromosomes consist of DNA tightly bound around the histones forming nucleosomes. A nucleosome consists of a histone octamer made of H2A, H2B, H3 and H4. Nucleosome flexible amino (NH2) and carboxy (COOH) tails can be post-translationally modified with modifications such as methylation, acetylation, phosphorylation and ubiquitination. K: lysine, S: serine.

induced immune responses in macrophages [129].

1.8 Epigenetic regulation of macrophages

Monocyte differentiation into macrophages encompasses large scale epigenetic reprogramming involving changes in H3K4me3, H3K4me1 and H3K27ac at promoters and enhancers [130]. Depending on the environmental signals present during differentiation, macrophages activate distinct signalling pathways which establish an enhancer landscape that is signal specific and determine the transcriptional output and macrophage phenotype [130–132]. The establishment of enhancer sites is driven by collaborative activity of pioneer lineage determining TFs (LDTFs), which compete with nucleosomes for binding to the DNA and recruit chromatin remodelers [110, 133]. LDTFs in macrophages are mainly PU.1 and CCAAT-enhancer-binding protein (C/EBP) [110]. Promoter landscape is established by more broadly expressed LDTFs, such as specificity protein 1 (SP-1), ying-yang 1 (YY1), nuclear transcription factor Y (NFY) an GA binding protein transcription factor subunit alpha (Gabpa).

Stimulation of macrophages with PAMPs such as LPS triggers metabolic and epigenetic reprogramming with subsequent transcription of associated immune response genes [111, 117, 133, 134]. Metabolites are used for histone modifications, e.g. acetyl-CoA for histone acetylation and metabolites also regulate activity of chromatin modifying enzymes [111]. PAMPs activate stimulus regulated TFs (SRTFs), such as NF-κB, AP-1 and IRF3, and induce their binding to available cis-regulatory regulatory elements at specific target genes to recruit chromatin modifiers and promote transcription [135]. Therefore the expression and activity of LDTFs during macrophage differentiation determines the set of available cis-regulatory elements for SRTFs and the resulting gene expression. In macrophages promoters and enhancers of many inflammatory cytokines and chemokines are in a “primed” state with partially opened chromatin conformation, activating histone marks and paused

Polymerase II present for rapid induction by binding of SRTFs [107, 117, 136]. Interestingly, even differentiated macrophages can undergo phenotypic shift upon short stimuli which is controlled by the chromatin state [132]. Cooperation between SRTFs and LDTFs after stimulation of differentiated macrophages promotes formation of de novo/ latent enhancers or trigger disassembly of enhancers in a signal specific manner [137, 138].

Cytokines, such as tumor necrosis factor (TNF), Type I IFNs and IFNγ, which are induced by PAMPs, induce secondary signalling pathways and further trigger modifications of chromatin and gene expression [138–140]. For instance, IFNγ downregulates expression of M2-like genes and LPS-induced negative feedback regulators though epigenetic mechanisms to potentiate pro-inflammatory response in macrophages [138, 139]. TNF treatment of macrophages prevents induction of inflammatory genes upon subsequent LPS stimulation termed "tolerization" and this TNF effect can be reversed by treatment with Type I IFNs [140]. Therefore, the interplay between pathogen PAMPs and induced cytokines triggers a very complex epigenetic and transcriptional response in macrophages to tailor an appropriate immune response.

Epigenetic changes that are induced in macrophages by different stimuli can persist over extended periods of time and influence the nature of response upon subsequent exposures by the same or different stimuli [141]. This phenomena is termed "innate immune memory" and two very well-known examples are LPS-induced "tolerance" and β-glucan-induced "training", which render induction of pro-inflammatory genes amplified or diminished, respectively [130]. Several pathogens modulate chromatin in macrophages to interfere with immune gene expression [129, 142]. Bacterial effectors modulate signalling pathways upstream of chromatin modifications or hijack the epigenetic machinery of the host. Furthermore, some bacteria encode effectors which translocate to the nucleus and mimic host chromatin modifying enzymes. Since epigenetic marks can be maintained even in the absence of triggering stimuli, infections likely affect the "innate immune memory" of the host.

1.9 Aim of the study

One of the main virulence mechanisms of the pathogenic *Yersinia* spp. is modulation of gene expression in macrophages [81]. Gene expression analysis using microarrays in mouse macrophage cell lines has been performed [99, 100], however there is a lack of global transcriptome analysis with RNA-seq in *Yersinia*-infected primary human macrophages. In macrophages gene expression is regulated at the level of chromatin [110] and it is not known whether *Yersinia* virulence factors target epigenetic marks to modulate transcription. Other bacterial pathogens regulate host chromatin and transcription to alter specific biological pathways [129], however it is not know which pathways might be targeted at gene expression and epigenetic level by *Yersinia*. Furthermore, MAPK and NF-κB pathways, which are suppressed by YopP, play a central role in modulation of histone marks and gene expression in macrophages [112]. Therefore, it could be speculated that YopP regulates chromatin and gene expression, but so far there are no data describing this. Moreover, the function of YopM

in the nucleus is still enigmatic and it is not know if YopM targets histone modifications. To address these points, the following questions were central for this work:

- How *Yersinia* virulence factors affect gene expression in primary human macrophages?
- Do *Yersinia* virulence factors modulate histone modifications and are they associated with gene expression?
- Which pathways are modulated at gene expression and histone mark level?
- Do YopP and YopM regulate gene expression and histone marks?
- How YopP modulates gene expression and histone marks?

2 Materials and Methods

2.1 Materials

2.1.1 Devices

TABLE 2.1 Devices

Device	Type, manufacturer
Accu-Jet	Accu-jet pro, Brand, Wertheim, Germany
Agarose gel electrophoresis	Agarose gel chamber, Roth, Karlsruhe, Germany
Bioanalyzer	Agilent 2100, Agilent Technologies, Santa Clara, USA
Cell counting chamber	Neubauer-cell counting chamber, Hartenstein, Würzburg, Germany
Cell culture incubators	CB Series, Binder, Tuttlingen, Germany
Centrifuge	Sorvall RC-5B, Thermo Scientific, Waltham, USA; 5417R and 5810R, Eppendorf, Hamburg, Germany; biofuge pico, Heraeus instruments, Hanau, Germany; Sigma 3-18K, Sigma-Aldrich, St. Louis, USA
Clean bench	Herasafe, Thermo Scientific, Waltham, USA
Freezer	-80 ℃: HERA freeze, Heraeus, Kendro Laboratory, Hanau, Germany; -20 ℃: comfort, Liebherr-International AG, Bulle, Switzerland
Fridge	4-8 ℃, Liebherr Premium, Liebherr_x0002_International AG, Bulle, Switzerland
Microscope	Microscope SZX12 with Camera DP10 , Olympus, Japan
Microwave	900W, Panasonic, Kadoma/Osaka, Japan
NanoDrop® ND-1000	PeqLab, Erlangen, Germany
pH-Meter	Seven easy, Mettler-Toledo, Giessen, Germany
Photometer	Ultrospec 3100 pro, Amersham/GE healthcare Europe, Munich, Germany
Pipettes	2, 10, 100, 200, 1000 µl, Research Plus, Eppendorf, Hamburg, Germany
Power supplies	Biorad power pac universal, Biorad power PC 200, Bio-Rad, Hercules, USA
Qubit	Qubit Fluorometer, Thermo Fisher Scientific, Waltham, USA

Continued on next page

Table 2.1 – *continued from previous page*

Device	Type, manufacturer
RT-qPCR machine	Rotorgene 6000 qPCR machine, Qiagen, Germany
Sequencer	NextSeq500, Illumina, San Diego, USA
Shaking incubator	Certomat BS-1, Sartorius, Göttingen, Germany
Sonicator for chromatin	BioruptorTM UCD-200, Diagenode, Belgium
Thermoblock	DRI-Block DB3 Techne, Bibby Scientific Limited, Staffordshire, UK
Transilluminator	Vilber Lourmat, ETX, Eberhardzell, Germany
UV-Transilluminator and Detector	ChemiDoc XRS, Bio-Rad, Hercules, USA
Vortex	REAX Topo, Heidolph Instruments, Schwabach, Germany
Water bath	Typ 1013, Gesellschaft für Labortechnik, Burgwedel, Germany
Weighing scale	440-47N, Kern, Balingen-Frommern, Germany

2.1.2 Disposables

TABLE 2.2 Disposables

Disposable	Type, manufacturer
µMacs Columns	MACS, Milteny Biotec GmbH, Bergisch, Gladbach, Germany
µMacs Columns separation column 25LE	MACS, Milteny Biotec GmbH, Bergisch, Gladbach, Germany
Bioanalyzer chips	DNA High Sensitivity Chip, RNA 6000 Nano Chip, Agilent Technologies, Santa Clara, USA
Bottle-top sterile filter units	Vacuum filtration system, capacity 500 ml, pore size 0.2 µm, Nalgene, Rochester, USA
CD14 Microbeads, human	MACS, Milteny Biotec GmbH, Bergisch, Gladbach, Germany
Coverslips	12 mm diameter, round, Hartenstein, Würzburg, Germany
Disposable cuvettes	1.5 ml, 12.5 x 12.5 x 45 mm, BRAND GmbH + CO KG,Wertheim, Germany
Disposable needles	0.40 x 20 mm ,0.55 x 25mm, 0.6 x 25 mm STERICAN disposable needles, B.Braun, Melsungen, Germany
Glass pasteur pipettes	230 mm, Heinz Herenz Medical and Laboratory Supplies, Hamburg, Germany
Multiwell plates	6-well, Sarstedt, Nümbrecht, Germany
Parafilm M	Bemis®, Pechiney Plastic Packaging, Neenah, USA
PhaseLock tubes	2-ml, heavy, Quantabio, Beverly, USA
Pipette tips	Sterile Biosphere filter tips and non-sterile 10, 100, 200, 1000 µl, Sarstedt, Nümbrecht, Germany

Continued on next page

Table 2.2 – *continued from previous page*

Disposable	Type, manufacturer
Plastic syringe	Sterile, 2 ml, 5 ml, 10 ml, 20 ml, B. Braun, Melsungen, Germany
Protein A/G magnetic beads	Pierce™ Magnet-ChIP-Kit, Thermo Fisher Scientific, Waltham, USA
Reaction tubes	0.2 ml, Biozym Scientific, Hessisch Odendorf, Germany; 0.5 ml, 1.5 ml, 2 ml, Sarstedt, Nürnbrecht , Germany; 15 ml, 50 ml Centrifuge Tubes, CELLSTAR, Greiner Bio-One, Kremsmuenster, Austria; qPCR Strip Tubes and Caps, 0.1 ml, Qiagen, Germany; Qubit assay tubes 0.5 ml, Thermo Fisher Scientific, Waltham, USA
Scalpels	Sterile, B. Braun, Melsungen , Germany
Serological pipettes	Sterile 2, 5, 10, 25 ml, Sarstedt, Nümbrecht, Germany
Syringe sterile filters	SFCA 0.2 µm, Thermo Fisher Scientific, Waltham, USA

2.1.3 Kits, enzymes, agents and inhibitors

TABLE 2.3 Kits, enzymes, agents and inhibitors

Kit, enzyme, agent, inhibitor	Provider, manufacturer
Accutase, Enzyme Cell Detachment Medium	eBioscience, San Diego, USA
DNase, RNase-Free DNase Set	Qiagen, Hilden, Germany
iScript cDNA Synthesis Kit	Bio-Rad, Hercules, USA
RNeasy Mini Kit	Qiagen, Hilden, Germany
RNAase A	Thermo Fisher Scientific, Waltham ,USA
Proteinase K	Thermo Fisher Scientific, Waltham ,USA
Glycogen	Thermo Fisher Scientific, Waltham ,USA
Maxima™ SYBR Green/ROX qPCR Master Mix (2X)	Thermo Fisher Scientific, Waltham ,USA
FastDigest Green Buffer (10X)	Thermo Fisher Scientific, Waltham ,USA
O'GeneRuler DNA Ladder, Ready-to-Use 50-1000 bp	Thermo Fisher Scientific, Waltham ,USA
Qubit dsDNA HS Assaykit	Thermo Fisher Scientific, Waltham ,USA
NEXTflex™ ChIP-Seq Kit	Bioo Scientific, Texas, USA
NEBNext Poly(A) mRNA Magnetic Isolation module	New England Biolabs, Ipswich, USA
NEBNext Ultra RNA Library Prep Kit for Illumina	New England Biolabs, Ipswich, USA
RedSAFE	Intron Biotechnology, Korea
SB203580	Cayman Chemical, Ann Arbor, USA
PD98059	Merck Millipore, Burlington, USA
Complete Protease inhibitor	Roche Diagnostics, Risch, Switzerland
Phosstop Phosphatase inhibitor	Roche Diagnostics, Risch, Switzerland

2.1.4 Growth media, additives and antibiotics

Media were sterilized by autoclaving for 20 min, 121 ℃ and 1.4 bar. Supplements, which could not be autoclaved, were sterile filtered with 0.22 µm filter.

TABLE 2.4 Media

Bacteria cultures	**Concentration**	**Components**
LB-medium (lysogenic broth), pH 7.5	10 g/l 5 g/l 5 g/l	Tryptone Yeast extract NaCl add 1000 ml H_2O
Eukaryotic cell culture	**Additives**	**Provider, manufacturer**
RPMI Medium 1640 + Glutamax		Gibco, Carlsbad, USA
	20 % (v/v) autologous serum	
	1 % (v/v) Penicillin/Streptomycin	Gibco, Carlsbad, USA

TABLE 2.5 Antibiotics

Antibiotics	**Solvent**	**Working concentration, µg/ml**	**Provider, manufacturer**
Kanamycin	ddH_2O	50	Sigma-Aldrich, St. Louis, USA
Chloramphenicol	EtOH	20	Roth, Karlsruhe, Germany
Nalidixic acid	1M NaOH	100	Sigma-Aldrich, St. Louis, USA

2.1.5 Buffers and chemicals

Chemicals were obtained from Amersham/GE Healthcare, Munich (Germany), BD Biosciences, Heidelberg (Germany), Biozym, Oldendorf (Germany), Dianova, Hamburg (Germany), Merck, Darmstadt (Germany), PAA, Pasching (Austria), PromoCell, Heidelberg (Germany), Roche, Mannheim (Germany), Roth, Karlsruhe (Germany), Sigma-Aldrich, St. Louis (USA) and Thermo Fisher Scientific, Waltham (USA).

Buffers were autoclaved for 20 min, 121 ℃ and 1.4 bar for sterilization or sterile filtered with 0.22 µm filter.

2.1.6 Antibodies

TABLE 2.6 Primary antibodies and working concentrations

Antigen	**Provider, catalogue number**	**Species**	**ChIP concentration**
H3K4me3	Merck Millipore, USA, 04–745	rabbit	4 µl
H3K4me1	Cell Signaling, USA, 5326S	rabbit	5 µl
H3K27ac	abcam, UK, ab4729	rabbit	2 µg
H3K27me3	Merck Millipore, USA, 07-449	rabbit	4 µl

2.1.7 Primers

TABLE 2.7 Primers used for ChIP-qPCR

Name	Sequence	Description
IDO1 F	GCCAGTATGAGCCTAAGCAGC	Promoter regions, H3K4me3 and H3K27ac DRs
IDO1 R	AGAGAGGCAGTGTGGAATAATGG	
IL6 F	GACAGCCACTCACCTCTTCAG	
IL6 R	AAGCCTACCCACCTCCTTTC	
IL1B F	CTGGCGAGCTCAGGTACTTC	
IL1B R	ACACATGAACGTAGCCGTCA	
PTGS2 F	TAACTGTATCCAGCCCCACTCC	
PTGS2 R	ACCCATGTCAAAACCGAGGTG	
RIOK3 F	TCTCAACCTCTCAGTCACCGCT	Used for normalization of H3K27ac signal
RIOK3 R	AAGCTGACATTTGCTGCCGCT	
NSA2 F	CAGCCTGAAAGGTCAGCGGT	
NSA2 R	TCGAGACTTGAGGCCGTTGC	
RPLP0 F	GTCAGGGATTGCCACGCAG	Used for normalization of H3K4me3 signal
RPLP0 R	GGCGATTGCGCGTGTCC	
GAPDH F	GCGTCTACGAGCCTTGCG	
GAPDH R	CTACCCTGCCCCCATACGA	
TBP F	CTGAGACAGCGGGCACGGTA	
TBP R	GCCTGAACCGAGAGACGGGA	
IB89 F	GCTGTAAGTGTTGTTGTTACTCGG	Background region; hg19 chr12:60,683,283-60,696,000
IB89 R	AGAAAGCCCAACCTCAGCACC	

2.1.8 Bacterial strains and eukaryotic cells

TABLE 2.8 *Y. enterocolitica strains*

Strain	Characteristics	Resistance	Reference
WA314	*Y. enterocolitica* serotype O:8, clinical isolate, pYVO8+	Nal	[143]
WAC	Plasmidless derivative of WA314	Nal	[143]
WA314ΔYopM	Derivative of WA314 harbouring the virulence plasmid pYVO8 in which the YopM gene had been replaced by a kanamycin resistance cassette from pUC4k	Kana	[53]
WA314ΔYopP	Derivative of WA314 in which the YopP gene was replaced by a chloramphenicol resistance	Chlor	[144]

TABLE 2.9 Eukaryotic cells

Cells	Characteristics	Reference
Human peripheral blood monocytes	Isolated monocytes were cultured for 6 days until differentiated into macrophages	Self-made isolation [145] from buffy coats, which were provided by Frank Bentzien, University Medical Center Eppendorf, Hamburg, Germany

2.1.9 Software and tools

TABLE 2.10 Software and tools

Software, tool	Provider/ reference
BEDTools 2.25.0	[146]
BWA 0.7.12-r1039 csaw 3.8	[147] [148]
DAVID 6.8	[149, 150]
deepTools 3.1.3	[151]
DESeq2 package (R-package)	[152]
diffReps	[153]
EaSeq 1.111	[154]
FastQC 0.11.5	http://www.bioinformatics.babraham.ac.uk/projects/fastqc/
FeatureCounts	[155]
GEO database	[156]
ggplot2 package (R-package)	[157]
heatmap.2 (R-package)	https://github.com/TomKellyGenetics/heatmap.2x
HOMER 4.11	[158]
ImageJ analysis software Version 1.52a	National Institute of Health, NIH. https://imagej.nih.gov/ij/
Integrative Genomics Viewer (IGV) 2.4.16	[159]
MACS2 2.1.2	[160]
MiKTeX Console 4.0.1	https://miktex.org/
Multi-symbol checker	HUGO Gene Nomenclature Committee (HGNC), [161]
pheatmap (R-package)	https://github.com/raivokolde/pheatmap
Picard 2.0.1	https://broadinstitute.github.io/picard/
PRIMER-Blast	[162]
Rotor Gene Q Software 2.3.1	Qiagen, Hilden, Germany
RseQC	[163]
RStudio 3.5.1	[164]
Samtools 1.9	[165]
SICER 1.1	[166]
SnapGene Viewer 4.3	Insightful Science, San Diego, USA
SRA toolkit	http://ncbi.github.io/sra-tools/
STAR	[167]
Texmaker 5.0.5	https://www.xm1math.net/texmaker
TrimGalore 0.5.0	http://www.bioinformatics.babraham.ac.uk/projects/trim_galore/
WPS Office	KINGSOFT Office, Beijing, China
UCSC Genome Browser	[168] http://genome.ucsc.edu/

Continued on next page

Table 2.10 – *continued from previous page*

Software, tool	Provider/ reference
limma package (R-package)	[169]
Inkscape 0.92.4	https://inkscape.org/

2.1.10 Next-generation sequencing data sets

All utilized next-generation sequencing data sets were download from GEO database [156].

TABLE 2.11 Utilized publicly available next-generation sequencing datasets

Dataset name	GEO ID	Series	Experiment
naive macrophages	GSM2262901	GSE85243	RNA-seq
naive macrophages	GSM2262902	GSE85243	RNA-seq
LPS stimulated macrophages	GSM2262906	GSE85243	RNA-seq
LPS stimulated macrophages	GSM2262907	GSE85243	RNA-seq
naive macrophages	GSM2679941	GSE100382	RNA-seq
naive macrophages	GSM2679942	GSE100382	RNA-seq
LPS stimulated macrophages	GSM2679944	GSE100382	RNA-seq
LPS stimulated macrophages	GSM2679945	GSE100382	RNA-seq
naive macrophages	GSM2262949	GSE85245	H3K27ac ChIP-seq
LPS stimulated macrophages	GSM2262992	GSE85245	H3K27ac ChIP-seq
naive macrophages	GSM2679933	GSE100381	H3K27ac ChIP-seq
LPS stimulated macrophages	GSM2679934	GSE100381	H3K27ac ChIP-seq

2.2 Methods

2.2.1 Cell culture methods

Isolation and cultivation of primary human macrophages

Human peripheral blood monocytes were isolated from buffy coats as described in Kopp et al. [145]. Cells were cultured in RPMI1640 containing 20 % autologous serum at 37 ℃ and 5 % CO_2 atmosphere. The medium was changed every three days until cells were differentiated into macrophages after 7 days. Macrophages were used for infection 1-2 weeks after the isolation.

Incubation with MAPK inhibitors

For MAPK pathway inhibition combination of 5 µM SB203580 (Cayman Chemical, USA) and PD98059 (Merck Millipore, USA), which target p38 and MEK1 respectively, was used. Inhibitors were added to macrophages 30-60 min before the infection for 6 h. For 3 h infection, 10 µM of inhibitors were used.

2.2.2 Microbiological methods

Conservation of bacteria

Glycerol stocks were prepared for long term storage of bacteria. For this LB medium containing 40 % (w/v) glycerol was mixed with the same amount of liquid bacterial culture from the exponential growth phase (OD_{600} = 0.3-0.6). The mixture was frozen in liquid nitrogen and transferred to -80 °C for long time storage.

Yersinia infection

On the day before the infection of primary human macrophages the cell medium was changed to RPMI1640 without antibiotics and serum and *Yersinia* precultures were grown overnight in LB medium with appropriate antibiotics at 27 °C and 200 x rpm. On the day of infection precultures were diluted 1:20 in fresh LB medium without antibiotics and incubated for 90 min at 37 °C and 200 x rpm to induce activation of the *Yersinia* T3SS machinery and Yop expression. Afterwards bacteria were pelleted by centrifugation for 10 min at 6000 x *g* and 4 °C and resuspended in 1 ml ice-cold PBS containing 1 mM $MgCl_2$ and $CaCl_2$. The optical density OD_{600} was adjusted to 3.6 and afterwards macrophages were infected at multiplicity-of-infection (MOI) of 100. Cell culture dishes were centrifuged for 2 min at RT and 200 x *g* to sediment bacteria on the cells and synchronize infection. Cells were incubated at 37 °C for an infection time depending on the experiment.

2.2.3 Chromatin immunoprecipitation (ChIP)

ChIP allows analyses of protein target binding sites to chromatin (see Figure 1.2). Initially cells are exposed to a crosslinker to fix interactions at the chromatin. Afterwards cells are lysed, nuclei are isolated and chromatin is fragmented to a size of about 200-500 bp, which constitutes to 1-3 nucleosomes. ChIP is performed by incubating fragmented chromatin with an antibody against a protein of interest, thus isolating target protein and bound DNA fragments. DNA is purified from the ChIP elution fraction and can be used to determine genomic distribution of target protein at selected loci by ChIP-quantitative real-time polymerase chain reaction (qPCR) or genome-wide by ChIP-sequencing (ChIP-seq) which employs next-generation sequencing (NGS).

In this work, distribution of modified histones, namely, H3K4me3, H3K27me3, H3K4me1 and H3K27ac was analysed by ChIP-seq. H3K4me3, H3K27me3, H3K4me1 and H3K27ac were selected because of their well-established role in regulation of gene expression and important function in macrophages [125, 128, 130, 170, 171]. H3K4me3 marks active promoters, H3K27me3 is found at repressed promoters and enhancers, H3K27ac marks active promoters and enhancers and H3K4me1 is characteristic for enhancers.

For the ChIP, macrophages (~3-10 x 10^6 cells per condition) were washed once with warm PBS and incubated for 30 min at 37 °C with accutase (eBioscience, USA) to detach the cells. The following ChIP steps were performed as described in [172], except that BSA-blocked ChIP grade protein A/G magnetic beads (Thermo Fisher Scientific, USA) were

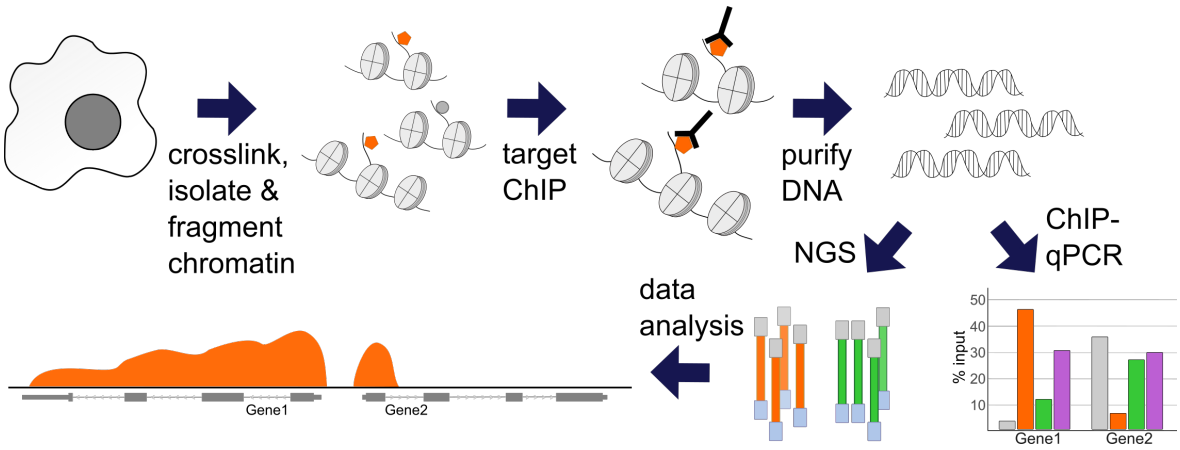

FIGURE 2.1: **ChIP workflow.** Cells are crosslinked, followed by isolation and fragmentation of the chromatin. An antibody against the target (here histone modification) is used to isolate target bound to associated DNA region (target ChIP). DNA is purified and used for ChIP-qPCR to analyse target enrichment at specific genomic locations or for NGS to map target distribution genome-wide.

added to the chromatin and antibody mixture and incubated for 2 h at 4 ℃ rotating to bind chromatin-antibody complexes. Samples were incubated for ~3 min with a magnetic stand to ensure attachment of beads to the magnet and mixed by pipetting during the wash steps. Eluted DNA was either subjected to ChIP-seq library preparation (section 2.2.5) or used for ChIP-qPCR experiments (section 2.2.4). Input chromatin DNA was prepared from 1/4 of chromatin amount used for ChIP.

2.2.4 Molecular biology methods

Agarose gel electrophoresis

Agarose gel electrophoresis was used to analyse DNA fragment size of sheared chromatin during ChIP protocol (section 2.2.3). 1.5 % w/v agarose gel was prepared in 1 x TAE buffer and RedSAFE (Intron Biotechnology, Korea) to enable visualization of DNA fragments. 200 ng of purified chromatin DNA was mixed with the loading dye (10 x FastDigest Green Buffer, Thermo Fisher Scientific, USA) and loaded in the wells. DNA ladder O'GeneRuler DNA Ladder, Ready-to-Use 50-1000 bp (Thermo Fisher Scientific, USA) was loaded to determine the size of DNA fragments. The gel was run at 100 V until the dye line was ~75-80 % of the way down the gel. DNA fragments were visualized using UV light on a Transilluminator (Bio-Rad, USA).

Measurement of DNA concentration after ChIP

Concentration of dsDNA in input and ChIP samples after DNA recovery (section 2.2.3) was measured using Qubit Fluorometer (Thermo Fisher Scientific, USA) and Qubit dsDNA HS Assaykit (Thermo Fisher Scientific, USA) following manufacturer's instructions.

Quantitative real-time polymerase chain reaction (qPCR)

The qPCR method was applied to confirm successful ChIP experiments (section 2.2.3) and monitor histone modification changes during infection using the Maxima SYBR Green/ROX qPCR Master Mix kit (Thermo Fisher Scientific, USA). Reaction volumes are listed in Table 2.12 and cycling conditions are listed in Table 2.13. SYBR Green dye emits fluorescence when bound to dsDNA, therefore DNA amplification can be measured in real-time by detecting changes in emitted fluorescence.

Primers were designed using PRIMER-Blast tool [162] with the optimal melting temperature of 60 ℃ and template length between 55 and 200 bp. For all primer pairs input chromatin DNA (section 2.2.3) was used to generate standard curves and verify amplification efficiency between 90-100 %. The specificity of primers was confirmed using reaction without a DNA template and melting curve analysis of PCR products.

qPCR was performed on a Rotorgene 6000 qPCR machine (Qiagen, Germany) and analysed with the Rotor-Gene 6000 software (Qiagen, Germany). A gain optimization was carried out at the beginning of the run. SYBR green fluorescence was recorded during elongation. After completion of the run, a melting curve analysis was performed.

Concentration of ChIP and input material was calculated based on the standard curve. To confirm successful ChIP experiment, ChIP enrichment was expressed as % input and calculated as follows: *ChIP DNA concentration/ input DNA concentration * 100 %*. In order to compare changes in enrichment at specific regions between different conditions, normalization was done with at least 2 selected control regions which did not show change in histone modifications during infection (section 2.1.7). This strategy was chosen because ChIP-qPCR and ChIP-seq experiments showed bias in ChIP efficiency (section 2.2.6). Specifically, the presence of bacterial material in the sample resulted in lower background (Figure 2.2) and higher enrichment in ChIP-seq.

TABLE 2.12 SYBR Green qPCR reaction setup

Component	**Amount**
2 x Maxima SYBR Green/ROX qPCR Master Mix	5 µL
Primer forward (10 µM)	0.3 µL
Primer reverse (10 µM)	0.3 µL
Template DNA	1.5 µL
H2O	up to 10 µL

TABLE 2.13 Cycling parameters for SYBR green qPCR

Number of cycles	**Temperature**	**Time**
1	95 ℃	10 min
40	95 ℃ 57 ℃ or 60 ℃ 72 ℃	15 s 30 s 30 s
1	70 ℃ to 95 ℃	

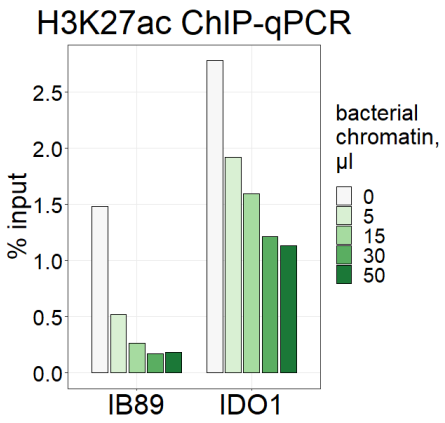

FIGURE 2.2: **H3K27ac ChIP-qPCR testing effect of addition of bacterial chromatin** Chromatin from mock was sheared and 0-50 µl of *Y. enterocolitica* sheared chromatin was added before H3K27ac ChIP. ChIP-qPCR was performed with mock background regions. It was evident that addition of bacterial chromatin reduces unspecific binding in the background.

Isolation of total RNA from eukaryotic cells

Total RNA of ~1-2 x 10^6 human macrophages was isolated using RNeasy extraction kit (Qiagen, Germany) including DNAse treatment according to manufacturer's instructions.

2.2.5 Next-generation sequencing

RNA sequencing (RNA-seq)

After isolation of total RNA (section 2.2.4) the RNA integrity was analysed with the RNA 6000 Nano Chip (Agilent Technologies, USA) on an Agilent 2100 Bioanalyzer (Agilent Technologies, USA). mRNA was extracted using the NEBNext Poly(A) mRNA Magnetic Isolation module (New England Biolabs, USA) and RNA-seq libraries were generated using the NEBNext Ultra RNA Library Prep Kit for Illumina (New England Biolabs, USA) as per the manufacturer's recommendations. Concentrations of all samples were measured with a Qubit 2.0 Fluorometer (Thermo Fisher Scientific, USA) and fragment lengths distribution of the final libraries was analysed with the DNA High Sensitivity Chip (Agilent Technologies, USA) on an Agilent 2100 Bioanalyzer (Agilent Technologies, USA). All samples were normalized to 2 nM and pooled equimolar. The library pool was sequenced on the NextSeq500 (Illumina, USA) with 1 x 75 bp and total ~19.9 to 23.8 million reads per sample.

ChIP-seq

ChIP-seq libraries were constructed with 1-10 ng of ChIP DNA or input control as a starting material. Libraries were generated using the NEXTflex™ ChIP-Seq Kit (Bioo Scientific, USA) as per manufacturer's recommendations. Concentrations of all samples were measured with a Qubit Fluorometer (Thermo Fisher Scientific, USA) and fragment length distribution of the final libraries was analysed with the DNA High Sensitivity Chip on an Agilent 2100 Bioanalyzer (Agilent Technologies, USA). All samples were normalized to 2 nM and pooled equimolar. The library pool was sequenced on the NextSeq500 (Illumina, USA) with 1 x 75 bp and total ~18.6 to 41 million reads per sample.

2.2.6 Bioinformatic data analysis

Conversion of publicly available data sets

Data sets were downloaded from the GEO database [156] as SRA files. Conversion process was done with SRA Toolkit program (http://ncbi.github.io/sra-tools/) following the manufacturer's instructions.

Quality control and trimming

FastQC program (http://www.bioinformatics.babraham.ac.uk/projects/fastqc) was used for quality control of FASTQ files, which contain the sequence data from the clusters that pass the filter on a flow cell. Sequencing reads containing bases with low quality scores (quality Phred score cutoff 20) or adapters were trimmed using TrimGalore program (http://www.bioinformatics.babraham.ac.uk/projects/trim_galore/).

ChIP-seq

Alignment to reference genome BWA program [147] was used to align reads from FASTQ files to hg19 human reference genome. Samtools [165] was used for manipulations (e.g. sorting, indexing, conversions) of the sequencing files. Picard (https://broadinstitute.github.io/picard/) was used for duplicate read removal. BEDTools [146] was used for generation of BED files. The following command was used for the alignment to hg19:

bwa mem -M <reference genome> <ChIP-seqfile.fastq> | samtools view -bT <reference genome> | samtools view -b -q 30 -F 4 -F 256 > <aligned-ChIP-seq-file.bam>

With this command BWA maps reads to the reference genome marking shorter split hits as secondary for Picard compatibility (*-M*) and samtools generates a BAM file (*-b*) skipping alignments with mapping quality less than 30 (*-q*), filtering out unmapped reads (*-F 4*) and secondary reads (*-F 256*).

Peak calling Peak calling was used to find regions with enrichment of target histone modifications on the genome over background. In this work, MACS2 peak calling [160] was used for H3K4me3 and H3K27ac which generally are narrowly distributed marks. MACS2 peaks were called against input control with *-q 0.01* parameter, which is minimum false discovery rate (FDR) cutoff. SICER peak calling [166] was used for H3K4me1 and H3K27me3 which are generally broad marks. With SICER the enrichment in ChIP samples was determined against input controls with default settings. SICER peaks were filtered for ChIP enrichment over background for fold change (FC) >2.

Peak merging and filtering BEDTools [146] was used for analysing overlaps between regions and merging regions of BED files. To generate a pooled peak file for each histone mark, overlapping peaks from replicates of each condition were merged and selected, thus excluding peaks appearing only in one replicate. Afterwards peaks from different conditions were merged together to form a file with all enriched regions for each histone modification

("all peak file"). Files were filtered to exclude blacklist regions [173], which are sequencing artefacts in NGS experiments.

Data normalization After normalization of ChIP-seq data based on sequencing depth, it was noticeable that infected cells (WAC- or WA314-treated) showed higher signal in peak regions and lower signal in background regions globally for all histone modifications when compared to mock. This kind of result has not been seen in macrophages [131, 140] and was unexpected, thus pointing to a bias in the data. Concentration measurement of input samples showed that infected cells have large amounts of bacterial DNA present. ChIP-qPCR showed that addition of *Yersinia* chromatin results in lower background (see Figure 2.2), indicating an efficiency bias where in ChIP-seq mock samples have higher proportion of the reads in the background than infected samples.

Csaw package [148] in R was employed to normalize for efficiency bias in ChIP-seq data. For determining the read counts across windows, window width of 150 (*width*), distance between consecutive windows of 100 (*spacing*), minimum mapping quality score of 50 (*minq*) and fragment length of 210 (*ext*) were used. The TMM (trimmed mean of M-values) method [174] was applied to eliminate systematic differences across windows with high-abundance of reads assuming that most binding sites in the genome are not differential binding sites. Calculated normalization factors were used to obtain the effective library size (bias-corrected library size), detect differential binding analysis (section 2.2.6), quantify tag counts (section 2.2.6) and generate figures and BigWig files (section 2.2.6).

BigWig file generation DeepTools [151] tool bamCoverage was used to convert BAM files into bigWig files for viewing ChIP-seq tracks in Integrative Genomics Viewer (IGV) [159]. Files were scaled using csaw normalization coefficients (section 2.2.6) using *–scaleFactor* option.

Identification of differential regions (DRs) DiffReps [153] with csaw normalization coefficients (section 2.2.6) was used to identify DRs of histone modifications between various conditions. DiffReps uses a sliding window to scan the genome in a fixed step size and identifies windows that show significant read count differences. For H3K4me1 and H3K27me3 *–nsd broad* parameter was used, which adjusts filtering of windows for broads peaks.

Accuracy of differential binding sites was examined in IGV. Significant DRs with log2 FC >1 and adjusted P-value <0.05 were filtered. Regions were further filtered to exclude regions that do not overlap MACS2 or SICER peaks from "all peak file" (section 2.2.6) and blacklist regions. Because some DRs still appeared to be in the background, regions with low read counts (less than 20 for any replicate in the enriched condition; less than 20 in the enriched condition for H3K4me3) were excluded. Additionally, for H3K27me3 regions with length less than 1700 bp were excluded as smaller regions appeared to be false positives. All filtered DRs for comparisons between mock, WAC and WA314 for each histone modification were pooled together and overlapping regions merged to generate "all changed regions file".

Classification and annotation of regions Promoter coordinates of ±2 kb from TSS and associated gene annotations were extracted from RefSeq hg19 gene annotations in UCSC Genome Browser [168] using EaSeq [154]. Regions overlapping promoter coordinates were defined as regions at promoters and annotated with associated genes, therefore one region could be annotated with multiple genes. Regions that did not overlap promoters were analysed for overlap with H3K4me1 regions to assign regions to enhancers. Enhancer regions were annotated to the closest gene in EaSeq. The remaining regions were classified as "undefined".

For the identification of "dynamic" and "constant" peak regions, peaks from "all peak files" for each histone modification were intersected with DRs from "all changed regions files" from diffReps using BEDTools [146]. Peaks intersecting any DR were defined as "dynamic regions", whereas the rest of the peaks were termed "constant regions".

Quantification of tag counts Raw counts for regions of interest were quantified in EaSeq [154]. Counts were normalized using effective library size derived from csaw normalization coefficients (section 2.2.6) to obtain normalized reads/kb with the formula: *(1+raw counts)/(effective library size/10^6)/bp per kb*. Normalized counts were used for visualization, clustering and to confirm reproducibility between replicates with principal component analysis (PCA) and correlation plots in R.

Clustering analysis Clustering of normalized tag counts at target regions was performed with R function heatmap.2. For H3K4me3 and H3K27ac promoter heatmap, regions from "all changed regions files" for H3K4me3 and H3K27ac that intersected promoter coordinates were used. For H3K27ac heatmap at enhancers, regions from "all changed regions file" that did not overlap promoters but overlapped H3K4me1 were used. For H3K4me3 promoter heatmap clustering distance based on Pearson correlation and Complete clustering method were used. For H3K27ac promoter heatmap only regions which did not overlap regions in H3K4me3 promoter heatmap were used for clustering. Clustering for H3K27ac promoter and enhancer heatmaps was performed with clustering distance based on Spearman correlation and Average clustering method. Clustering distance, clustering method and number of clusters were selected so that all meaningful clusters were identified by the analysis. Clusters were further assembled into classes based on the pattern of histone modifications across conditions.

Comparison to public data Spearman correlation heatmap was generated with H3K27ac tag counts from regions in H3K27ac "all peak file" using data generated here and publicly available data from LPS-treated and naive macrophages (section 2.1.10). Tag counts for the public data were normalized with csaw coefficients for efficiency bias; normalization to the library size gave the same results. Batch effect between different data sets was removed using limma package [169].

Analysis of latent enhancers Latent enhancers were defined as sites with H3K4me1 signal increase outside promoters without pre-existing H3K4me1 signal. To find latent enhancers for WAC/WA314 vs mock up, H3K4me1 DRs outside promoters were intersected with all H3K4me1 peaks in mock (pooled peaks from both replicates merging overlapping peaks). If there was no intersection, the H3K4me1 change was defined as taking place at latent enhancers.

RNA-seq

Read alignment Reads were aligned to the human reference assembly hg19 using STAR [167]. FeatureCounts [155] was employed to obtain the number of reads mapping to each gene.

Analysis of differentially expressed genes (DEGs) Statistical analysis of differential expression was carried out with DESeq2 [152] using raw counts as an input and the experimental design *~batch + condition*. Significantly enriched genes were defined with log2 FC >1 and adjusted P-value <0.05. Normalized rlog counts for each gene were obtained after batch effect removal with limma package [169] and used for downstream analysis and visualization. Reproducibility between replicates was confirmed by PCA analysis and sample distance heatmaps.

Clustering analysis and heatmaps Clustering analysis of all DEGs from comparisons between mock, WAC, WA314 at 1.5 h and 6 h was done with rlog counts in R with pheatmap package. Clustering was performed with clustering distance based on Pearson correlation and Ward.D2 clustering method. Clustering distance, clustering method and number of clusters were selected so that all meaningful clusters were identified by the analysis. For RNA-seq heatmaps rlog counts from DESeq2 analysis were scaled by row (row Z-score) and low to high expression levels are indicated by blue-white-red color gradient. 2 representative replicates were shown for each sample.

Comparison to public data Public expression data sets were analysed as described above. Batch effect was observed when rlog counts from public data and data in this study were compared. To make datasets comparable rlog counts of all DEGs from this study were converted to Z-scores and used to generate a dendrogram of sample distances based on Spearman correlation and Complete clustering method.

Analysis of association between ChIP-seq and RNA-seq

Gene lists from RNA-seq and ChIP-seq were compared based on gene symbols to find the number of overlapping genes and determine how many genes showed associated epigenetic and gene expression changes. In some cases old gene symbols were used in the RNA-seq lists, therefore they did not match the symbols in ChIP-seq lists for which RefSeq annotation from UCSC with new symbols was used. All old symbols in RNA-seq lists, which

did not have a matching symbol in RefSeq annotation, were replaced with the new symbol using Multi-symbol checker tool [161].

Relative overlap was calculated to express overlap of genes between ChIP-seq and RNA-seq classes. Relative overlap was obtained by dividing the number of overlapping genes from two input classes with the total number of genes from the first input class and then with total number of genes from the second input class, thus normalizing the overlap for the number of input genes.

Pathway analysis

Gene Ontology (GO) and Kyoto Encyclopedia of Genes and Genomes (KEGG) terms were determined for RNA-seq and ChIP-seq gene lists by using DAVID webtool [149, 150].

Transcription factor (TF) motif enrichment analysis

TF motif enrichment for known motifs was performed using HOMER package [158]. Command *findMotifsGenome.pl* was used and a list of genomic coordinates was supplied as an input; the exact size of supplied regions was used by setting parameter *-size given*.

Boxplot

Boxplots were generated using ggplot2 in R. Boxes encompass the twenty-fifth to seventy-fifth percentile changes. Whiskers extend to the tenth and ninetieth percentiles. Outliers are depicted with black dots. The central horizontal bar indicates the median.

Calculation of percentage YopP effect

Percentage YopP effect was calculated as ratio of FC between WA314ΔYopP vs WA314 and WAC vs WA314 (Suppression and Prevention) or WA314 vs mock (Up and Down). % YopP effect was presented (Figure 3.13, Tables 6.6 and 6.5) for individual strongly WA314-regulated genes and regions from inflammatory response and Rho GTPase pathway, which associated with gene expression and histone modifications changes in Suppression and Prevention profiles. Specifically, only genes and regions were selected, which overlapped WAC vs WA314 DEGs and DRs, respectively. Normalized tag counts were calculated for the target regions and used to obtain FC.

Rho GTPase pathway gene analysis

The target gene list with 534 Rho GTPase pathway genes was compiled from publicly available data and included 370 effectors binding GTP-Rho GTPases [175–177], 66 GAPs, 77 GEFs [178] and 23 Rho GTPases [179, 180]. In Senoo et al. [180] the list of human Rho GTPases was from the supplementary material. The list of genes does not match the list of genes including activities (534 vs 536) as some genes possess multiple activities.

3 Results

3.1 Transcriptome analysis of *Y. enterocolitica* infected primary human macrophages

3.1.1 T3SS effectors modulate gene expression induced by bacterial PAMPs

Until now, a systematic and comprehensive analysis of how gene expression in human macrophages is modulated by the *Yersinia* virulence factors is missing. Therefore, a global transcriptome analysis of in vitro differentiated primary human macrophages mock-infected or infected with *Y. enterocolitica* wild type strain WA314 or its avirulent derivative WAC for 1.5 and 6 h was performed (Figure 3.1A). The T3SS is absent in WAC (see section 2.1.8) and therefore WAC served to distinguish the effects of the *Yersinia* PAMPs from the effects of the T3SS effectors. Total RNA of the uninfected or infected macrophages was isolated and subjected to RNA-seq (Figure 3.1A). PCA confirmed high reproducibility between replicates (Figure 3.1B). Moreover, there was a clustering of samples infected for 1.5 h and mock, whereas samples infected for 6 h clustered distinctly (Figure 3.1B), indicating the main alterations of gene expression after 6 h of infection.

Next, we analysed the number of significantly differentially expressed genes (DEGs; fold change >2, adjusted P-value <0.05) in pairwise comparisons between mock, WAC and WA314 at 1.5 and 6 h. 6329 DEGs were identified when taking all comparisons together (Figure 3.1C, 3.2A). WAC upregulated 603 genes vs mock at 1.5 h, indicating early inflammatory response to the *Y. enterocolitica* PAMPs (Figure 3.1C). In comparison, 55 genes were induced by WAC vs WA314 (Figure 3.1C) of which 54 were also upregulated by WAC vs mock (Figure 6.1A), reflecting early suppression of PAMP-induced transcription by WA314. In contrast, 137 genes were downregulated by WAC vs mock of which 1 was also downregulated by WAC vs WA314, indicating no prevention of PAMP-induced downregulation by WA314 (Figures 3.1C, 6.1B).

At 6 h of infection WAC and WA314 vs mock induced 5 and 4 times more genes and downregulated 16 and 4 times more genes, respectively, than at 1.5 h of infection (Figure 3.1C). This is in line with the PCA (Figure 3.1B) showing the main changes in gene expression at 6 h of infection. WA314 suppressed late induction of genes by WAC as 1278 (42 %) of the 3020 genes upregulated by WAC vs mock were also upregulated by WAC vs WA314 (Figure 3.1D). At 6 h of infection WA314 prevented late downregulation of genes by WAC as 834 (39 %) of the 2152 genes downregulated by WAC vs mock were also downregulated by WAC vs WA314 (Figure 3.1E). Therefore, virulence factors of WA314 counteract transcriptional changes induced by the PAMPs of *Yersinia*.

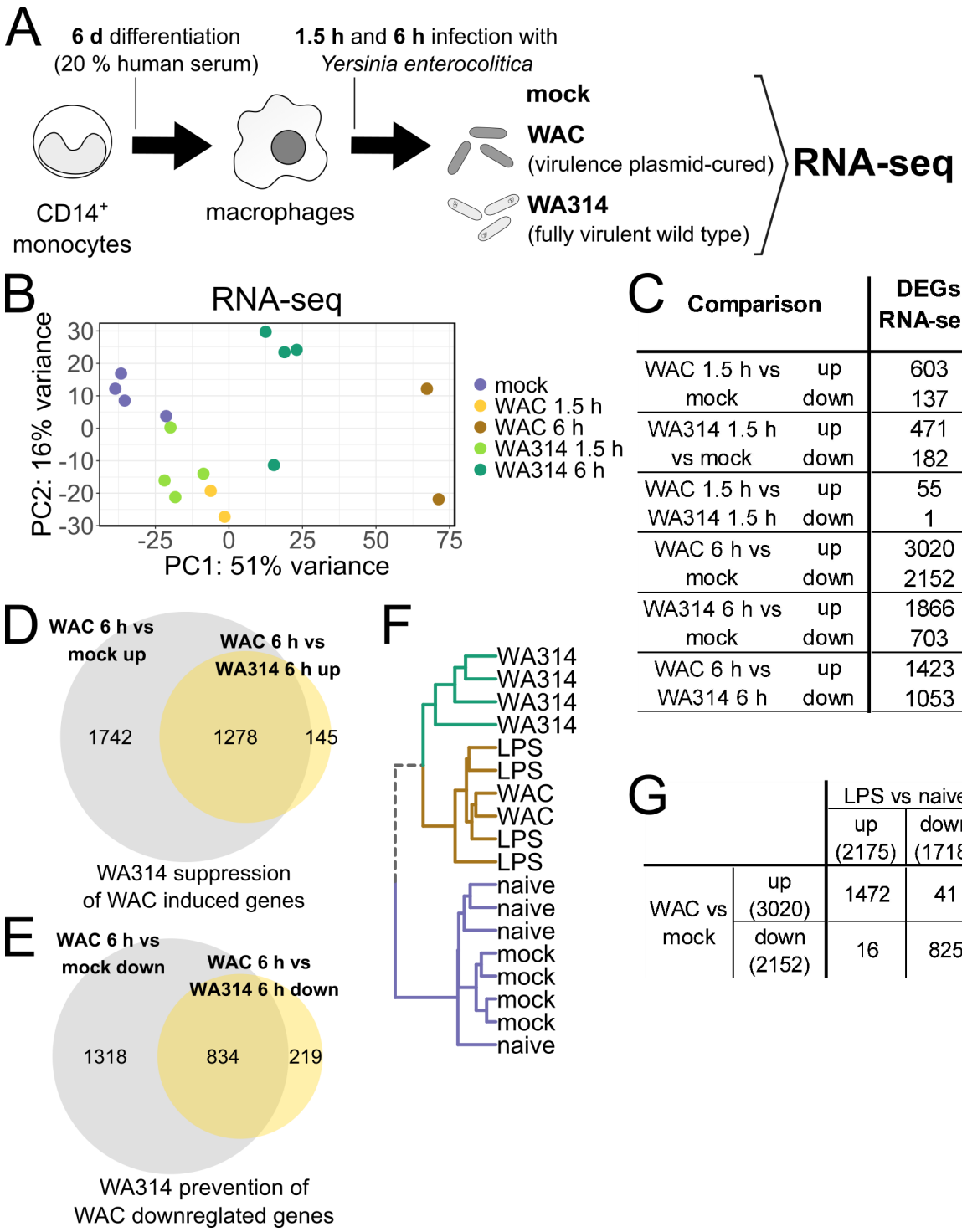

FIGURE 3.1: **PAMP induced gene expression is counteracted by *Yersinia* virulence factors. (A)** Experimental design. CD14$^+$ monocytes were isolated from fresh buffy coats and differentiated into macrophages with 20 % human serum for 6 days. Macrophages at least from two independent donors were infected with *Yersinia enterocolitica* strains WAC, WA314 or mock-infected for 1.5 h and 6 h and samples were subjected to RNA-seq. **(B)** PCA of RNA-seq rlog gene counts for each sample replicate used in the analysis. 1000 genes with the highest row variance were used for plotting. **(C)** Number of RNA-seq DEGs (log2 FC >1 and adjusted P-value <0.05) for comparisons between mock, WAC and WA314 at 1.5 h and 6 h identified by DESeq2 analysis. **(D, E)** Venn diagrams of DEG overlaps. **(F)** Dendrogram of RNA-seq data from *Yersinia*-infected and mock macrophages and public datasets of LPS-treated and naive macrophages. DEGs from **(C)** were used for the analysis. **(G)** Number of overlapping DEGs between WAC 6 h vs mock and LPS vs naive macrophages from publicly available datasets. Numbers in the brackets indicate the total number of DEGs for each comparison.

We investigated whether LPS contributes as a PAMP in *Yersinia* triggering gene expression changes in macrophages. For this publicly available RNA-seq datasets from LPS-treated primary human macrophages [131, 140] were compared to the data from this study. Hierarchical clustering of sample distances based on Spearman correlation showed three distinct groups: i) WAC and LPS; ii) WA314 and iii) naive macrophages and mock (Figure 3.1F). Moreover, 49 % and 38 % of the genes that were up- or downregulated by WAC vs mock, were accordingly regulated by LPS vs naive macrophages (Figure 3.1G). Overall, these data suggest LPS as one of the main PAMPs in *Yersinia* inducing transcriptional changes which are counteracted by the T3SS effectors of WA314.

3.1.2 Expression changes associate with distinct profiles of regulation and biological pathways

In order to visualize patterns/profiles of gene expression and relate them to biological pathways a heatmap of all DEGs between mock-, WAC- and WA314-infected cells (see Figure 3.1C) was created. By clustering analysis the DEGs were grouped into four classes R1-R4 (color coded in Figure 3.2A), which showed distinct patterns of gene expression. In classes R1 and R2 WAC upregulated gene expression and this was suppressed by WA314 (Figure 3.2A), which was assigned to the profile “Suppression”. The temporal dynamics of suppression were distinct in R1 and R2. Class R1 represented early (at 1.5 h) suppressed genes that were also suppressed late (at 6 h) and class R2 included late suppressed genes (Figure 3.2A). Class R3 genes showed generally the highest expression levels in WA314-infected cells after 6 h and this profile was named “Up” (Figure 3.2A). In class R4 WA314 prevented the downregulation of genes by WAC (Figure 3.2A), therefore this profile was termed “Prevention”. WA314 clearly opposed the PAMP-induced up- or downregulation of genes as ~90 % of DEGs belonged to Suppression and Prevention profiles (Figure 3.2A). However, for many genes expression levels of WA314-infected cells were in between mock- and WAC-infected cells reflecting incomplete counteraction (Figure 3.2A: R2 and R4 classes).

Genes of the different profiles and classes were enriched in distinct Gene Ontology (GO) terms (Figure 3.2C). The early and late suppressed genes (class R1, green code) were enriched in immune and LPS response genes (Figure 3.2C) as shown with the pro-inflammatory cytokine TNF, which is rapidly induced upon TLR4 activation (Figure 3.2B) [117]. In comparison, the late suppressed genes in class R2 (orange coding) were enriched for protein polyubiquitination, antiviral response and type I IFN signalling (Figure 3.2C). These genes contain several ISGs with myxovirus resistance 2 (MX2) shown as an example gene (Figure 3.2B). ISGs are secondary response genes in LPS signalling and are induced by autocrine/paracrine IFNα/β signalling [181]. Profile “Up” (class R3) was enriched in cilium morphogenesis and Wnt signalling (Figure 3.2C) with the Wnt receptor component frizzled class receptor 4 (FZD4) shown as a representative gene (Figure 3.2B) [182]. Wnt signalling directs macrophage differentiation, regulates phagocytosis and mediates expression of anti-inflammatory mediators IL-10 and TGF-β via induction of β-catenin nuclear translocation [182]. Genes in profile Prevention (R4) were enriched in DNA replication, repair and transcription and metabolic regulation (Figure 3.2C), such as steroid biosynthesis,

fatty acid and lipid metabolism, Krebs cycle (isocitrate dehydrogenase 1 (IDH1) and aconitase 2 (ACO2)), N-Glycan biosynthesis and t-RNA biosynthesis (Table 6.1). This data suggests that *Yersinia* modulates metabolic reprogramming in macrophages which is induced by PAMP signalling [183]. Interestingly, 8 % (212) of the genes in R4 belong to C2H2 domain zinc-finger genes (ZNFs), as illustrated by ZNF519 (Figure 3.2B), which encode mainly transcriptional repressors associated with heterochromatin [184–186]. Suppression (class R1 and R2) and Up (class R3) profiles were also enriched for distinct transcriptional regulators (Figure 3.2C). Suppression profile contained members of basic leucine zipper domain (bZIP), basic helix-loop-helix (bHLH), STAT (e.g., Stat1/6), rel homology domain (RHD), E26 transformation-specific (ETS) and IRF (e.g., IRF1/4/5) families [187]. In comparison, Up profile encompassed nuclear receptors (NRs) retinoic acid receptor gamma (RARG), peroxisome proliferator activated receptor alpha (PPARA) and nuclear receptor subfamily 1 group D member 1 (NR1D1) as well as C2H2 domain ZNFs KLF2, KLF12 and ikaros family zinc-finger 4 (IKZF4) [187, 188]. This data suggests a complex control of expression of transcriptional regulator networks by *Yersinia*. Notably, although primary human macrophages are post-mitotic and do not undergo cell division in vitro [189], Suppression (R1 and R2) and Prevention (R4) profiles were enriched in pathways involved in the cell cycle (Figure 3.2C). Suppression involved negative regulators of cell proliferation (CDKN1A, CDKN2A, RB1), whereas Prevention included positive regulators of cell-cycle (CDK1, MCM2, CCNE1 and E2F1) [190], suggesting that PAMP signalling during *Yersinia* infection downregulates processes associated with macrophage proliferation.

Overall, the T3SS-associated effectors of *Yersinia* extensively modulate gene transcriptional programs in human macrophages to counteract the *Yersinia* PAMP-induced regulation of inflammatory, metabolic, cell cycle and transcriptional regulator genes. Additionally, in the Up profile the *Yersinia* effectors directly modulate genes involved in Wnt signalling and transcription (Figure 3.2D).

3.2 *Yersinia* reprograms macrophage epigenome

3.2.1 Acetylation at enhancers is the most dynamic histone mark

Histone modifications play a key role in macrophage gene transcription during stimulation [107]. We wondered whether *Y. enterocolitica* coordinate reprogramming of gene transcription in macrophages through histone modifications. Macrophages were mock-infected or infected with WAC or WA314 for 6 h and subjected to ChIP-seq experiments (Figure 3.3A). Global epigenetic analyses were performed for four H3 marks: H3K4me3 marking active promoters; H3K4me1 marking enhancers; H3K27ac marking active promoters and enhancers; and H3K27me3 marking inactive promoters and enhancers [125, 128, 170, 171]. Altogether, 7 %, 3 %, 43 % and 0.1 % of the H3K4me3, H3K4me1, H3K27ac and H3K27me3 regions (MACS2 or SICER peaks), respectively, were dynamic between at least 2 conditions: mock, WA314 or WAC; Figure 3.3B). Of all dynamic histone marks, roughly 55 % of the H3K4me3, 52 % of the H3K4me1, 24 % of the H3K27ac and 50 % of the H3K27me3 regions were at promoters (±2 kb from TSS; Figure 3.3C). Furthermore, roughly 44 % of the H3K4me3, 48 % of

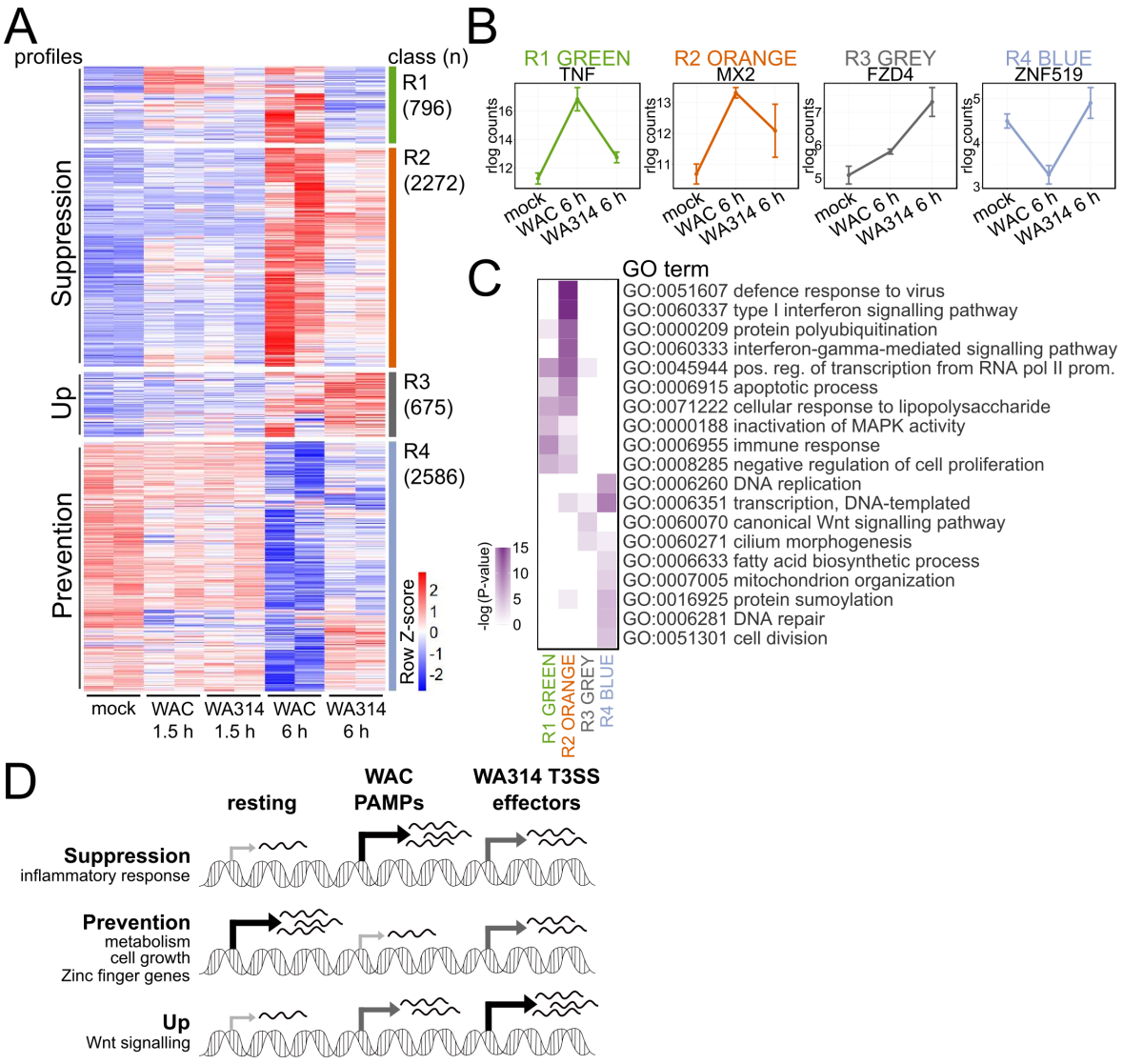

FIGURE 3.2: **Clustering and GO analysis of DEGs. (A)** Heatmap from clustering of all DEGs from mock, WAC and WA314 comparisons at 1.5 and 6 h. Clustering identified 4 major classes R1-R4 (color coded, right side) where (n) is the number of genes in each class. Profiles describing relation of expression levels between mock, WAC and WA314 are indicated on the left. Rlog counts of DEGs were row-scaled (row Z-score). **(B)** Line plots of mean rlog counts of representative genes from R1-R4 in **(A)** depicting gene expression profile of each class. Error bars represent standard deviation (SD). **(C)** Heatmap showing log10 transformed P-values and enriched GO terms for each class in **(A)**. Darker color indicates lower P-value and higher significance of enrichment. **(D)** Scheme summarizing the effect of *Yersinia* on gene expression in macrophages.

the H3K4me1, 73 % of the H3K27ac and 33 % of the H3K27me3 regions were at enhancers (H3K4me1-enriched regions outside promoters; Figure 3.3C). Overall histone modification changes in *Yersinia*-infected macrophages occurred at promoters of 6228 genes and at enhancers of 7730 genes in total encompassing 10994 unique genes (Figure 3.3D). These results suggest a large scale epigenetic reprogramming of macrophages during *Yersinia* infection.

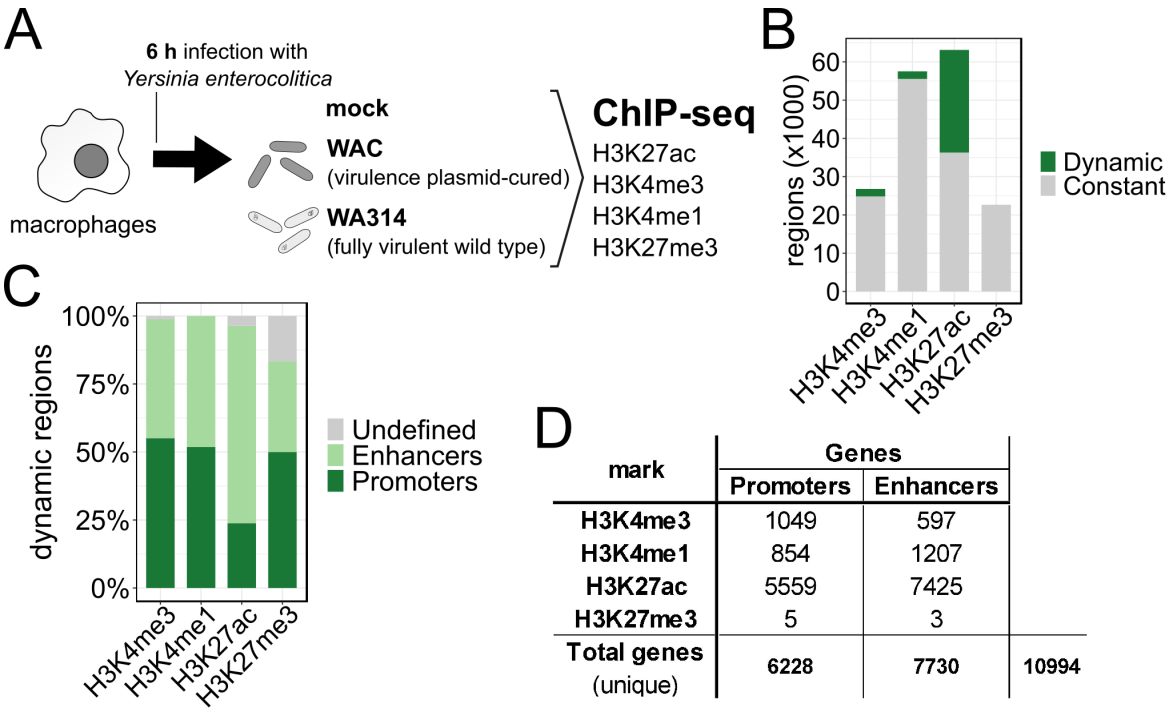

mark	Genes	
	Promoters	Enhancers
H3K4me3	1049	597
H3K4me1	854	1207
H3K27ac	5559	7425
H3K27me3	5	3
Total genes (unique)	6228	7730	10994

FIGURE 3.3: **Analysis of *Yersinia*-induced histone modifications. (A)** Experimental design. Primary human macrophages from at least two independent donors were infected with *Yersinia enterocolitica* strains WAC, WA314 or mock-infected for 6 h and samples were subjected to ChIP-seq for histone modifications H3K27ac, H3K4me3, H3K4me1 and H3K27me3. **(B)** Bar plot showing proportion of dynamic and constant regions from ChIP-seq for analysed histone marks during *Yersinia* infection. **(C)** Bar plot showing distribution of dynamic regions from **(B)** at gene promoters and enhancers. **(D)** Number of genes associated with differential regions (DRs) at promoters or enhancers for comparisons between mock, WAC and WA314 taken together for all histone marks.

3.2.2 *Yersinia* effectors suppress histone modifications induced by PAMPs

We analysed the number of differential regions (DRs) with significantly (diffReps FC >2, adjusted P-value <0.05) up- or downregulated histone marks in the pairwise comparisons between mock, WAC and WA314 (Table 3.1). Around 14-times more H3K27ac DRs than H3K4me3 DRs (22431 vs 1600; only unique regions counted) were detected (Table 3.1). For H3K4me1, there were 2156 unique DRs whereas H3K27me3 marks were essentially unchanged (Table 3.1), suggesting that they do not play a relevant role in the epigenetic reprogramming of macrophages by *Yersinia*.

Similar to what was found with gene expression (Figures 3.1D, E), WA314 blocked upregulation of 571 (53 %) of the H3K4me3 DRs induced by WAC vs mock (Figure 3.4A). Along this line, WA314 blocked 2881 (42 %) H3K27ac DRs from being upregulated (Figure 3.4B) and 2627 (40 %) H3K27ac DRs from being downregulated by WAC vs mock (Figure 3.4C). A Spearman correlation heatmap of the H3K27ac regions from Figure 3.3B and two public data sets of naive and LPS-treated macrophages [131, 140] showed a strong correlation within two groups: i) WAC-infected and LPS-treated macrophages; ii) mock-, WA314-infected and naive macrophages (Figure 3.4D). This data suggests that PAMPs of WAC induce epigenetic alterations mainly through its LPS and this is counteracted by WA314 to bring histone mark levels close to uninfected macrophages.

TABLE 3.1 Differential regions (DRs) and unique regions for the analysed histone marks

Comparison		H3K4me3	H3K4me1	H3K27ac	H3K27me3
WAC vs mock	up	1081	584	6902	0
	down	173	523	6650	3
WA314 vs mock	up	280	425	5057	1
	down	44	363	3600	3
WAC vs WA314	up	740	391	5464	1
	down	104	249	6687	6
Unique regions		1600	2156	22431	13

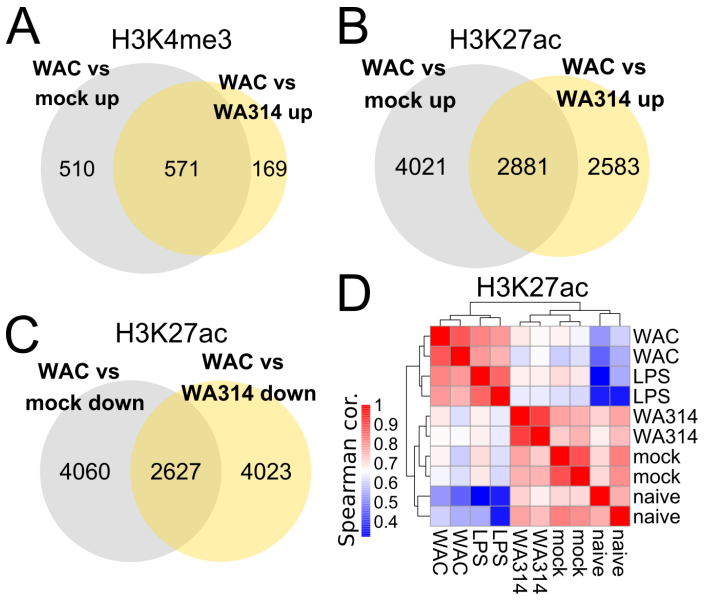

FIGURE 3.4: **Analysis of virulence factor modulation of PAMP-induced histone marks. (A-C)** Venn diagrams showing overlaps of differential regions (DRs) for H3K4me3 **(A)** and for H3K27ac **(B, C)**. **(D)** Heatmap showing Spearman correlation (cor.) of H3K27ac tag density at all H3K27ac regions from mock-, WAC- and WA314-infected samples and publicly available H3K27ac ChIP-seq data of naive and LPS treated macrophages. Low to high correlation is indicated by blue-white-red color scale.

3.3 Analysis of H3K4me3 and H3K27ac changes at promoters

3.3.1 Promoter H3K4me3 and H3K27ac show distinct profiles of regulation

The effect of *Y. enterocolitica* on active promoter marks H3K4me3 and H3K27ac at gene promoters was further evaluated. All promoter H3K27ac and H3K4me3 DRs of mock-, WAC- and WA314-infected macrophages were grouped in 10 clusters (color coded), which were assembled in 6 classes and 2 modules (Figure 3.5A). Promoter module 1 (P1; classes P1a and b) includes all H3K4me3 DRs and these regions generally show concordant H3K27ac changes (Figures 3.5A, B). In contrast, promoter module 2 (P2; classes P2a, b, c and d) contains all H3K27ac DRs with mainly unchanged H3K4me3 levels (Figures 3.5A, C). Notably, P1 and P2 promoter classes resembled the profiles of the transcriptional classes R1-R4 (see

Figure 3.2A). In class P1a and P2a, WAC induced histone marks and this was opposed by WA314, resembling a Suppression profile (Figures 3.5A-D). In P1b and P2d, WAC downregulated histone marks and this was counteracted by WA314, equalling a Prevention profile (Figures 3.5A-D). H3K27ac was selectively downregulated by WA314 in P2b in comparison to mock and WAC, therefore this profile was named “Down” (Figures 3.5A, C). In contrast, H3K27ac was selectively induced in P2c resembling Up profile (Figures 3.5A, C). The majority of the promoter H3K4me3 and H3K27ac DRs were associated with Suppression (P1a, P2a) and Prevention (P1b, P2d) profiles (Figure 3.5A), therefore *Y. enterocolitica* virulence factors mainly function to oppose PAMP-triggered histone modifications. Furthermore, modulation of H3K27ac marks in Down (P2b) and Up (P2c) profiles appears to be a specific activity of the T3SS effectors.

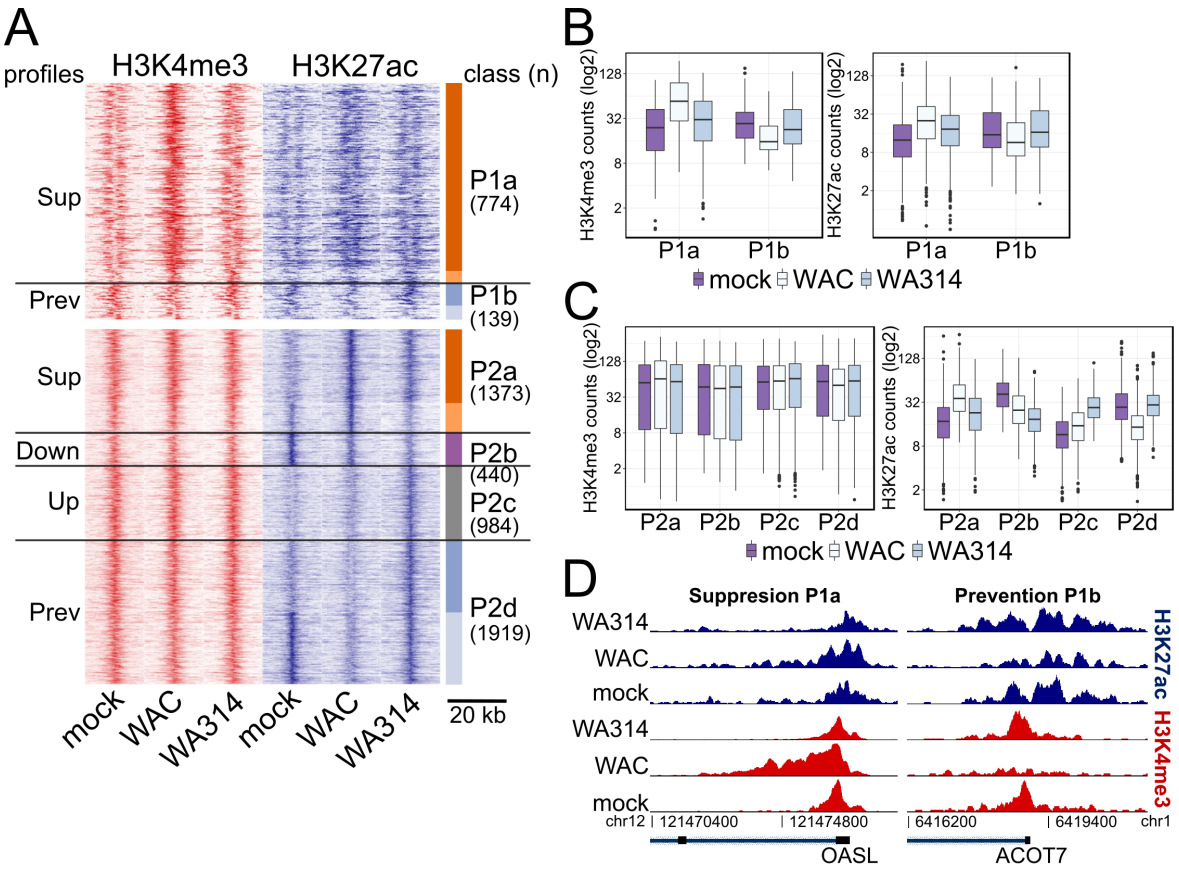

FIGURE 3.5: **Clustering of H3K4me3 and H3K27ac DRs at promoters. (A)** Heatmap showing clustering of H3K4me3 (upper part, module P1) and H3K27ac (lower part, module P2) DRs at promoters. H3K4me3 and H3K27ac tag density is shown for regions in both modules. Identified clusters (colour coded bars on the right side) were grouped in classes P1a-P2d. Rows are genomic regions from -10 to +10 kb around the centre of the analysed regions. (n) indicates the number of regions in different classes. Profiles describing relation of histone mark levels between mock, WAC and WA314 are indicated on the right. Sup: Suppression, Prev: Prevention. **(B-C)** Boxplots of H3K4me3 and H3K27ac tag counts for the regions in each class in **(A)** for P1 **(B)** and P2 **(C)** modules. Data are representative of at least two independent experiments. **(D)** Peak tracks of H3K4me3 (red) and H3K27ac (blue) tag densities at promoter regions from Suppression and Prevention profiles in P1.

3.3.2 Promoter H3K4me3 and H3K27ac changes associate with transcription

We analysed whether *Yersinia*-induced H3K4me3 and H3K27ac changes at promoters correlated with expression of the associated genes using above described RNA-seq data. The strongest correlation was observed for DRs upregulated in WAC vs mock where 73 % of the H3K4me3 DRs (Figure 3.6A) and 46 % of the H3K27ac DRs (Figure 3.6B) showed enhanced transcription of the associated genes. In the pairwise comparisons between mock, WAC and WA314 taken together 42 % of the H3K4me3 DRs (Figure 3.6A) and 24 % of the H3K27ac DRs (Figure 3.6B) were on average associated with altered gene expression. Analysis of the change in gene expression of P1 and P2 associated genes showed the strongest relation between histone marks and gene expression in Suppression (P1a, P2a) and Prevention (P1b, P2a) profiles (Figures 3.6C).

We next analysed the overlaps of genes in classes R1-R4 (Figure 3.2A) and P1a-P2d (Figure 3.5A). Overlaps were visualised in a heatmap and revealed that the genes in Suppression classes P1a, P2a, R1, R2 overlapped most strongly (Figure 3.6D). Moreover, there were strong overlaps also for the Up classes P2c and R3 and Prevention classes P1b, P2d, and R4 (Figure 3.6D). Down Profile was not present in RNA-seq classes (Figure 3.2A) and in line with this, promoter class P2b showed no substantial overlap with RNA expression (Figure 3.6D). It can be concluded that *Y. enterocolitica* reprograms chromatin modifications at promoters of human macrophages by inhibiting the PAMP-induced deposition and removal of H3K27ac- and H3K4me3 marks to regulate associated gene expression (Figure 3.6E).

3.4 Effectors modify chromatin at distal regulatory elements

3.4.1 Enhancer states are altered by virulent *Yersinia* in macrophages

The next analysis steps focused on histone modification changes during *Y. enterocolitica* infection at enhancers defined as H3K4me1 positive regions outside promoters. First, genome-wide heatmap of all H3K27ac DRs at enhancers of mock-, WAC- and WA314-infected macrophages was generated encompassing 16408 regions (Figure 3.7A). Regions were grouped into six clusters (color coded) and assembled in four classes E1, E2, E3 and E4 equalling to Suppression, Down, Up and Prevention profiles, respectively (Figures 3.7A, B). In mock-treated macrophages enhancers were either poised (H3K27ac absent or low) as in classes E1 and E3 or constitutive (H3K27ac present) as in classes E2 and E4 (Figures 3.7A, B) [137]. In WAC-treated macrophages poised enhancers in E1 were activated by deposition of H3K27ac, whereas constitutive enhancers in E4 were repressed by removal of H3K27ac (Figures 3.7A, B). WA314 suppressed activation of poised enhancers in E1 and prevented downregulation of constitutive enhancers in E4 (Figures 3.7A, B), thus counteracting WAC effects in classes containing the majority of enhancer regions. In addition, WA314 downregulated constitutive enhancers in E2 and induced poised enhancers in E3 (Figures 3.7A, B). We further studied H3K4me1 induction at latent enhancer regions, characterised by the absence of H3K4me1 marks in uninfected macrophages [137]. 222 latent enhancers gained H3K4me1- and H3K27ac marks in WAC-infected macrophages (Figure

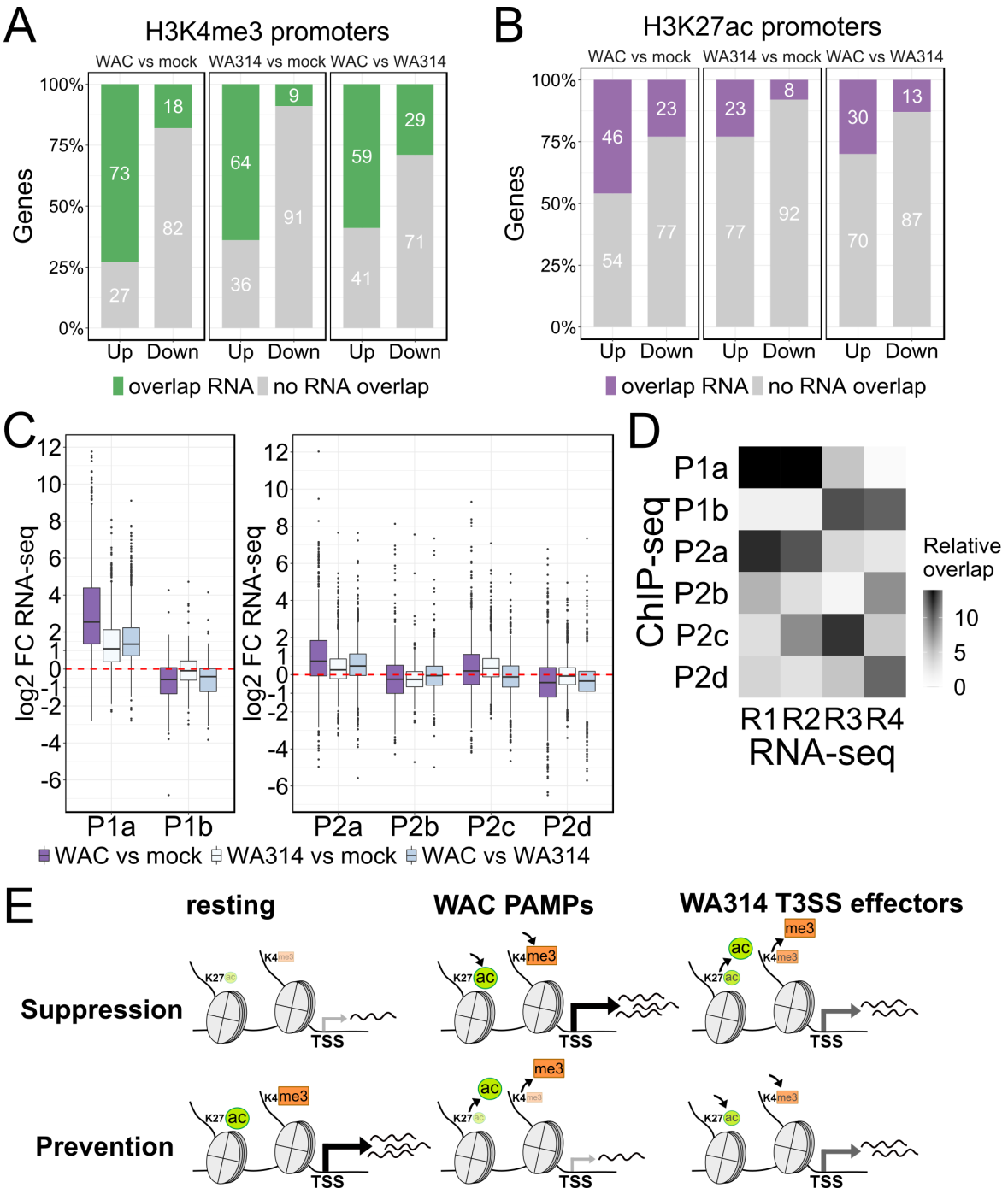

FIGURE 3.6: **Analysis of association between promoter histone mark changes and gene expression. (A, B)** Bar plots showing fraction of genes associated with H3K4me3 **(A)** and H3K27ac **(B)** DRs at promoters which also show associated change (log2 FC >1 and adjusted P-value <0.05) in gene expression. **(C)** Boxplot showing RNA-seq log2 FC for genes associated with classes in modules P1 (left) and P2 (right). **(D)** Heatmap presentation showing relative overlap of genes from RNA-seq classes R1-4 and H3K4me3 and H3K27ac classes P1a-P2d. Dark to light color scale indicates low to high overlap. **(E)** Scheme summarizing *Yersinia* counter-regulation of PAMP-induced changes of H3K4me3 and H3K27ac at promoters to modulate gene expression.

3.7C). WA314 infection also increased H3K4me1 levels, however H3K27ac levels were induced in only a fraction of latent enhancers (Figure 3.7C). This suggests that WA314 blocks PAMP-induced upregulation of H3K27ac marks in a part of the latent enhancers (Figure

3.7C) and therefore modulates latent enhancer conversion into active/ constitutive state.

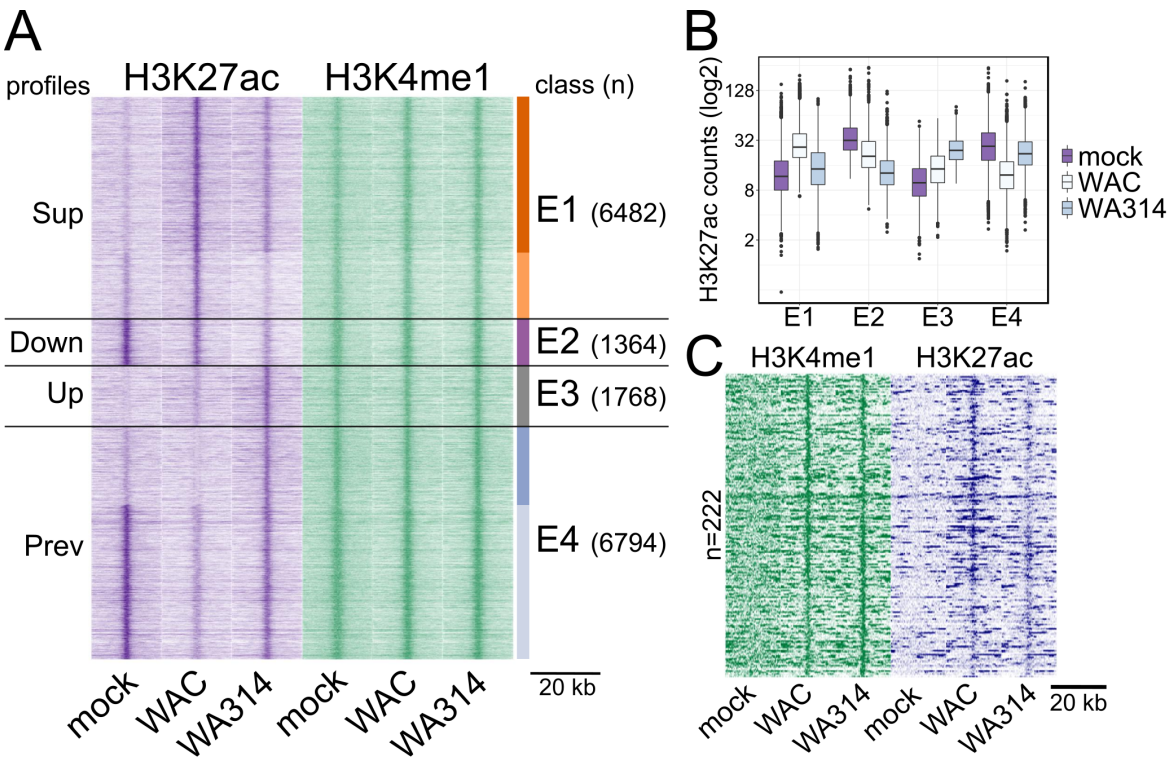

FIGURE 3.7: **Analysis of H3K27ac and H3K4me1 changes at enhancers. (A)** Heatmap showing clustering of H3K27ac DRs at enhancers. H3K4me1 tag counts are shown for the associated regions. Clustering yielded 6 clusters (color coded, right side) which were assembled into 4 classes E1-4. Profiles describing relation of histone mark levels between mock, WAC and WA314 are indicated on the right. **(B)** Boxplot of H3K27ac tag counts for the regions in each class in **(A)**. Data are representative of two independent experiments. **(C)** Heatmap showing H3K4me1 and H3K27ac tag counts at latent enhancers for WAC and WA314 vs mock. In **(A)** and **(C)** rows are genomic regions from -10 to +10 kb around the center of the analysed regions. “n” indicates the number of regions.

3.4.2 Enhancer H3K27ac changes frequently occur without associated gene expression

By analysing the correlation between gene expression and H3K27ac enhancer changes, we found that 5 % to 29 % enhancer-associated genes showed respective expression change (Figure 3.8A), which was lower than for promoter modifications (8 % to 73 %; Figures 3.6A, B). A heatmap of pairwise overlaps of genes in classes E1-E4 (Figure 3.7A) and R1-R4 (Figure 3.2A) showed the highest overlaps between classes from the same profiles for Suppression (E1 and R1, R2) and Prevention (E4 and R4; Figure 3.8B). E3 overlapped strongly with Up class R3 and Suppression classes R1/2, whereas Down profile E2 overlapped the most with Suppression class R1 (Figure 3.8B). Furthermore, H3K4me1 changes in latent enhancers (Figure 3.7C) showed increased expression of the associated genes (Figure 3.8C). We conclude that there were changes in enhancer modifications which associated with gene expression changes, however many H3K27ac alterations occurred without a corresponding gene expression change.

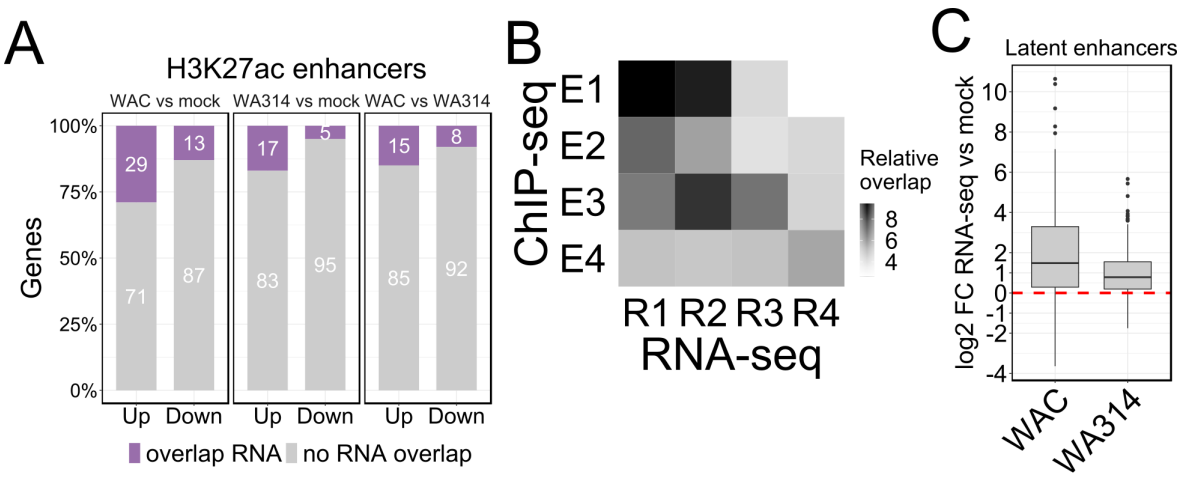

FIGURE 3.8: **Analysis of association between epigenetic changes at enhancers and gene expression. (A)** Bar plots showing fraction of genes associated with H3K27ac DRs at enhancers which also show associated change (log2 FC >1 and adjusted P-value <0.05) in gene expression. **(B)** Heatmap presentation showing relative overlap of genes from RNA-seq classes R1-4 and H3K27ac enhancer classes E1-4. Dark to light color scale indicates low to high overlap. **(C)** Boxplot showing RNA-seq log2 FC for WAC and WA314 vs mock for genes associated with latent enhancers in Figure 3.7C.

3.4.3 Histone marks at promoters and enhancers are regulated in a coordinated manner

A heatmap of pairwise overlaps of genes associated with classes E1 to E4 (Figure 3.7A) and P1a to P2d (Figure 3.5A) was produced to analyse if *Yersinia* altered histone marks at promoters and enhancers in a coordinated way (Figure 3.9A). The strongest overlaps were found between classes with the same profiles: E1/P1a/P2a (Suppression), E2/P2b (Down), E3/P2c (Up) and E4/P1b/P2d (Prevention; Figure 3.9A). Further analysis revealed that ~59 % (509) of genes from E1/P1a/P2a overlaps were common with genes in Suppression classes R1 and R2 and ~27 % (197) of genes from E4/P1b/P2d overlaps were found in Prevention class R4 (Figure 3.9B). Genes from E3/P2c overlaps were the most common with genes from Suppression class R2 while genes from E2/P2b overlaps did not show an overlap with a distinct profile (Figure 3.9B). Overall, these data suggest that *Yersinia* effectors counteract a fraction of PAMP induced gene expression by coordinated modulation of histone modifications at gene promoters and enhancers (Figure 3.9C, D).

3.5 *Yersinia* modulates histone marks and expression of genes in specific pathways

We analysed which genes from profiles in R1-R4 (Figure 3.2A) overlapped with genes from corresponding profiles either at promoters (P1a-P2d; Figures 3.5A, 3.6D) and/or enhancers (E1-4; Figures 3.7A, 3.8B). In total 1579 (52 %) genes from Suppression classes R1 and R2 associated with genes in Suppression classes P1a, P2a or E1 (Figure 3.10A). In comparison, 924 (36 %) genes in Prevention class R4 associated with genes in Prevention classes

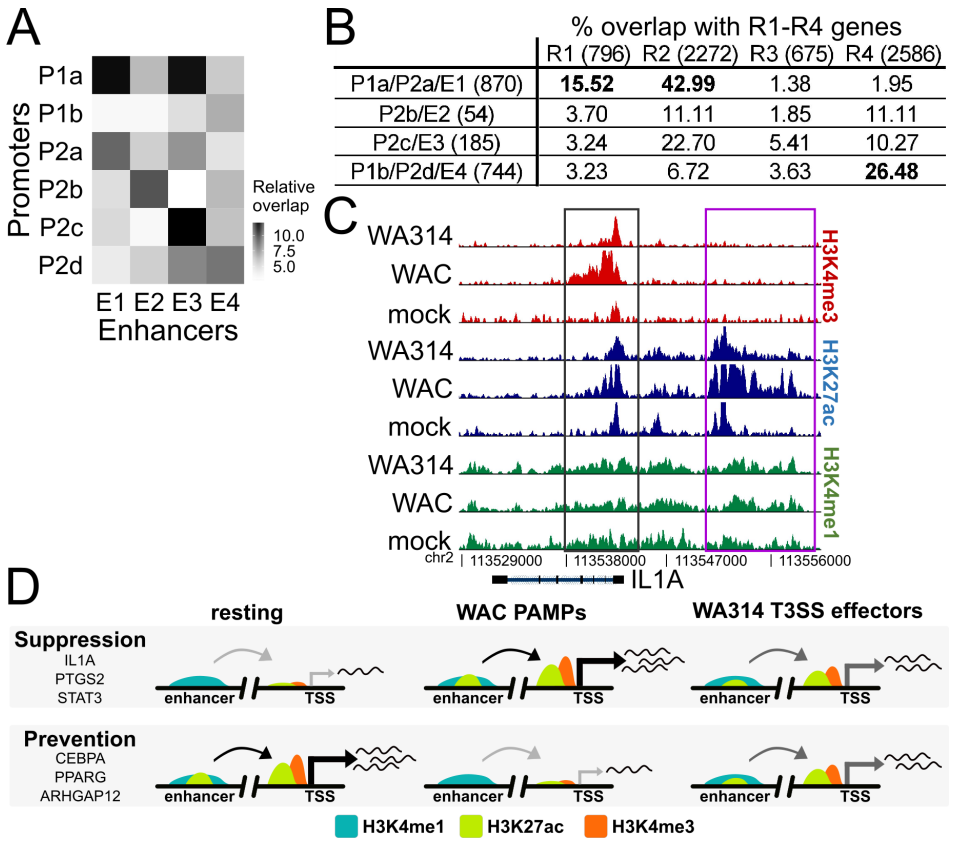

FIGURE 3.9: **Analysis of co-regulation of histone marks at promoters and enhancers and gene expression. (A)** Heatmap presentation showing relative overlap of genes from promoter classes P1a-P2d and enhancer classes E1-4. Dark to light color scale indicates low to high overlap. **(B)** Percentage of genes from promoter and enhancer overlaps in **(A)** overlapping genes from RNA-seq classes R1-4. Overlapping promoter and enhancer genes from the same profiles were pooled (Suppression: P1a/P2a/E1, Down: P2b/E2, Up: P2c/E3, Prevention: P1b/P2d/E4). Numbers in brackets indicate the number of genes associated with RNA-seq classes and promoter and enhancer overlaps. Highlighted values are described in the text. **(C)** Peak tracks of H3K4me3 (red), H4K27ac (blue) and H3K4me1 (green) tag densities showing *Yersinia*-induced changes at promoter (black line) and enhancer (purple line) regions of IL1A gene which is also regulated at the expression level and equals to the Suppression profile. **(D)** Scheme summarizing coordinated regulation of histone marks at gene promoters and enhancers to modulate transcription by *Yersinia*. Representative genes belonging to each profile are indicated.

P1b, P2d or E4, whereas 142 (21 %) genes from Up class R3 associated with genes in Up classes P2c or E3 (Figure 3.10A).

Suppression genes were enriched for transcription, apoptosis, protein polyubiquitination and immune signalling, involving pro-inflammatory cytokines, chemokines, feedback regulators and IFN signalling mediators (Figures3.10B, C and Table 6.2). Up genes were enriched for transcriptional regulators (Figures 3.10B, D) and included several regulators of macrophage immune response, such as IKZF4 [191–193], PPARA [194] and forkhead box O1 (FOXO1) [195–197]. Prevention profile genes were enriched in metabolic pathways, integrin signalling encompassing several integrin genes, potassium transport and regulation of GTPase activity (Fig 3.10B). Interestingly, regulated genes included Rho GTPases Rho related BTB domain containing (RhoBTB) 1 and RhoBTB2 and several Rho GTPase GAPs, such as ARHGAP35, oligophrenin-1 (OPHN1), ARHGAP12, ARHGAP11A and ARHGAP9

(Table 6.2) [178, 179]. Finally, genes associated with latent enhancers (Figure 3.7C) were associated with transcriptional regulation, immune signalling, GTPase activation and apoptosis (Table 6.3).

TF motif analysis of promoter and enhancer regions associated with Suppression genes (Figure 3.10A) revealed binding sites of known inflammatory regulators from the RHD- (NFκB-p65-Rel), IRF- (ISRE, IRF2, IRF1) and bZIP- (Fra1, Fra2, Fosl2, Jun-AP1) families (Figures 3.10E, F). Also Up profile regions (Figure 3.10A) were enriched for RHD (NFκB-p65-Rel) binding sites (Figures 3.10E, F), implicating that *Yersinia* modulates NF-κB signalling to upregulate expression of certain target genes. Prevention profile (Figure 3.10A) was enriched for distinct motifs from ETS (SpiB, PU.1) family (Figures 3.10E, F), which are known to interact extensively with other TFs [198], and PU.1 is a LDTF in macrophages [107].

Taken together, the histone modifications that *Y. enterocolitica* reorganizes at promoters and enhancers of macrophages act to reprogram central transcriptional programs, including inflammatory, metabolic and GTPase pathways, by modulation of PAMP signalling and transcription regulator expression networks.

3.5.1 Extensive regulation of Rho GTPase pathway genes by *Yersinia*

We identified that genes involved in the small Rho GTPase signalling are regulated at histone mark and gene expression level during *Yersinia* infection in Prevention profile (Figure 3.10B, Table 6.2). Small Rho GTPases are molecular switches which cycle between primarily cytosolic GDP-bound inactive state and mainly membrane-localized GTP-bound active state [199]. GTP hydrolysis and transition into inactive GDP-bound state is promoted by GTPase activating proteins (GAPs), whereas GDP to GTP exchange resulting in GTP-bound state is facilitated by guanine nucleotide exchange factors (GEFs) [199]. Additionally, GDP dissociation inhibitors (GDIs) sequester Rho GTPases in the cytosol and inhibit GDP dissociation thus modulating GTPase interactions with GAPs, GEFs and downstream effectors [199]. As central regulators of actin cytoskeleton dynamics Rho GTPases are directly targeted by several *Yersinia* effectors to inhibit phagocytosis [16]. Whether Rho GTPase signalling genes are targeted also at gene expression and epigenetic level by *Yersinia* effectors is not known, therefore we studied this question in a more detail.

We compiled a target small Rho GTPase pathway gene list with 534 genes encompassing 370 effectors [175–177], 66 GAPs, 77 GEFs [178] and 23 Rho GTPases [179, 180]. First, we analysed which of these target genes are DEGs and to which classes and profiles they belong to. From the all target genes 206 (39 %) were differentially expressed during *Yersinia* infection (Figure 3.11A). Majority of the genes (108) belonged to the Suppression profile, whereas 22 and 76 genes belonged to Up and Prevention profiles, respectively (Figure 3.11A). We further analysed target genes with epigenetic changes from promoter (P1a-P2d) and enhancer (E1-E4) classes. Overall, 324 (61 %) target genes associated with H3K4me3 or H3K27ac changes at promoters or enhancers encompassing 1023 regions (Figure 3.11B). Majority of the regions belonged to Suppression (433 regions, 42 % total) and Prevention profiles (378 regions, 37 % total; Figure 3.11B). Histone modifications were

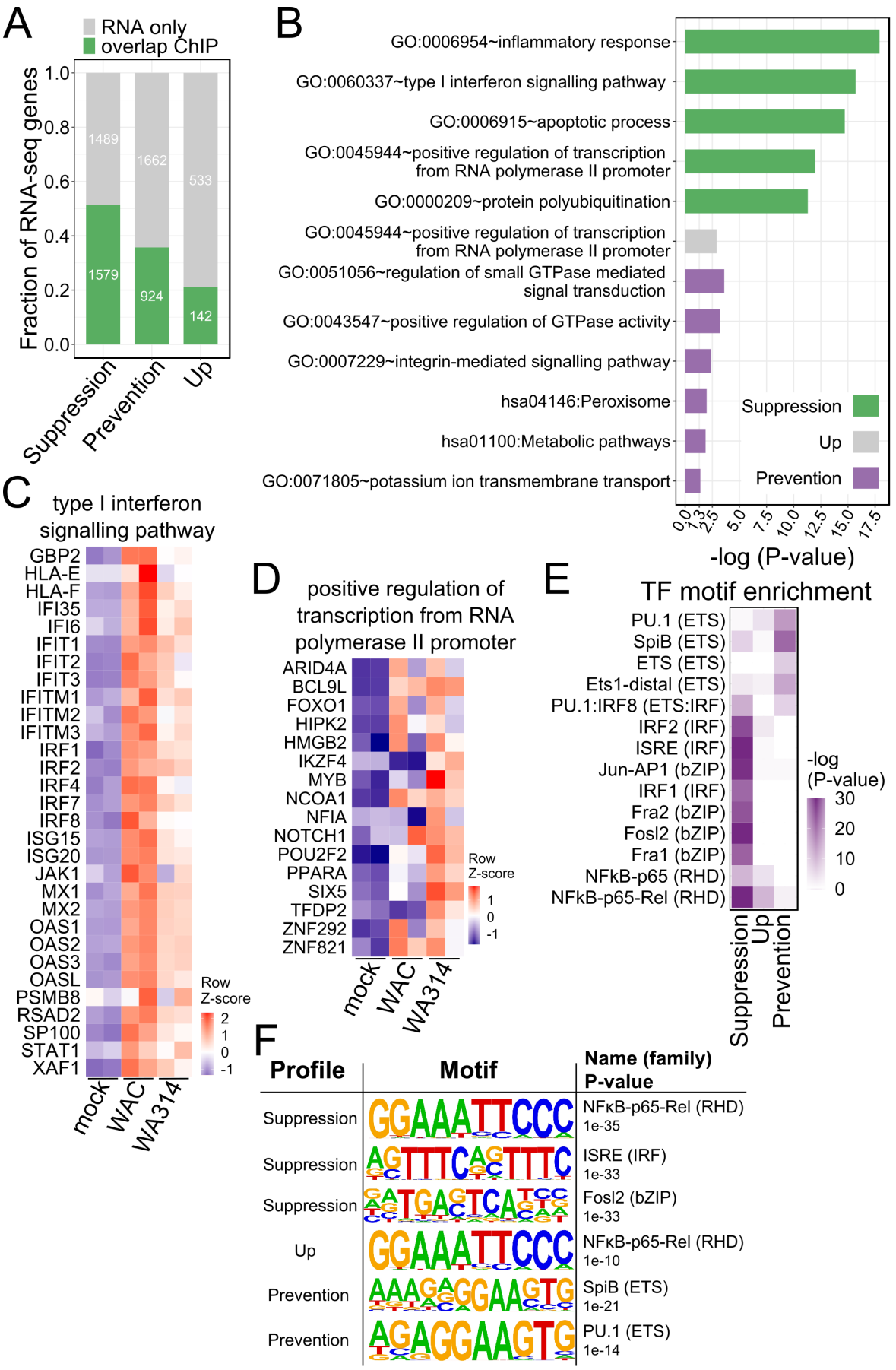

FIGURE 3.10: *(Continued on the next page.)*

FIGURE 3.10: **Analysis of genes modulated at histone modification and gene expression level by *Yersinia*. (A)** Barplot showing fraction and number (numbers in bars) of genes from RNA-seq profiles Suppression, Prevention and Up overlapping genes from a corresponding profile from ChIP-seq. **(B)** Barplot showing log10 transformed P-values and enriched GO and KEGG terms for genes with RNA-seq and ChIP-seq overlaps in **(A)**. Longer bar indicates lower P-value and thus higher significance of enrichment. **(C, D)** Heatmaps of row-scaled (row Z-score) RNA-seq rlog gene counts for genes from pathways in **(B)**. **(E)** Heatmap showing log10 transformed P-value for TF motif enrichment in promoter and enhancer regions associated with ChIP-seq and RNA-seq overlaps in **(A)**. Darker color indicates lower P-value and thus higher significance of enrichment. **(F)** Representative TF motifs from **(E)**.

found to be associated with 58 %, 68 %, 62 % and 74 % of all effectors, GAPs, GEFs and Rho GTPases, respectively (Figure 3.11C). RNA-seq and ChIP-seq overlaps of target genes were analysed for each profile to identify genes regulated both at gene expression and histone modification level. Overall, 63 %, 36 % and 51 % of target genes from RNA-seq profiles Suppression, Up and Prevention, respectively, associated with histone mark changes from the same profile (Figure 3.11D). These overlapping genes encompassed 19 %, 33 %, 22 % and 35 % of all target effectors, GAPs, GEFs and Rho GTPases, respectively (Figure 3.11C). For the overlapping genes from Suppression and Prevention profiles WA314 expression levels were frequently between mock and WAC (Figure 3.12A), indicating an incomplete counteraction of the PAMP signalling. For the Up profile, target genes were mostly induced by both WAC and WA314 (Figure 3.12A), suggesting an induction by PAMPs and not by a specific activity of the T3SS effectors.

We analysed the Rho GTPase specificity of GAPs, GEFs and effectors of genes with RNA-seq and ChIP-seq overlaps using information from publicly available data [175–178]. In the Prevention profile 60 % (6 out of 10) active GAPs were specific exclusively towards Rac1, which was higher than in the Suppression profile (25 %, 2 out of 8) and all GAPs [178] (36 %, 18 out of 50; Figures 3.12A, B). Furthermore, 50 % (3 out of 6) of all active GEFs in the Prevention profile were specific for cell division cycle 42 GTP binding protein (Cdc42), which was higher than in the Suppression profile (33 %, 1 out of 3) and all GAPs [178] (27 %, 12 out of 45; Figures 3.12A, C). However, the expression levels of Cdc42 GEFs between WAC and WA314 were only marginally different (Figure 3.12A), indicating that WA314 did not prevent PAMP downregulation of these genes. For the Suppression and Up profiles generally there was no enrichment of specific GAPs and GEFs when compared to all GAPs and GEFs [178] (Figures 3.12A-C). Overall, the major effect of *Yersinia* effectors appears to be targeting of Rac1 GAPs.

Analysis of Rho GTPase effector specificity [175–177] revealed that effectors for 20 and 15 Rho GTPases were encompassed in Suppression and Prevention profiles, respectively, with majority of Rho GTPases overlapping between both profiles (Table 6.4). Cdc42 effectors were the most numerous both in Suppression (12 out of 46) and Prevention profiles (7 out of 18) followed by Rac1 and RhoA effectors (Table 6.4). Notably, only Suppression profile contained RhoBTB1/2 effectors (Table 6.4). Up profile effectors were not enriched for a certain Rho GTPase (Table 6.4). Investigation of function with STRING database [200] revealed effectors in Suppression and Prevention profiles involved in actin cytoskeleton dynamics (ABI1, ACTN1, FNBP1, BAIAP2, DIAPH1), transcription (STAT3, SPEN, PKN2) and MAPK pathway (SH3RF1, ROCK2, MAP3K4). Moreover, several effectors are reported to

be involved in epigenetic modulation (DIAPH1 [201], BASP1 [202], PKN2 [203–205], STAT3 [139], ROCK2 [206–210]), suggesting regulation of epigenetic modifications by the Rho GTPase pathway.

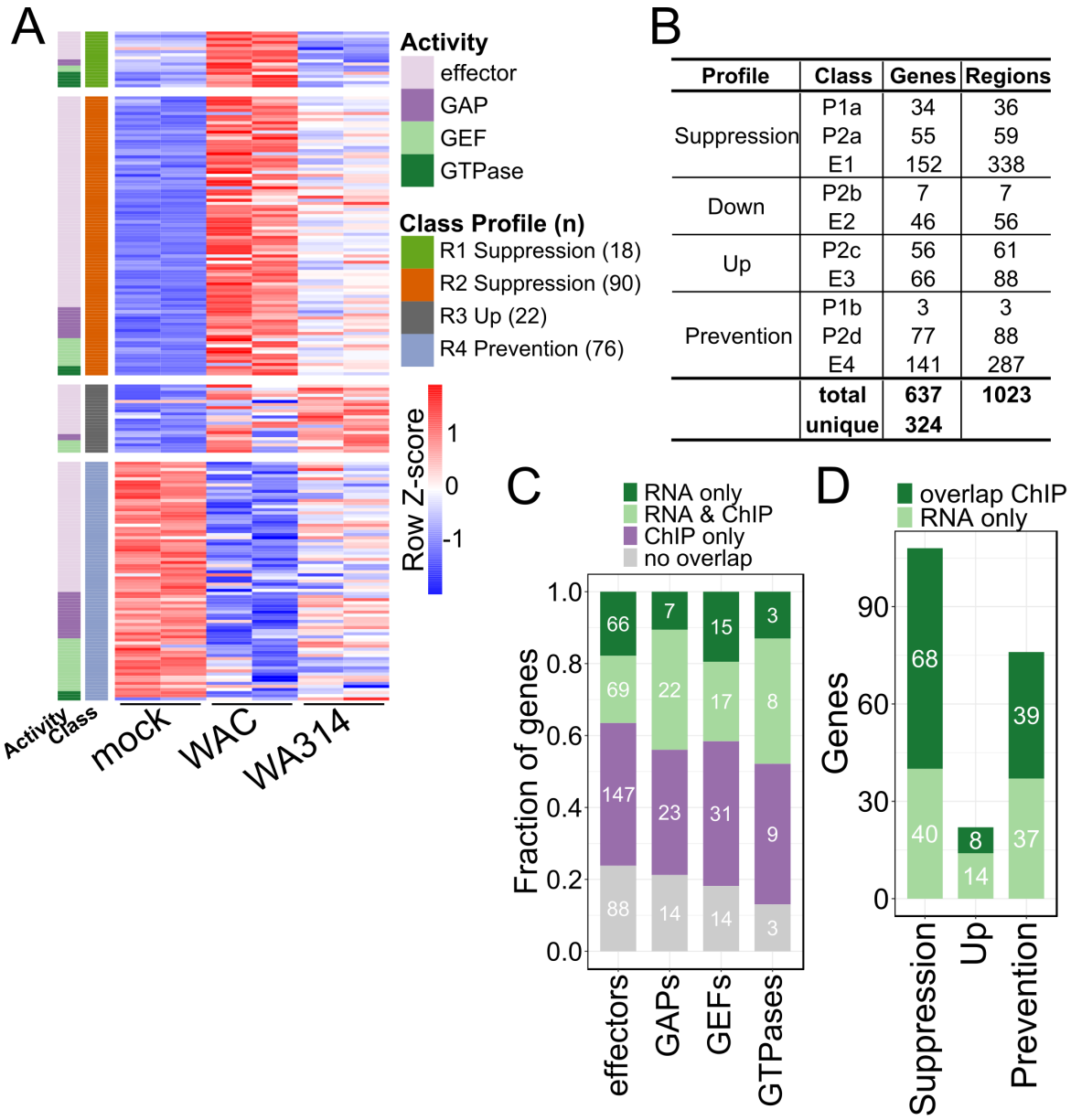

Profile	Class	Genes	Regions
Suppression	P1a	34	36
	P2a	55	59
	E1	152	338
Down	P2b	7	7
	E2	46	56
Up	P2c	56	61
	E3	66	88
Prevention	P1b	3	3
	P2d	77	88
	E4	141	287
	total	**637**	**1023**
	unique	**324**	

FIGURE 3.11: **Analysis of gene expression and histone modification changes of Rho GTPase pathway genes during *Yersinia* infection.** **(A)** Heatmap of all DEGs from Rho GTPase pathway grouped in classes R1-R4 where (n) refers to the number of genes. Classes and activity are colour coded on the left side. Rlog counts were row-scaled (row Z-score). **(B)** Number of Rho GTPase pathway genes associated with regions in promoter and enhancer classes. **(C)** Barplot showing fraction and number (numbers in bars) of effectors, GAPs, GEFs and Rho GTPases with RNA-seq and/ or ChIP-seq change. **(D)** Barplot showing fraction and number (numbers in bars) of genes from RNA-seq profiles in **(A)** associated with promoter and/ or enhancer regions from the same profile.

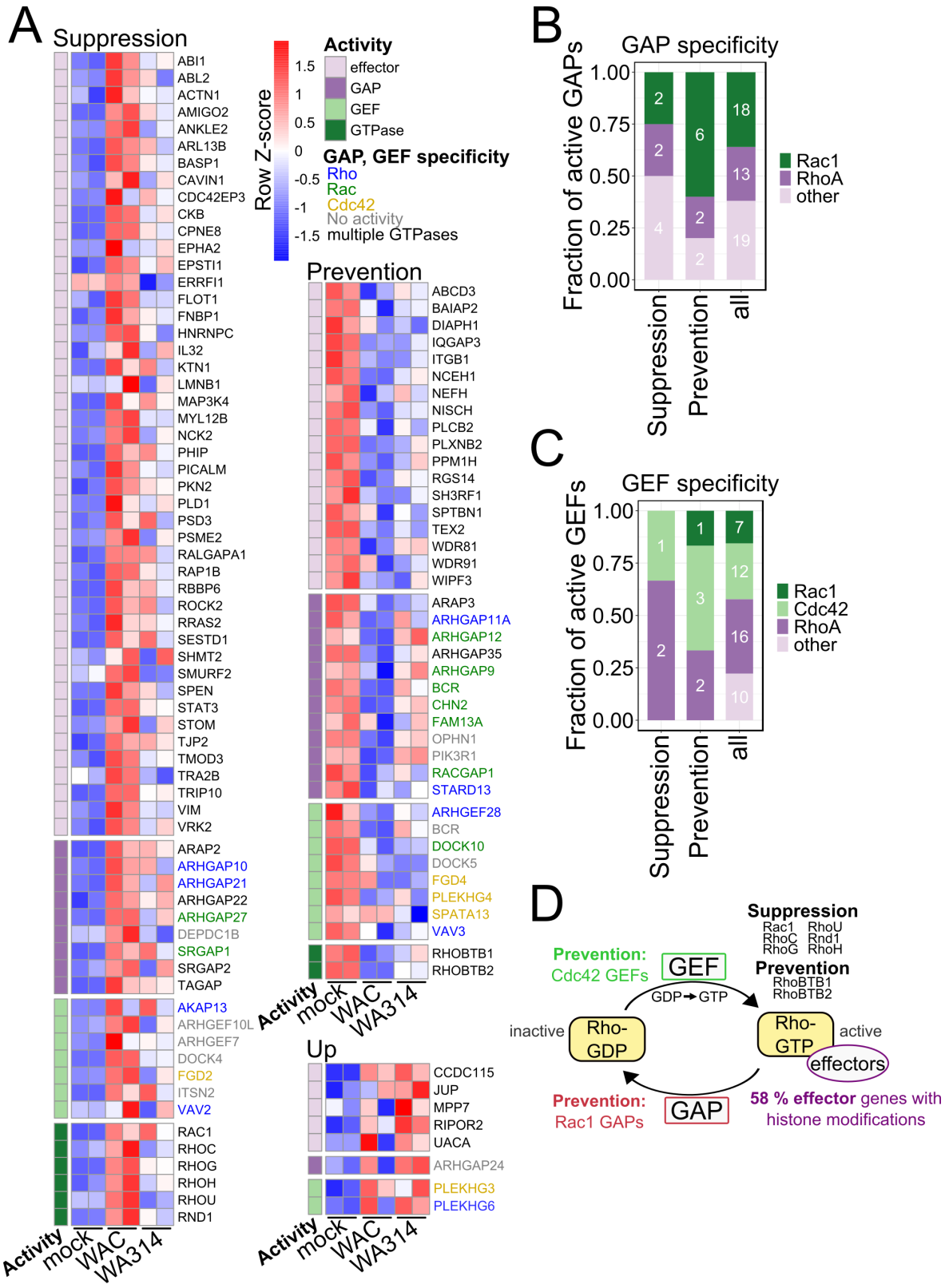

FIGURE 3.12: **Analysis of modulated Rho GTPase pathway gene specificity and function. (A)** Heatmaps of RNA-seq rlog gene counts for genes with RNA-seq and ChIP-seq overlaps in Figure 3.11D. Activity of genes is colour coded on the left side. The Rho GTPase specificity of GAPs and GEFs is colour coded for gene symbols. Rlog counts were row-scaled (row Z-score). **(B, C)** Barplots showing Rho GTPase specificity of all active GAPs **(B)** and GEFs **(C)** associated with overlaps in Figure 3.11D for Suppression and Prevention profiles and all GAPs and GEFs analysed. **(D)** Scheme depicting Rho GTPase cycle and the main results about epigenetic and transcriptomic modulation of Rho GTPase pathway genes by *Yersinia*.

Suppression and Prevention profiles contained three classical Rho GTPases (Rac1, RhoC, RhoG) and five atypical Rho GTPases (RhoH, RhoU, RND1, RhoBTB1, RhoBTB2) [211]. Most atypical Rho GTPases are not regulated by GAPs and GEFs but at the level of transcription and protein stability [211, 212]. Atypical GTPases play a role in various cellular functions (e.g. RhoBTB in tumour suppression [212]) but also in the regulation of activity of classical Rho GTPases [213, 214]. Notably, RhoBTB1 and RhoBTB2 were found in the Prevention profile whereas their effectors were found in the Suppression profile (Figure 3.12A, Table 6.4). Furthermore, Rac1, Rac1 activator RhoG and atypical GTPases RhoH and RhoU were found in the Suppression profile (Figure 3.12A). These Rho GTPases are able to interact with Rac effectors and modulate the activity and functions of Rac [176, 199, 212, 213, 215]. Thus, *Y. enterocolitica* targets Rac directly by Yops [16] and epigenetic and transcriptomic modulation of Rac activating Rho GTPases (Suppression profile) and inactivating GAPs (Prevention profile) to promote lowered cellular activity of Rac.

In summary, *Yersinia* extensively targets expression and histone modifications of Rho GTPase pathway genes, suggesting another level of regulation of Rho GTPases by *Yersinia* effectors (Figure 3.12D).

3.6 Analysis of the role of YopM and YopP on WA314 effects

3.6.1 YopP but not YopM induces epigenetic changes

The *Y. enterocolitica* T3SS effectors YopP and YopM modulate inflammatory gene expression in *Yersinia*-infected macrophages [81]. Therefore, we investigated whether YopP and/or YopM contribute to transcriptional and epigenetic reprogramming by virulent *Y. enterocolitica*. Macrophages were infected for 6 h with WA314 strains lacking YopP or YopM (WA314ΔYopP or WA314ΔYopM; see section 2.1.8) and subjected to RNA-seq and H3K4me3 and H3K27ac ChIP-seq (Figure 3.13A). PCA analysis of RNA-seq data showed that WA314ΔYopP, WA314ΔYopM and WA314 replicates clustered together in separate clusters (Figure 3.13B), indicating modulation of transcription by YopM and YopP. Accordingly, 1616 DEGs were detected between WA314ΔYopP and WA314 and 804 DEGs were found between WA314ΔYopM and WA314 (Figure 3.13E). PCA analysis of H3K4me3 and H3K27ac ChIP-seq data revealed clustering of WA314ΔYopM and WA314 replicates, whereas WA314ΔYopP replicates were clearly separate (Figures 3.13C, D). This data suggest that YopP but not YopM contributes to the WA314 induced epigenetic changes. In line with this, only 24 H3K4me3 regions and 7 H3K27ac regions were differentially regulated between WA314ΔYopM and WA314 (Figure 3.13E). In contrast, 684 H3K4me3 regions and 5094 H3K27ac regions were altered between WA314ΔYopP and WA314 (Figure 3.13E). This data suggests that YopP impacts gene transcription via modulation of H3K4me3 and H3K27ac histone marks, whereas YopM effects on transcription occur without regulating these histone marks.

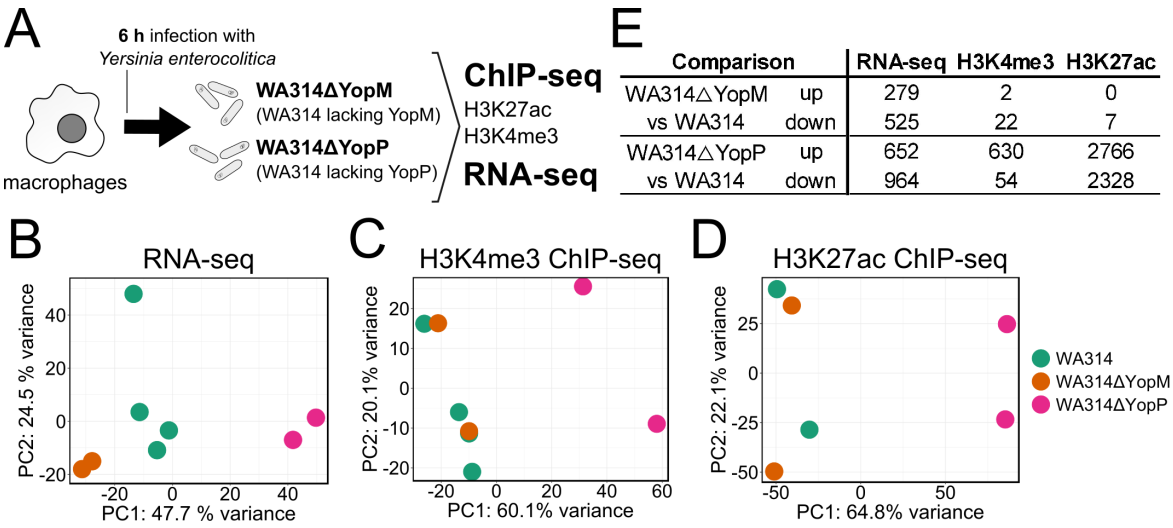

E

Comparison		RNA-seq	H3K4me3	H3K27ac
WA314ΔYopM	up	279	2	0
vs WA314	down	525	22	7
WA314ΔYopP	up	652	630	2766
vs WA314	down	964	54	2328

FIGURE 3.13: **ChIP-seq and RNA-seq analysis with *Y. enterocolitica* lacking YopM or YopP. (A)** Experimental design. Primary human macrophages were infected with *Y. enterocolitica* strains lacking YopM (WA314ΔYopM) or YopP (WA314ΔYopP) for 6 h and subjected to RNA-seq and H3K4me3 and H3K27ac ChIP-seq. **(B-D)** PCA of rlog gene counts from all DEGs in R1-4 **(B)**, H3K4me3 tag counts from regions in P1 module **(C)** and H3K27ac tag counts from regions in P1-2 modules and E1-4 classes **(D)** for each WA314, WA314ΔYopM and WA314ΔYopP replicate analysed. **(E)** Number of DEGs from RNA-seq and DRs from H3K4me3 and H3K27ac ChIP-seq for WA314ΔYopM and WA314ΔYopP vs WA314.

3.6.2 YopP is a major regulator of *Yersinia*-induced histone marks and gene expression

We studied what proportion of the WA314-induced transcriptional (Figure 3.2A) and epigenetic changes (Figures 3.5A, 3.7A) were due to YopP in the profiles Suppression, Prevention, Up and Down. For this, the percentage YopP effect was calculated from the ratio of FC between WA314ΔYopP vs WA314 and either WA314 vs WAC (Suppression and Prevention profiles) or WA314 vs mock (Up and Down profiles). The median YopP effect on the histone modifications was 42 % and ranged from 8.9 % - 57.2 % in the different profiles with lower YopP contribution to Up and Down profiles (Figures 3.14A, B). The median YopP effect on gene expression for genes associated with histone modifications ranged from 45.4 % - 63.4 % (Figures 3.14C, D). Overall, YopP generally accounts for almost half of the effects of *Yersinia* on chromatin marks and gene expression, however other Yops except YopM also significantly contribute to this virulence activity.

3.6.3 YopP regulates inflammatory and Rho GTPase pathway genes

We analysed closer the role of YopP on Rho GTPase pathway associated with Suppression and Prevention profiles (Figure 3.12A). The average YopP effect on gene expression in Suppression and Prevention profiles was 46. 6 % and 78.5 %, respectively (Table 6.5). However, at the level of individual genes the YopP effect was widely spread from 2 % to 177 % (Figure 3.15A, Table 6.5). We further analysed the inflammatory response genes associated with Suppression profile (Figure 3.10B) and found that the average YopP effect on gene expression was 46.5 %, however YopP effect spread widely from -57 % to 103 % for

A

Profile	Class	% YopP effect
Suppression	P1a	57.2
	P2a	43.4
	E1	48.6
Down	P2b	8.9
	E2	25.2
Up	P2c	25.9
	E3	28.3
Prevention	P1b	40.5
	P2d	52.0
	E4	53.2
Median		**42.0**

C

Profile	Class	% YopP effect
Suppression	R1	49.5
	R2	45.4
Up	R3	63.4
Prevention	R4	54.4
Median		**51.9**

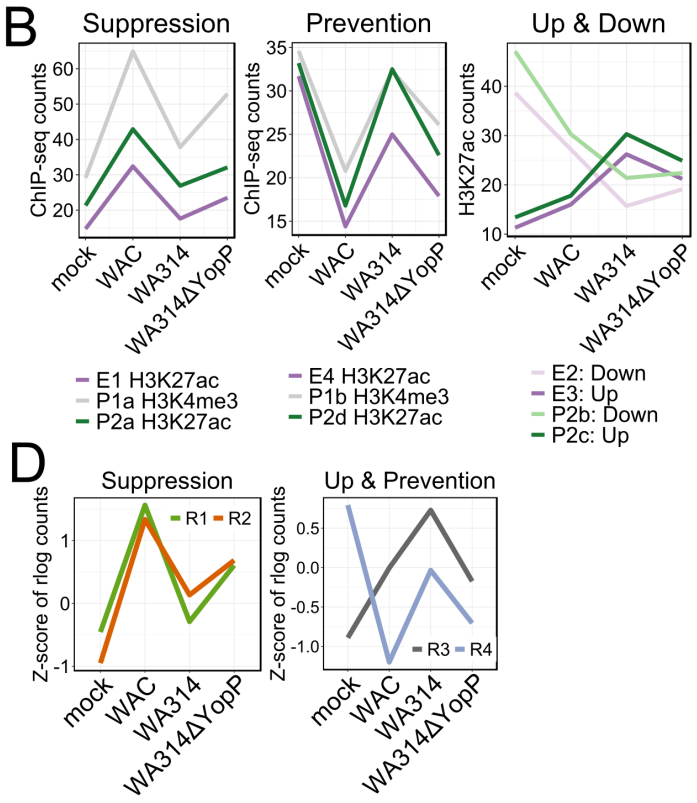

FIGURE 3.14: **Analysis of YopP contribution to gene expression and chromatin modification profiles. (A, C)** % YopP effect (median value) for classes of histone modifications **(A)** and RNA-seq genes associated with histone modifications **(C)**. "Median": median value when taking % YopP effect from all classes together. **(B, D)** Line plots of the average H3K4me3 or H3K27ac counts for regions **(B)** and average Z-score of rlog counts for genes associated with histone modifications **(D)** in the different profiles.

the individual genes (Figure 3.15B, Table 6.6). Generally, YopP-dependent gene expression changes associated with corresponding changes in histone modifications, however some YopP regulated genes were associated with histone modifications not induced by YopP (Figure 3.15C, D, Table 6.5, Table 6.6). These data suggest that YopP is a major regulator of Rho GTPase and inflammatory pathway gene expression and histone modifications in a complex interplay with the other effectors.

YopP/J blocks inflammatory gene expression by inhibiting NF-κB and MAPK signalling initially triggered by the *Yersinia* PAMPs [81]. NF-κB- and MAPK pathways control different histone modifications in the nucleus [107] and thus we wondered whether the observed effect of YopP on H3K4me3 and H3K27ac is due to the inhibition of these pathways. For this primary human macrophages were treated with specific MAPK inhibitors (SB203580 plus PD98059) during *Yersinia* infection followed by ChIP-qPCR. MAPK inhibition blocked the WA314ΔYopP-induced deposition of H3K4me3 at the indoleamine 2,3-dioxygenase 1 (IDO1) but not at the IL1B gene promoters (Figure 3.15E) as well as the deposition of H3K27ac at the IL6 and prostaglandin-endoperoxide synthase 2 (PTGS2) promoters (Figure 3.15F). WA314ΔYopP in combination with the MAPK inhibitors inhibited deposition of histone modifications as efficient as WA314, indicating that MAPK inhibition mimics YopP activity (Figures 3.15E, F). Altogether these data suggest that YopP inhibits the deposition of H3K4me3 and H3K27ac marks by it's known activity of MAPK inhibition.

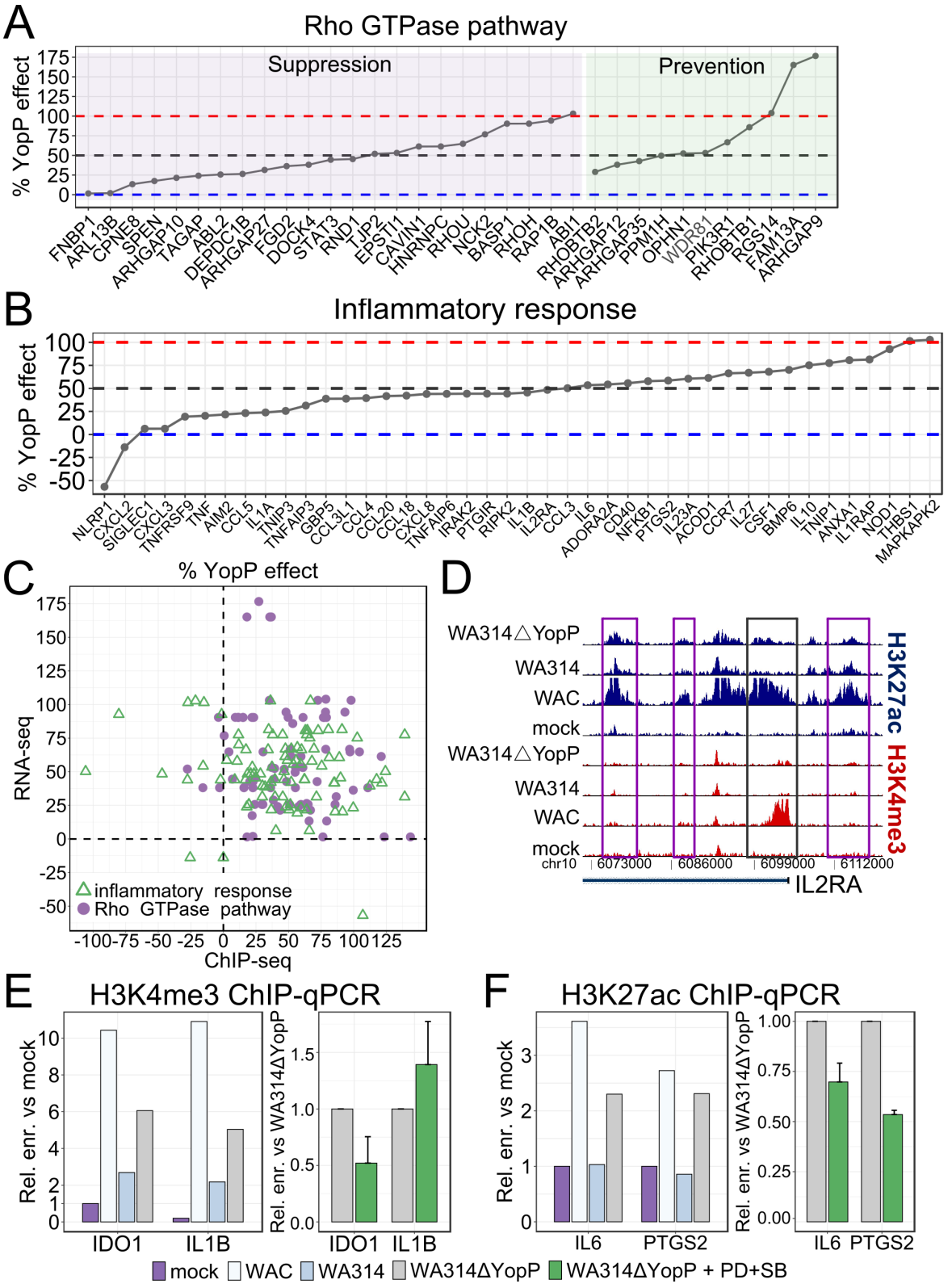

FIGURE 3.15: **Analysis of YopP effect on inflammatory response and Rho GTPase pathways. (A, B)** Line plots of % YopP effect on gene expression for genes associated with histone modifications and gene expression in inflammatory response **(A)** and Rho GTPase pathway **(B)**. Only genes and regions that overlapped WAC vs WA314 up DEGs and DRs, respectively, were used. **(C)** Scatter plot of % YopP effect for RNA-seq and ChIP-seq for genes and regions associated with pathways from **(A)** and **(B)**. **(D)** Peak tracks of H3K4me3 (red) and H3K27ac (blue) tag densities showing changes at IL2RA gene promoter (black line) and enhancers (purple lines) not induced by YopP. **(E, F)** Bar plots of H3K4me3 **(E)** and H3K27ac **(F)** ChIP-qPCR analysis from mock, WAC, WA314 and WA314ΔYopP infection (left panel) and WA314ΔYopP infection with or without MAPK pathway inhibitors (PD+SB; right panel). ChIP-qPCR signal was expressed as relative enrichment (rel. enr.) vs mock (left panel) or vs WA314ΔYopP without inhibitors (right panel). Error bars indicate SD. At least 2 biological replicates were used, on the left panel one representative replicate is shown.

4 Discussion

Pathogenic *Yersinia* spp. modulate host gene expression as one of the main virulence strategies to inhibit immune response in macrophages [81]. Up to now, the effect of *Yersinia* virulence factors on host gene expression has been analysed in mouse macrophage cell lines utilizing microarray. The involvement of chromatin modifications in *Yersinia*-induced gene expression changes is not known.

The main aim of this study was to analyse the effect of *Y. enterocolitica* virulence factors on gene expression and histone modifications in primary human macrophages by performing a global gene expression and histone modification analysis with RNA-seq and ChIP-seq, respectively.

4.1 *Yersinia* virulence factors regulate gene expression in macrophages

Primary human macrophages were mock-infected or infected with *Y. enterocolitica* strains WA314 (wild type) or WAC (virulence plasmid-cured) for 1.5 h and 6 h and subjected to RNA-seq to elucidate the modulation of gene expression by *Yersinia* virulence plasmid-encoded factors at early and late time points (Figures 3.1,3.2). We detected 6329 DEGs, which is a much larger number of DEGs when compared to microarray gene expression analysis in mouse macrophages, which identified 50 and 857 DEGs [99, 100]. This difference might be because microarray encompasses a limited number of probes and has lower sensitivity than RNA-seq [216]. Furthermore, mouse and human macrophages show large differences in response to stimulation [217]. Additionally, mouse macrophages undergo *Yersinia*-induced cell death 4-8 h post-infection [218, 219], thus the infection time in mouse macrophage microarrays was limited to 2-2.5h [99, 100]. Primary human macrophages are highly resistant to *Yersinia*-induced cell death, which appears after 20 h of infection or later [218, 219]. Therefore infection times for 1.5 h and 6 h could be used in this study minimizing cell death-driven expression changes. We were able to study rapidly induced primary response genes (PRGs) and later induced secondary response genes (SRGs), which require new protein synthesis for induction [117–119]. We observed a strong induction of type I IFN signalling including IFN stimulated genes (ISGs), which are SRGs in TLR4 signalling, and which were not detected as DEGs in mouse macrophages [99, 100, 181]. Therefore, a much larger number of DEGs could be also attributed to detection of SRGs which are induced by feedback loops of PRGs, such as IFNβ, IL10 and TNF [139, 140, 181].

Clustering analysis of all DEGs yielded 3 profiles describing gene expression in WA314 in relation to mock and WAC (Figure 3.2). WA314 suppressed induction and prevented

downregulation of gene expression by WAC in the Suppression and Prevention profiles, respectively. In the Up profile WA314 generally showed the highest expression levels when compared to mock and WAC. Suppression and Prevention profiles comprised the vast majority of all DEGs (~90 %), indicating that the main activity of effectors is to counteract gene expression induced by bacterial PAMPs. The remainder of the genes in the Up profile signified regulation by specific activity of the T3SS effectors. Similar profiles were also identified in the microarray analysis with *Yersinia*-infected mouse macrophages [99, 100]. Additionally, these studies detected genes altered independently of the virulence factors and genes with the lowest expression in WA314 [99, 100]. 60 % of all DEGs, including several cytokines and pro-inflammatory proteins, were found to belong to a general response of macrophages to an infection and were not modulated by the effectors [99]. In the work here, PCA showed that WAC and WA314 cluster together at 1.5 h but were clearly separate at 6 h post-infection (Figure 3.1B). Thus, there is induction of expression changes independently of the virulence factors as in Sauvonnet et al. [99] at early time points and extensive modulation by effectors later in infection. In Hoffmann et al., the majority of genes resembled Suppression profile and Prevention profile was not identified [100]. This is similar to results from 1.5 h post-infection, where only 56 DEGs were detected between WAC and WA314 and the vast majority (55) were suppressed by WA314 (Figure 3.1C). It can be concluded, that microarray studies show comparable results to primary human macrophage infection after 1.5 h, when supposedly the amounts and activity of translocated effectors are not sufficient to extensively suppress PAMP-induced signalling and there is no modulation of SRGs.

Notably, WA314 expression levels were frequently between mock and WAC, indicating an incomplete counteraction of PAMP-induced gene expression changes (Figure 3.2A). PAMP-induced signalling is more rapid than translocation and activity of effector proteins as both WA314 and WAC activate NF-κB and MAPK pathways initially followed with a delayed suppression by WA314 [27, 96]. Moreover, NF-κB and MAPK pathway blockage simultaneously with TLR4 activation is sensed as a danger signal, which induces caspase-8 dependent cell death protective for the host [81]. Therefore, *Yersinia* must balance suppression of inflammation and induction of cell death.

4.2 *Yersinia* modulates expression of genes important for macrophage immune response

Genes from Suppression profile were enriched for inflammatory response (Figure 3.2C) which is in line with known immunosuppression by *Yersinia* [81, 99, 100]. Additionally, Suppression profile was associated with type I IFN signalling and antiviral response (Figure 3.2C), which are known to be induced by LPS [220]. Type I IFNs promote an antiviral state which can be both beneficial or harmful for pathogenic bacteria [220]. Type I IFNs prevent TNF induced tolerance, thus promoting expression of NF-κB target genes [140]. Moreover, ISGs are negative and positive regulators of pro-inflammatory and ISG gene expression, respectively [221]. Overall, these data suggest a very complex role of type I IFN signalling during *Yersinia* infection.

Suppression profile was also associated with genes involved in protein polyubiquitination, encompassing E3 ligases, E2 enzymes and proteasome components (Figure 3.2C). Ubiquitination is a key component in immune signalling, for instance, by regulating NF-κB nuclear translocation [222]. Moreover, bacterial pathogens frequently mimic host E3 ligases to alter host cell ubiquitination landscape and modify specific pathways [223]. Future studies deserve investigation whether *Yersinia* targets transcription of genes from ubiquitination machinery to target specific cellular processes in macrophages.

Distinct transcriptional regulators were enriched in all profiles Suppression, Prevention and Up (Figure 3.2C). Suppression profile associated with known inflammatory mediators from STAT, RHD, and IRF families [224]. These included Stat1 and IRF1/5, which promote M1 polarization and pro-inflammatory response, and Stat6 and IRF4, which trigger M2 differentiation and anti-inflammatory response [224]. Thus, Suppression profile involves transcriptional regulators which both promote and reduce inflammation likely to ensure effective response against infection but also limit the harm of excessive inflammation. Prevention profile was mainly enriched for C2H2 domain ZNF transcriptional regulators. In line with this, ZNFs were downregulated in mouse macrophages in response to LPS [225]. ZNFs contain a kruppel-associated box (KRAB) domain, which is involved in gene repression [186] and promote heterochromatin spreading [226], thus *Yersinia* might limit inflammatory gene expression by preventing downregulation of repressive ZNFs. Up profile contained TF KLF2, which is specifically upregulated by *Yersinia* [100] and negatively regulates NF-κB activity [227]. Other Up profile TFs included nuclear receptors (NRs) RARG, PPARA and NR1D1 [188], which suppress inflammatory response [194, 228, 229]. This suggests that virulent *Yersinia* target specific TFs to modulate PAMP response.

Suppression and Prevention profiles were also associated with cell cycle regulation, although monocyte derived macrophages in vitro are in a terminally differentiated state and do not divide [189]. Interestingly, recently it was shown that primary human macrophages stimulated with LPS enter G0 cell-cycle arrest, thus inducing an anti-retroviral state [190]. This state is characterized with no changes in DNA synthesis and mitosis but there is down- and upregulation of transcripts triggering cell-cycle progression and arrest, respectively [190]. In line with these results, Suppression and Prevention profiles were associated with genes promoting cell cycle arrest and triggering cell-cycle progression, respectively. In vivo where macrophages can proliferate, G0 arrest might prevent division of cells infected by bacteria [190]. Alternatively, cell-cycle regulators might participate in other roles, such as in cytokine production [190]. Antiviral state might also promote cell death [230], which is unfavourable for *Yersinia* [81].

Prevention profile was strongly enriched for various metabolic pathways. Activation of macrophages rewires metabolic pathways, which control inflammatory gene expression, activity and PTMs of proteins and epigenetic marks among others [111]. Thus, by modulating metabolism, *Yersinia* could target various essential processes in macrophages. Prevention associated with Krebs cycle enzymes ACO2 and IDH1, which convert citrate to isocitrate and isocitrate to α-ketoglutarate, respectively [111], thus likely resulting in excess citrate in WAC infection. This is in line with citrate accumulation during LPS stimulation, which is

used for protein acetylation and generation of inflammatory mediators [111]. LPS also induces accumulation of lanosterol due to the downregulation of genes involved in cholesterol metabolism [231], consistent with the Prevention profile. Lanosterol triggers reduction of Stat1/2 signalling, ISG expression and cytokine production, thus protecting against endotoxic shock [231]. Moreover, lanosterol increases membrane fluidity, ROS production and phagocytosis, thus promoting killing of bacteria [231]. Prevention profile associated with several key fatty acid (FA) biosynthesis enzymes, such as, fatty acid synthase (FASN), carnitine O-palmitoyltransferase 2 (CPT2), acetyl-CoA carboxylase 1 (ACACA) and fatty acid desaturase 2 (FADS2). In line with this, downregulation of unsaturated FAs and associated enzymes has been shown in macrophages upon TLR activation [232]. These FAs serve as anti-inflammatory mediators, thereby downregulation promotes TLR4-induced inflammatory signalling. Overall, by Prevention of metabolic pathway genes, *Yersinia* potentially suppress inflammation (Krebs cycle enzymes and FA synthesis) and bacterial killing (cholesterol synthesis). Future studies will be necessary to confirm that transcriptional changes of metabolic genes correlate with cellular metabolite levels.

In summary, *Yersinia* effectors extensively regulate macrophage gene expression to counteract PAMP-induced gene expression changes. *Yersinia* targets genes from numerous biological pathways of which only inflammatory signalling has been described as *Yersinia* target so far [81]. This opens up a lot of potential for future studies to understand how these pathways play a role in *Yersinia* and bacterial infection in general to modulate macrophage immune response.

4.3 Macrophage epigenetic reprogramming by *Yersinia*

We performed ChIP-seq analysis with four histone marks, H3K4me1, H3K4me3, H3K27me3 and H3K27ac, to analyse if observed *Yersinia*-induced gene expression changes are associated with chromatin changes (Figure 3.3). H3K27ac at enhancers was the most dynamic mark during infection, whereas the active promoter mark H3K4me3 and the enhancer mark H3K4me1 were modulated to a much smaller extent and the repressive H3K27me3 mark was virtually unchanged. In line with these data, extensive remodelling of H3K27ac at enhancers takes place during macrophage differentiation and stimulation [130, 137, 233, 234], whereas H3K27me3 is largely unaltered in macrophages [131, 140, 235, 236].

Clustering of H3K4me3 and H3K27ac differential regions (DRs) at promoters and enhancers revealed the same profiles as for RNA-seq, namely, Suppression, Prevention and Up (Figures 3.5, 3.7). Additionally, profile Down was identified for the H3K27ac mark where WA314 showed the lowest levels when compared to mock and WAC. Similarly to gene expression, most of the regions belonged to Suppression and Prevention, showing that *Yersinia* effectors mainly counteract PAMP-induced gene expression and histone modifications. Consistent with this, WAC and mock showed the strongest correlation with LPS-stimulated and naive macrophages, respectively, when comparing RNA-seq and H3K27ac ChIP-seq data from this study and publicly available data (Figures 3.1F, 3.4D) [131, 140]. In contrast, WA314 was distinct from mock and WAC, indicating modulation of PAMP-induced

signalling. Therefore, in addition to known *Yersinia* modulation of PAMP-triggered gene expression changes [81], here we also report for the first time counteraction of PAMP-induced chromatin modifications to alter the state of promoters and enhancers in macrophages.

Importantly, as a live bacteria *Yersinia* possess other PAMPs besides LPS which might contribute to gene expression and chromatin mark changes [81]. For instance, LPS biosynthesis metabolites ADP-L-β-d-heptose (ADP-heptose) and d-β-d-heptose 1-phosphate (HBP) can enter the host cell cytosol and trigger expression of inflammatory cytokine genes [81]. Also adhesins YadA and invasin induce expression of pro-inflammatory genes [94, 95]. LcrV and lipoproteins activate TLR2 [237], whereas bacterial DNA is detected by TLR9 upon destruction of bacteria in phagosomes [238]. Therefore, LPS likely represents only one of the PAMPs in *Yersinia* which contributes to complex immune stimulation in macrophages during infection.

4.4 Epigenetic changes at promoters and enhancers associate with transcription

H3K4me3 changes at promoters showed the strongest association with gene expression, followed by H3K27ac at promoters and H3K27ac at enhancers (Figures 3.6, 3.8). As H3K4me3 and H3K27ac are characteristic for active genes [125, 128], gain and removal of these marks resulted in increased and decreased expression, respectively. Generally, promoters with H3K4me3 changes showed concordant H3K27ac changes, therefore alterations of two activating histone marks might indicate a strong activation at these promoters and robust induction of transcription. In line with these results, H3K4me3 and H3K27ac gain at promoters correlates with gene induction in macrophages [110, 117, 130, 140, 233].

Many genes were altered epigenetically with H3K27ac at enhancers without a corresponding gene expression change (Figures 3.3D, 3.8A). A possible explanation might be that enhancer-target gene associations are unclear. Here enhancers were annotated with the closest gene. However, enhancers are usually located far away from the genes they regulate and one enhancer can be associated with multiple genes and vice versa [127]. Methods analysing interactions between regions in the genomic space would be necessary to assign enhancers to their target genes accurately [127]. Moreover, gene transcription is defined by the sum of all gene-associated chromatin modifications and bound proteins, thus a change in one histone mark might not reflect the overall chromatin landscape and the transcriptional state [107]. Stimulation can also prime specific regions to trigger a rapid response upon subsequent activation of macrophages. For instance, type I IFNs and IFNγ induce open chromatin conformation, increased histone acetylation, H3K4me3 and recruitment of TFs without an increase in transcription at inflammatory gene promoters and enhancers to prime genes [140, 233]. Upon stimulation, primed genes are induced more rapidly and show prolonged recruitment of TFs and RNA polymerase II [140, 233]. Priming is essential for rapid immune response of macrophages as many LPS inducible genes are in a primed state before stimulation [107, 110, 117, 118]. Moreover, as histone marks associated with Up and Down profiles showed weaker association with transcription than

Suppression and Prevention profiles (Figures 3.6C, 3.8B, 3.9B), the specific activity of T3SS effectors on chromatin might be involved in priming of macrophages.

We also observed that *Yersinia* induces H3K4me1 at latent enhancers, which play a role in macrophage priming and modulate enhancer landscape in differentiated cells in a signal specific manner (Figure 3.7C) [137]. Interestingly, virulence factors did not modulate H3K4me1 at latent enhancers but suppressed H3K27ac induction at subset of these enhancers, thus interfering with their activation state. H3K4me1 at latent enhancers persists even when the inducing stimulus is removed enabling faster and stronger response upon restimulation [137]. Therefore, virulent *Yersinia* suppress activation of latent enhancers but H3K4me1 "scar" likely remains the same way as with WAC infection to affect macrophage response during subsequent exposures. Genes associated with latent enhancers included transcription factors and immune response regulators (Table 6.3). Thus, *Yersinia* affects macrophage "memory" via latent enhancers of the central immune response pathways.

Modulation of host chromatin by bacterial pathogens to alter gene expression is a known phenomena [129]. However, most studies have analysed chromatin modification and gene expression changes at selected loci and genes by qPCR and a very few studies have performed genome-wide analysis during bacterial infection [239–243]. For instance, RomA from *Legionella pneumophila* translocates to the host cell nucleus and induces H3K14me3, thus reducing activating H3K14ac levels and repressing immune gene transcription [239]. *Mycobacterium tuberculosis* (MTB) in human monocyte-derived dendritic cells and *Salmonella typhimurium* in human primary macrophages induce DNA demethylation at distal regulatory elements which is accompanied with the H3K27ac gain and altered gene expression [240, 241]. Interestingly, MTB also induces latent enhancers [240] as seen here with *Yersinia* infection.

In summary, *Yersinia* modulates H3K4me3 and H3K27ac at promoters and enhancers to regulate expression of the associated genes. Moreover, *Yersinia* might also affect priming and the available enhancer landscape, thus altering responsiveness of macrophages upon secondary stimulation.

4.5 Distinct biological pathways are associated with common gene expression and histone mark profiles

We found that a notable fraction of DEGs (52 %, 36 % and 21 % of genes from Suppression, Prevention profiles, respectively) associated with epigenetic changes during *Yersinia* infection (Figure 3.10A) including co-regulation of histone marks at gene promoters and enhancers (Figure 3.9). As not all *Yersinia*-induced gene expression changes are modulated by the histone marks investigated in this work, other mechanisms must be also involved. These might include recruitment of factors mediating RNA polymerase II pausing, transition into elongation and transcription speed, displacement of repressive and activating factors, production and availability of transcriptional regulators, premature termination, RNA degradation and transcriptional bursting. Future studies warrant investigation of these mechanisms in *Yersinia*- mediated gene expression.

Genes with associated gene expression and histone mark changes were generally enriched for the same pathways as described earlier for RNA-seq (see section 4.2). Namely, Suppression was enriched for inflammatory signalling, polyubiquitination, type I IFN signalling, apoptosis and transcription. Up profile was enriched for transcriptional regulators, such as IKZF4, PPARA and FOXO1. IKZF4 acts both as gene activator and repressor in the LPS response [192], cooperates with macrophage lineage determining TF PU.1 to drive activation of myeloid specific enhancers and regulates expression of PU.1 [193]. FOXO1 is a key regulator of cell metabolism, cell cycle and cell death [244] and has been described to enhance TLR4 mediated inflammatory response [195, 196] but also to promote expression of the anti-inflammatory cytokine IL-10 in macrophages [197]. Prevention profile was enriched for metabolic pathways and integrin signalling containing several integrin genes. Although integrins promote bacterial uptake and inflammatory response during *Yersinia* infection [16, 93–95], integrins also induce active form of immunosuppresive cytokine TGF-β [245, 246]. Therefore, T3SS effectors might prevent downregulation of integrins to activate TGF-β and suppress inflammatory response, while anti-phagocytosis effectors suppress integrin-mediated uptake of bacteria. Interestingly, Prevention profile was also enriched for small GTPase pathway involving genes from the Rho GTPase pathway, which is directly targeted by several Yops to modulate phagocytosis [16]. Overall, this data suggests that *Yersinia* modulates gene expression and histone modifications to affect central pathways in macrophage immune response.

4.6 *Yersinia* regulates Rho GTPase pathway genes

GTPase signalling, including small Rho GTPase pathway genes, was the most enriched pathway in the Prevention profile (see section 3.5). In line with this, downregulation of Rho GTPase signalling genes upon LPS stimulation of macrophages has been evidenced before [139, 247], but comprehensive analysis of epigenetic and transcriptional regulation of Rho GTPase pathway genes during infection is lacking. Therefore, we carried out an analysis with 534 Rho GTPase pathway target genes, including effectors, GAPs, GEFs and Rho GTPases (see section 3.5.1). Notably, 216 (39 %) and 324 (61 %) of all Rho GTPase pathway genes were associated with RNA-seq and ChIP-seq changes, respectively. Furthermore, 36 % - 63 % of the Rho GTPase genes from RNA-seq profiles Suppression, Prevention and Up also showed a respective histone modification change. As most of the modulated genes and regions belonged to Prevention and Suppression profiles, majority of changes are induced by PAMPs of WAC and counteracted by T3SS effectors of WA314.

We revealed increased fraction of Rac-specific GAPs in the Prevention profile. Rac is a major facilitator of phagocytosis in macrophages during *Yersinia* infection [16], therefore *Yersinia* effectors might prevent downregulation of Rac GAPs to promote Rac GTP hydrolysis and inactivation. In contrast, Suppression profile contained Rac1, Rac1 activator RhoG and atypical Rho GTPases RhoH and RhoU, which can regulate Rac function and activity [176, 199, 212, 213, 215]. Overall, these data suggest that *Yersinia* downregulates Rac activity in cells at multiple levels: i) direct targeting by Yops ii) Prevention of Rac GAPs and

ii) Suppression of Rac1 and it's activators. The strong modulation of Rac activity during infection might be also crucial for other processes besides phagocytosis, such as chemotaxis, production of ROS and gene expression [248].

Additionally, we found that effectors from Suppression and Prevention profiles are active towards most of the Rho GTPase families and play a role in actin cytoskeleton, but also processes like transcription and MAPK signalling. Thus, *Yersinia* potentially affect various downstream effector functions of the majority of small Rho GTPases. Interestingly, the effectors for RhoBTB1/2 GTPases in the Prevention profile were found in the Suppression profile. This might implicate some feedback regulation, where PAMP-downregulation of RhoBTB1/2 induces compensatory upregulation of respective effectors to keep RhoBTB1/2 signalling active. Although not clear, similar feedback mechanisms might be also associated with other Rho GTPase pathway genes where altered activity or expression of Rho GTPases could induce feedback regulation. Future experiments are clearly necessary to elucidate in detail how Rho GTPase activity and PAMP-signalling affects epigenetic modifications and gene expression of Rho GTPase pathway genes and subsequent Rho GTPase activity.

4.7 YopP is a major regulator of gene expression and chromatin modifications during infection

We performed RNA-seq and ChIP-seq analysis with *Yersinia* strains lacking either YopM or YopP to reveal if these two effectors are modulating *Yersinia*-induced gene expression and chromatin modifications. YopP is a prominent suppressor of inflammatory gene expression due to the inhibition of NF-κB and MAPK pathways [81], which regulate histone modifications in macrophages [107], therefore a strong effect of YopP on gene expression and chromatin modifications was anticipated. YopM also modulates MAPK pathway and gene expression [70], and translocates to the nucleus [65]. However, the nuclear function of YopM is not clear and we envisioned that YopM might regulate histone modifications. Both YopM and YopP induced gene expression changes when compared to WA314, however, only deletion of YopP altered H3K27ac and H3K4me3 marks (Figure 3.11). This implicates that YopM does not regulate gene expression through H3K4me3 and H3K27ac but potential other mechanisms (see section 4.5), which require further investigation.

YopP-induced gene expression changes associated with histone modifications when analysing inflammatory response and Rho GTPase pathway genes (Figure 3.13). Generally, YopP mediated about a half of WA314 effects on gene expression, histone modifications and associated pathways (Figures 3.12, 3.13). However, YopP contribution to individual genes and histone marks spread over a broad range (Figure 3.13), indicating that the degree of YopP regulation of separate genes and regions is very variable. In line with this, suppressive action of YopP on gene expression was shown not to be uniform and some genes were stronger affected by YopP than others [100]). It was proposed that genes are not controlled to the same extent by YopP-mediated pathways or that they are downstream of several independent signalling cascades [100]. We could show that the inhibition of MAPK pathway by

YopP mediates deposition of histone marks, but the another YopP target, NF-κB, pathway is very likely involved as well.

Partial role of YopP on gene expression and histone modifications indicates that other effectors are also involved in these processes. It is unclear exactly how and which other Yops participate, however some pathways modulated by other Yops than YopP are known to regulate histone modifications and gene expression and therefore might play a role in *Yersinia*-induced effects. For instance, small Rho GTPase signalling mediates NF-κB and MAPK activation [249, 250] and actin polymerisation regulates nuclear translocation of myocardin related transcription factor (MRTF), which functions as a cofactor of serum response factor (SRF) [251]. Therefore, actin cytoskeleton modulating effectors YopO, YopE, YopT and YopH potentially also regulate histone modifications and gene expression. Moreover, YopH suppresses PI 3-kinase/Akt cascade [25], which downregulates NF-κB activity and promotes anti-inflammatory phenotype in macrophages [252]. Thus, YopH might be involved in incomplete counteraction of PAMP response by WA314 (see section 4.1) by increasing NF-κB activity. Furthermore, YopQ mediates formation and size of YopB/D pores in the host cell membrane [15], therefore likely affecting K^+ efflux, which mediates histone phosphorylation and inflammatory gene expression [253]. Future RNA-seq and ChIP-seq studies with other Yop deletion mutants will be necessary to elucidate the role of each effector in *Yersinia*-induced gene expression and histone marks.

As we found YopP to be a major regulator of chromatin marks and gene expression of Rho GTPase pathway genes (Figure 3.13E, F), YopP might be yet another virulence factor involved in the modulation of phagocytosis during *Yersinia* infection. Phagocytosis assays with Yop deletion mutants showed that YopP does not play a role in bacterial uptake [57]. However, these experiments were performed in mouse macrophage J774 cells and polymorphonuclear leukocytes after short infection times of 30 min. If YopP regulates phagocytosis though chromatin marks and gene expression, the effect would be expected to be visible after longer periods of infection when proteins have been translated and have exerted their activity in the cell. Supporting this idea are the results showing that a pretreatment for 24 h with TLR ligands in macrophages and monocytes promotes phagocytosis through induction of phagocytotic gene program via p38 signalling, which increases mRNA and protein levels of scavenger receptors [254]. Therefore, we propose that *Yersinia* effectors modulate Rho GTPase activity and phagocytosis through direct and early targeting of Rho GTPases in addition to later modulation of PAMP-induced epigenetic and transcriptomic Rho GTPase pathway gene program.

5 Summary

Pathogenic *Yersinia* spp. extensively suppress expression of inflammatory genes via injection of virulence plasmid-encoded factors into macrophages. At this point a global analysis of virulence factor regulation of gene expression in primary human macrophages is missing and it is not known whether epigenetic modifications are involved. To address these questions we performed a global gene expression and epigenetic analysis with RNA-seq and ChIP-seq, respectively, in primary human macrophages mock-infected or infected with *Y. enterocolitica* wild type strain WA314 or virulence plasmid-cured strain WAC. ChIP-seq was performed for histone modifications H3K4me1, H3K4me3, H3K27me3 and H3K27ac to analyse association between *Yersinia*-induced transcription and alterations of chromatin state at promoters and enhancers.

WA314 extensively counteracted WAC/ PAMP-induced gene expression and associated H3K4me3 and H3K27ac histone modifications at promoters and enhancers. Effectors suppressed gene expression and respective histone marks of inflammatory response genes and prevented downregulation of metabolic pathway genes. Furthermore, we revealed that expression and chromatin marks associated with Rho GTPase pathway genes were substantially regulated by *Yersinia* with 324 (61 %) of 534 genes regulated epigenetically. Transcriptional and epigenetic analysis with YopM and YopP effector mutant strains revealed that YopP was a major regulator of the WA314 effects, but other yet uncharacterised factors were involved as well. Moreover, YopP modulation of histone marks was due to the known YopP inhibitory activity of the MAPK pathway.

Overall, we show that the main activity of *Yersinia* virulence factors is to counteract PAMP-induced effects on gene expression and chromatin modifications in macrophages primarily through the activity of YopP (Figure 5.1). Major epigenetic and transcriptomic regulation of Rho GTPase pathway genes suggests another level of Rho GTPase targeting by *Yersinia* to modulate actin cytoskeleton.

Zusammenfassung

Pathogene *Yersinia* spp. unterdrücken erheblich die Expression von entzündlichen Genen durch eine Injektion von Virulenzplasmid kodierten Faktoren in Makrophagen. Bislang ist noch keine globale Analyse der Virulenzfaktorregulation der Genexpression in primären humanen Makrophagen durchgeführt worden und es ist nicht bekannt, ob epigenetische Modifikationen daran beteiligt sind. Um auf diese Fragen einzugehen, führten wir eine globale Genexpression sowie eine epigenetische Analyse mit RNA-seq bzw. ChIP-seq in primären humanen Makrophagen durch, die entweder nicht infiziert oder mit *Y. enterocolitica* Wildtyp-Stamm WA314 oder mit Virulenzplasmidlosem Stamm WAC infiziert wurden. ChIP-seq wurde für die Histonmodifikationen H3K4me1, H3K4me3, H3K27me3 und H3K27ac durchgeführt, um die Zusammenhang zwischen der *Yersinia*-induzierten Transkription und den Veränderungen des Chromatinzustands bei Promotoren und Enhancern zu analysieren.

WA314 wirkte der WAC / PAMP-induzierten Genexpression und assoziierte Histonmodifikationen von H3K4me3 und H3K27ac an Promotoren und Enhancern erheblich entgegen. Die Effektoren unterdrückten die Genexpression und die jeweiligen Histonmarkierungen von Entzündungsreaktionsgenen und sowie verhinderten die Herunterregulierung von Stoffwechselweggenen. Wir haben außerdem festgestellt , dass *Yersinia* maßgeblich die Expressions und Chromatinmarkierungen, die mit Rho-GTPase-Signalwegs-Genen assoziiert sind, wobei 324 (61 %) der 534 Genen epigenetisch regulierte. Eine Transkriptions- und epigenetische Analyse mit YopM- und YopP-Effektormutantenstämmen zeigte YopP als einen Hauptregulator der WA314-Effekte, aber jedoch andere noch nicht charakterisierte Faktoren waren auch beteiligt. Des Weiteren wurde festgestellt, dass die YopP-Modulation von Histonmarkierungen auf die bekannte YopP inhibitorische Aktivität des MAPK-Weges zurückgeführt werden kann.

Insgesamt zeigen wir, dass die Hauptaktivität von *Yersinia*-Virulenzfaktoren darin besteht, den PAMP-induzierten Effekten auf die Genexpression und Chromatinmodifikationen in Makrophagen hauptsächlich durch die Aktivität von YopP entgegenzuwirken (Abbildung 5.1). Die beachtliche epigenetische und transkriptomische Regulation der Gene des Rho GTPase-Signalwegs deutet auf eine andere Ebene des Rho GTPase-Targetings von *Yersinia* zur Modulation des Aktin-Zytoskeletts hin.

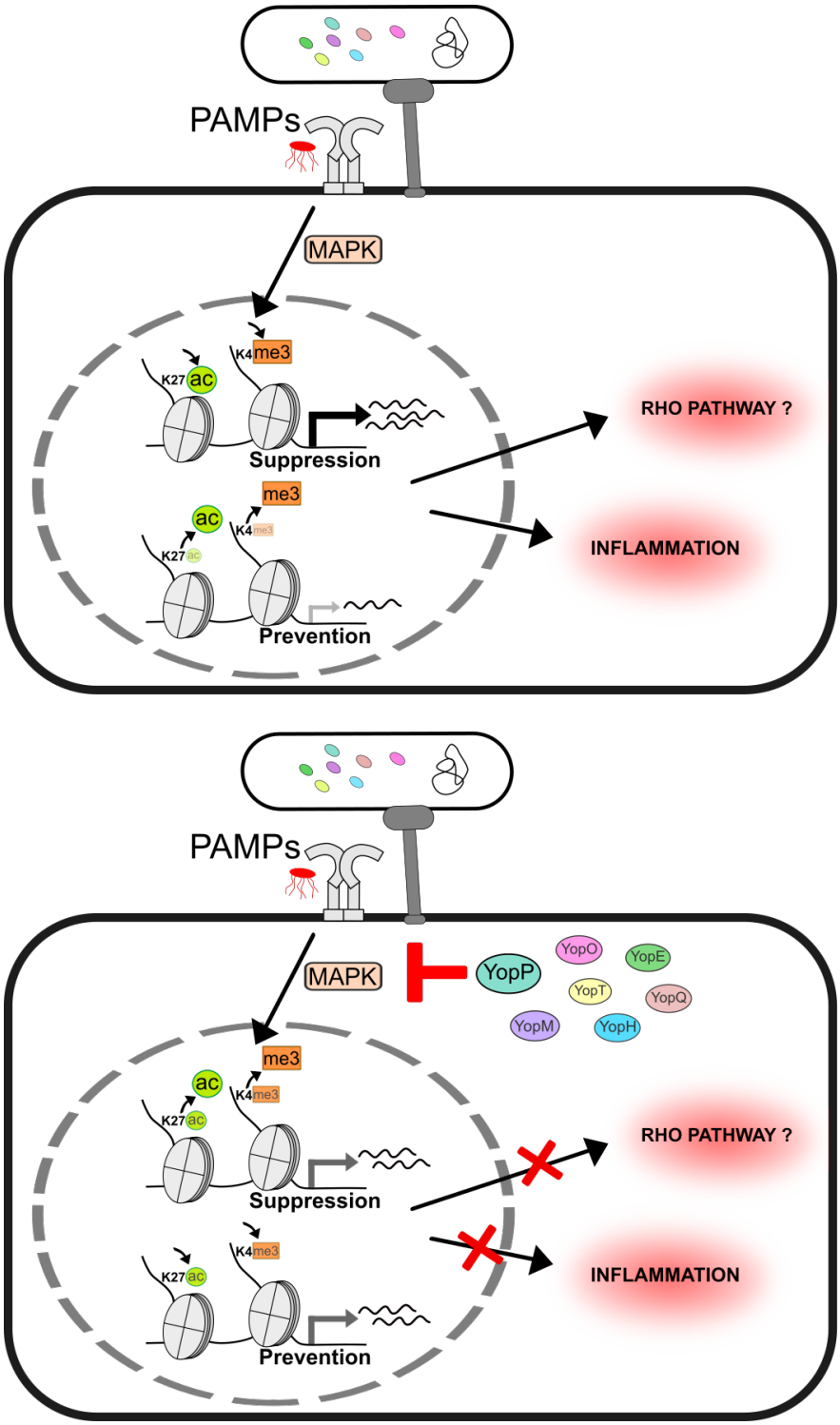

FIGURE 5.1: **Summary schematic of *Yersinia*-induced gene expression and histone modification changes in macrophages.** PAMPs of *Y. enterocolitica* activate MAPK pathway which trigger deposition or removal of H3K4me3 and H3K27ac at specific target gene promoters and enhancers to modulate gene expression and subsequent inflammation and potentially Rho GTPase pathway (top). *Yersinia* T3SS effectors mainly through the activity of YopP counteract PAMP-induced signalling to suppress deposition of H3K4me3 and H3K27ac (Suppression) and prevent removal of H3K4me3 and H3K27ac (Prevention; bottom). *Yersinia* modulation of histone marks affects subsequent gene expression and associated inflammatory processes and possibly Rho GTPase pathway in macrophages.

6 Supplementary material

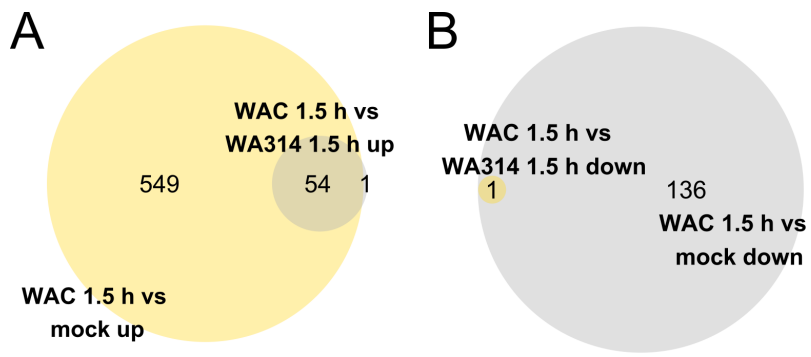

FIGURE 6.1: **Analysis of DEG overlaps. (A, B)** Venn diagrams showing overlap of DEGs.

TABLE 6.1 Metabolic pathways associated with Prevention profile in RNA-seq

Term: hsa00100:Steroid biosynthesis **Genes (6)**: MSMO1, SQLE, FAXDC2, DHCR7, NSDHL, DHCR24
Term: hsa01212:Fatty acid metabolism **Genes (10)**: CPT2, HACD3, HACD2, EHHADH, MCAT, ACACA, FASN, FADS2, ACAT2, OXSM
Term: hsa00970:Aminoacyl-tRNA biosynthesis **Genes (13)**: QRSL1, TARS2, PSTK, PARS2, NARS2, MARS2, IARS2, FARSA, LARS2, DARS2, SARS2, GATB, EARS2
Term: hsa00510:N-Glycan biosynthesis **Genes (11)**: MGAT4A, ST6GAL1, FUT8, ALG10B, ALG1, ALG6, ALG10, ALG11, DOLPP1, MAN1C1, DOLK
Term: hsa00561:Glycerolipid metabolism **Genes (11)**: LPL, AGPAT5, DGAT2, ALDH1B1, DGKG, DGKZ, LCLAT1, PNPLA3, GPAM, GPAT3, LPIN3

TABLE 6.2 Selected pathways associated with Suppression and Prevention profile genes with gene expression and histone modification changes

Profile: Suppression **Term**: GO:0006954 inflammatory response **P-value**: 1.20E-18 **Genes (83)**: PTGS2, TBK1, IL18, IL19, TLR2, NFKB1, IL15, SGMS1, NFKB2, IL10, CCRL2, PTGIR, NOD1, CCL3L1, SEMA7A, IL1RAP, TICAM1, IL1B, FAS, TNIP1, IL1A, TNIP3, IRAK2, NFKBIZ, DAB2IP, PTGER2, SP100, ADGRE2, GBP5, LYN, IL27, RELA, CCL4L2, CD40, IFI16, NLRP1, SIGLEC1, TNFRSF9, TNFAIP6, CCR7, RIPK2, NFE2L2, TNFAIP3, ACOD1, CCL1, CCL3, IL36G, NMI, TNF, ADORA2A, CSF1, CXCL3, CXCL2, CCL8, CXCL8, MAPKAPK2, CCL5, CCL4, IL23A, CCL20, MEFV, REL, RAC1, TNFRSF18, BCL6, PTX3, THBS1, BMP2, IL6, IL2RA, HCK, SPHK1, ANXA1, CCL18, AIM2, EPHA2, GGT5, APOL3, P2RX7, HDAC9, PLA2G4C, IGFBP4, BMP6
Profile: Prevention **Term**: GO:0051056 regulation of small GTPase mediated signal transduction pathways **P-value**: 2.53E-04 **Genes (17)**: BCR, VAV3, SIPA1L3, ARHGAP35, RACGAP1, FAM13A, ARHGAP12, STARD13, RHOBTB2, RHOBTB1, OPHN1, CHN2, ARHGAP11A, ARAP3, RAP1GAP2, ARHGAP9, FGD4

TABLE 6.3 Pathways associated with latent enhancers

Term: GO:0000122 negative regulation of transcription from RNA polymerase II promoter **P-value**: 5.90E-05 **Genes (19)**: ATF7IP, SP100, JARID2, SMAD7, EDN1, PKIG, EZH2, NFKB1, ZEB2, REST, FOXP1, KDM2B, REL, BCL11A, H2AFY2, NEDD4L, RBPJ, CUX1, NFATC2
Term: GO:0060333 interferon-gamma-mediated signalling pathway **P-value**: 3.93E-04 **Genes (6)**: ICAM1, SP100, IRF6, PML, IRF1, OAS2
Term: GO:0006915 apoptotic process **P-value**: 4.20E-03 **Genes (13)**: STEAP3, TNFRSF9, SGK1, IL2RA, BCL2, IL19, PML, IRF1, NFKB1, EFNA5, NR3C1, TNFAIP3, AHR
Term: GO:0005096 GTPase activator activity **P-value**: 9.25E-04 **Genes (13)**: TBC1D16, RALGAPA2, TIAM2, PREX2, CHN1, MYO9B, CDC42EP3, SRGAP1, DOCK4, ADPRH
Term: GO:0006954 inflammatory response **P-value**: 6.21E-03 **Genes (10)**: TNFRSF9, TNFAIP6, CCR7, SP100, IL2RA, REL, IL19, CCL3L3, NFKB1, TNFAIP3

TABLE 6.4 Rho GTPase specificity of effector proteins with gene expression and histone modification change for different profiles

Specificity	Suppression	Prevention	Up
Cdc42	12	7	1
Rac1	12	6	1
RhoA	9	5	2
RhoB	8	2	2
Rac3	7	2	1
RhoC	7	2	1

Continued on next page

Table 6.4 – *continued from previous page*

Specificity	Suppression	Prevention	Up
Rac2	5	1	1
Rnd3	5	1	0
RhoBTB1	5	0	0
RhoBTB2	5	0	0
RhoF	5	0	0
RhoD	4	1	0
RhoG	4	1	1
RhoJ	4	1	2
RhoQ	4	1	2
RhoV	3	2	0
Rnd2	3	1	0
RhoH	3	0	2
Rnd1	3	0	0
RhoU	2	1	0
unique	**46**	**17**	**5**

TABLE 6.5 Summary of Rho GTPase pathway genes belonging to Suppression (top) and Prevention (bottom) profiles which show strong regulation by WA314 (FC >2, adjusted P-value <0.05) in RNA-seq and ChIP-seq

Symbol	Class ChIP-seq	Class RNA-seq	% YopP effect ChIP-seq	% YopP effect RNA-seq	Chr	Start	End	H3 mark
ABL2	P1a	R1	24	26	chr1	179105201	179111300	K4me3
ABL2	P1a	R1	60	26	chr1	179112801	179114000	K4me3
ABL2	P1a	R1	83	26	chr1	179105201	179111300	K27ac
ABL2	P1a	R1	63	26	chr1	179112801	179114000	K27ac
ABL2	E1	R1	30	26	chr1	179142801	179146200	K27ac
ABL2	E1	R1	51	26	chr1	179155901	179158600	K27ac
ABL2	E1	R1	30	26	chr1	179158801	179161800	K27ac
DEPDC1B	P2a	R1	64	26	chr5	59994701	59996500	K27ac
HNRNPC	P1a	R1	60	61	chr14	21721801	21736600	K4me3
HNRNPC	E1	R1	121	61	chr14	21711101	21713800	K27ac
RHOH	P1a	R1	50	90	chr4	40197901	40202300	K4me3
RHOH	P1a	R1	9	90	chr4	40197901	40202300	K27ac
RHOH	E1	R1	11	90	chr4	40180501	40187700	K27ac
RHOH	E1	R1	-4	90	chr4	40239101	40246500	K27ac
RHOU	P2a	R1	4	65	chr1	228871501	228874600	K27ac

Continued on next page

Table 6.5 – *continued from previous page*

Symbol	Class ChIP-seq	Class RNA-seq	% YopP effect ChIP-seq	% YopP effect RNA-seq	Chr	Start	End	H3 mark
RHOU	E1	R1	104	65	chr1	228913201	228916400	K27ac
RHOU	E1	R1	30	65	chr1	228960101	228965300	K27ac
RHOU	E1	R1	97	65	chr1	228976901	228979500	K27ac
ABI1	P1a	R2	35	103	chr10	27141901	27148800	K4me3
ABI1	P1a	R2	94	103	chr10	27141901	27148800	K27ac
ABI1	E1	R2	72	103	chr10	27118901	27120100	K27ac
ARHGAP10	E1	R2	67	21	chr4	148927201	148930400	K27ac
ARHGAP10	E1	R2	44	21	chr4	148950301	148952700	K27ac
ARHGAP27	E1	R2	87	31	chr17	43452601	43454400	K27ac
ARL13B	P2a	R2	23	2	chr3	93698201	93700200	K27ac
BASP1	P1a	R2	77	90	chr5	17218201	17232100	K4me3
BASP1	P1a	R2	14	90	chr5	17218201	17232100	K27ac
BASP1	E1	R2	61	90	chr5	17180801	17183400	K27ac
BASP1	E1	R2	11	90	chr5	17184201	17186600	K27ac
BASP1	E1	R2	15	90	chr5	17186601	17188600	K27ac
BASP1	E1	R2	23	90	chr5	17220401	17223000	K27ac
BASP1	E1	R2	22	90	chr5	17238201	17240500	K27ac
BASP1	E1	R2	77	90	chr5	17266001	17268800	K27ac
BASP1	E1	R2	79	90	chr5	17283601	17286400	K27ac
CAVIN1	P1a	R2	52	61	chr17	40571301	40576100	K4me3
CPNE8	E1	R2	79	13	chr12	39165801	39171400	K27ac
CPNE8	E1	R2	66	13	chr12	39243501	39246300	K27ac
DOCK4	E1	R2	-3	38	chr7	111691301	111697900	K27ac
DOCK4	E1	R2	23	38	chr7	111699301	111702400	K27ac
DOCK4	E1	R2	-16	38	chr7	111718301	111726900	K27ac
DOCK4	E1	R2	36	38	chr7	111751001	111757700	K27ac
DOCK4	E1	R2	111	38	chr7	111790001	111791300	K27ac
EPSTI1	P1a	R2	61	53	chr13	43561301	43566500	K4me3
EPSTI1	P1a	R2	38	53	chr13	43561301	43566500	K27ac
EPSTI1	E1	R2	56	53	chr13	43465801	43468400	K27ac
FGD2	E1	R2	100	36	chr6	37058901	37060700	K27ac
FNBP1	E1	R2	18	2	chr9	132671301	132674700	K27ac
FNBP1	E1	R2	76	2	chr9	132745701	132748400	K27ac
FNBP1	E1	R2	123	2	chr9	132752101	132755200	K27ac
FNBP1	E1	R2	144	2	chr9	132792501	132793700	K27ac

Continued on next page

Table 6.5 – *continued from previous page*

Symbol	Class ChIP-seq	Class RNA-seq	% YopP effect ChIP-seq	% YopP effect RNA-seq	Chr	Start	End	H3 mark
NCK2	P2a	R2	1	77	chr2	106361501	106365700	K27ac
RAP1B	P1a	R2	48	94	chr12	69006201	69017500	K4me3
RAP1B	P1a	R2	75	94	chr12	69006201	69017500	K27ac
RAP1B	E1	R2	93	94	chr12	69041201	69043000	K27ac
RND1	E1	R2	25	45	chr12	49274901	49279200	K27ac
SPEN	E1	R2	22	17	chr1	16220001	16221700	K27ac
STAT3	P2a	R2	7	44	chr17	40539701	40542700	K27ac
STAT3	E1	R2	39	44	chr17	40505601	40508800	K27ac
TAGAP	P1a	R2	58	24	chr6	159458701	159465400	K4me3
TAGAP	E1	R2	42	24	chr6	159510901	159515500	K27ac
TJP2	P1a	R2	-26	52	chr9	71788801	71793200	K27ac
TJP2	E1	R2	47	52	chr9	71794501	71796500	K27ac
Suppression average			**49.7**	**46.6**				
ARHGAP12	E4	R4	16	38	chr10	31997801	31999600	K27ac
ARHGAP12	E4	R4	55	38	chr10	32039701	32043800	K27ac
ARHGAP35	E4	R4	48	43	chr19	47478401	47482400	K27ac
ARHGAP35	E4	R4	23	43	chr19	47483201	47484800	K27ac
ARHGAP35	E4	R4	20	43	chr19	47486201	47489200	K27ac
ARHGAP35	P2d	R4	72	43	chr19	47364701	47365700	K27ac
ARHGAP9	P2d	R4	27	177	chr12	57869501	57872300	K27ac
FAM13A	E4	R4	18	165	chr4	89738901	89739900	K27ac
FAM13A	E4	R4	36	165	chr4	89750301	89751400	K27ac
FAM13A	E4	R4	37	165	chr4	89876001	89882900	K27ac
OPHN1	E4	R4	39	52	chrX	67424701	67425700	K27ac
PIK3R1	E4	R4	79	67	chr5	67547601	67548700	K27ac
PIK3R1	E4	R4	51	67	chr5	67714401	67717400	K27ac
PIK3R1	P2d	R4	97	67	chr5	67509301	67511000	K27ac
PPM1H	E4	R4	55	50	chr12	63025101	63027300	K27ac
RGS14	P2d	R4	79	104	chr5	176783701	176786000	K27ac
RHOBTB1	P2d	R4	53	86	chr10	62701401	62704300	K27ac
RHOBTB2	E4	R4	38	29	chr8	22835301	22836700	K27ac
WDR81	P2d	R4	56	53	chr17	1623701	1629700	K27ac
Prevention average			**47.3**	**78.5**				

TABLE 6.6 Summary of inflammatory response genes belonging to Suppression profile which show strong suppression by WA314 (FC >2, adjusted P-value <0.05) in RNA-seq and ChIP-seq

Symbol	Class ChIP-seq	Class RNA-seq	% YopP effect ChIP-seq	% YopP effect RNA-seq	Chr	Start	End	H3 mark
ACOD1	P1a	R1	47	61	chr13	77521701	77527000	K4me3
ADORA2A	P1a	R1	75	54	chr22	24818601	24825300	K4me3
ADORA2A	P2a	R1	-16	54	chr22	24827901	24833900	K27ac
AIM2	E1	R2	64	22	chr1	159059401	159062100	K27ac
AIM2	E1	R2	50	22	chr1	159082801	159084800	K27ac
AIM2	P1a	R2	37	22	chr1	159044001	159047300	K4me3
ANXA1	E1	R1	64	81	chr9	75770201	75771900	K27ac
ANXA1	E1	R1	73	81	chr9	75879801	75881200	K27ac
ANXA1	E1	R1	63	81	chr9	75730601	75734800	K27ac
ANXA1	E1	R1	64	81	chr9	75756001	75757700	K27ac
BMP6	E1	R2	12	70	chr6	7728801	7733500	K27ac
CCL18	E1	R2	52	42	chr17	34381801	34384300	K27ac
CCL18	P2a	R2	36	42	chr17	34390301	34391900	K27ac
CCL20	E1	R1	85	42	chr2	228681701	228682700	K27ac
CCL20	P1a	R1	85	42	chr2	228677701	228682900	K4me3
CCL20	P1a	R1	-36	42	chr2	228677701	228682900	K27ac
CCL3	P1a	R1	124	50	chr17	34417501	34420700	K4me3
CCL3	P1a	R1	-21	50	chr17	34412701	34416200	K27ac
CCL3	P1a	R1	-4	50	chr17	34417501	34420700	K27ac
CCL3L1	P2a	R1	32	39	chr17	34625201	34628200	K27ac
CCL4	P1a	R1	112	39	chr17	34429701	34436200	K4me3
CCL4	P1a	R1	3	39	chr17	34429701	34436200	K27ac
CCL5	P1a	R2	16	23	chr17	34200201	34208600	K27ac
CCL5	P1a	R2	100	23	chr17	34200201	34208600	K4me3
CCR7	E1	R2	34	66	chr17	38697601	38701000	K27ac
CCR7	P1a	R2	13	66	chr17	38715401	38722600	K27ac
CCR7	P1a	R2	60	66	chr17	38715401	38722600	K4me3
CD40	E1	R2	54	56	chr20	44735101	44737900	K27ac
CD40	P1a	R2	59	56	chr20	44745901	44752400	K4me3
CSF1	E1	R1	57	68	chr1	110431401	110432700	K27ac
CXCL2	P1a	R1	-39	-14	chr4	74959201	74964800	K27ac
CXCL3	E1	R1	40	6	chr4	74898201	74900200	K27ac
CXCL8	E1	R1	-2	44	chr4	74585901	74596500	K27ac
CXCL8	P1a	R1	17	44	chr4	74606201	74613700	K4me3
CXCL8	P1a	R1	-22	44	chr4	74606201	74613700	K27ac

Continued on next page

Table 6.6 – *continued from previous page*

Symbol	Class ChIP-seq	Class RNA-seq	% YopP effect ChIP-seq	% YopP effect RNA-seq	Chr	Start	End	H3 mark
GBP5	P1a	R2	35	39	chr1	89733901	89740400	K4me3
IL10	E1	R1	66	75	chr1	206925001	206928200	K27ac
IL10	P1a	R1	103	75	chr1	206945701	206947700	K4me3
IL1A	E1	R1	18	24	chr2	113550201	113558300	K27ac
IL1A	P1a	R1	48	24	chr2	113536001	113542600	K4me3
IL1B	P1a	R1	4	45	chr2	113584701	113600700	K27ac
IL1B	P1a	R1	90	45	chr2	113584701	113600700	K4me3
IL1RAP	E1	R2	35	81	chr3	190249701	190253100	K27ac
IL1RAP	E1	R2	81	81	chr3	190282801	190284800	K27ac
IL1RAP	E1	R2	91	81	chr3	190303601	190305600	K27ac
IL23A	P1a	R1	89	61	chr12	56731801	56737900	K4me3
IL23A	P1a	R1	9	61	chr12	56731801	56737900	K27ac
IL27	E1	R2	70	67	chr16	28510701	28513600	K27ac
IL27	P1a	R2	52	67	chr16	28507301	28523100	K4me3
IL27	P1a	R2	11	67	chr16	28507301	28523100	K27ac
IL2RA	E1	R2	28	48	chr10	6086101	6089000	K27ac
IL2RA	E1	R2	21	48	chr10	6073901	6078900	K27ac
IL2RA	E1	R2	-47	48	chr10	6111501	6117500	K27ac
IL2RA	P1a	R2	6	48	chr10	6099501	6105200	K27ac
IL2RA	P1a	R2	19	48	chr10	6099501	6105200	K4me3
IL6	P1a	R1	37	53	chr7	22766101	22771400	K4me3
IL6	P1a	R1	-1	53	chr7	22766101	22771400	K27ac
IRAK2	E1	R1	40	44	chr3	10232501	10242600	K27ac
IRAK2	P1a	R1	23	44	chr3	10206201	10213400	K27ac
MAPKAPK2	E1	R1	-21	103	chr1	206852701	206855700	K27ac
MAPKAPK2	E1	R1	67	103	chr1	206886901	206887900	K27ac
MAPKAPK2	E1	R1	36	103	chr1	206878501	206882200	K27ac
NFKB1	E1	R2	68	58	chr4	103539201	103542100	K27ac
NFKB1	P1a	R2	11	58	chr4	103424001	103434100	K4me3
NLRP1	P2a	R2	107	-57	chr17	5488701	5489700	K27ac
NOD1	E1	R2	-80	93	chr7	30503901	30506600	K27ac
NOD1	P2a	R2	-1	93	chr7	30510801	30517500	K27ac
PTGIR	P1a	R2	62	44	chr19	47123501	47129400	K4me3
PTGS2	E1	R1	3	58	chr1	186583201	186591800	K27ac
PTGS2	P1a	R1	56	58	chr1	186637601	186654100	K4me3

Continued on next page

Table 6.6 – *continued from previous page*

Symbol	Class ChIP-seq	Class RNA-seq	% YopP effect ChIP-seq	% YopP effect RNA-seq	Chr	Start	End	H3 mark
PTGS2	P1a	R1	0	58	chr1	186637601	186654100	K27ac
RIPK2	P1a	R2	46	44	chr8	90771201	90781800	K4me3
SIGLEC1	P1a	R2	66	6	chr20	3688701	3691500	K4me3
THBS1	E1	R1	-27	101	chr15	39718601	39720400	K27ac
THBS1	P2a	R1	-15	101	chr15	39872601	39873700	K27ac
TNF	P1a	R1	92	20	chr6	31541901	31549700	K4me3
TNF	P1a	R1	8	20	chr6	31541901	31549700	K27ac
TNFAIP3	E1	R1	46	31	chr6	138222801	138233600	K27ac
TNFAIP3	E1	R1	40	31	chr6	138166001	138176200	K27ac
TNFAIP3	E1	R1	71	31	chr6	138212201	138217500	K27ac
TNFAIP3	P1a	R1	139	31	chr6	138185901	138187400	K4me3
TNFAIP3	P1a	R1	-1	31	chr6	138185901	138187400	K27ac
TNFAIP6	P1a	R2	62	44	chr2	152212301	152230300	K4me3
TNFAIP6	P1a	R2	1	44	chr2	152212301	152230300	K27ac
TNFRSF9	P1a	R2	57	19	chr1	7995901	8001700	K4me3
TNIP1	P1a	R2	7	77	chr5	150460601	150467900	K27ac
TNIP1	P1a	R2	139	77	chr5	150442601	150450600	K4me3
TNIP1	P1a	R2	64	77	chr5	150460601	150467900	K4me3
TNIP1	P1a	R2	1	77	chr5	150453201	150460500	K27ac
TNIP1	P1a	R2	15	77	chr5	150442601	150450600	K27ac
TNIP3	E1	R2	20	26	chr4	122075501	122079400	K27ac
TNIP3	P1a	R2	51	26	chr4	122078401	122086300	K4me3
TNIP3	P1a	R2	1	26	chr4	122078401	122086300	K27ac
		Average	**37.7**	**46.5**				

7 Abbreviations

°C	degree Celsius
A	adenine
ABI1	Abl interactor 1
ac	acetylation
ACACA	acetyl-CoA carboxylase 1
ACO2	aconitase 2
ACTN1	actinin alpha 1
ADP	adenosine diphosphate
Ail	attachment and invasion locus
aka	also known as
AP-1	activator protein 1
APS	ammonium persulfate
ATP	adenosine triphosphate
BAIAP2	BAR/IMD domain containing adaptor protein 2
bHLH	basic helix-loop-helix
BMDMs	bone marrow derived macrophages
bp	basepair
BSA	bovine serum albumin
bZIP	basic leucine zipper domain
C	cytosine
C/EBP	CCAAT-enhancer-binding proteins
$CaCl_2$	calcium chloride
Cdc42	cell division cycle 42 GTP binding protein
ChIP	chromatin immunoprecipitation
chlor	chloramphenicol
CLR	C-type lectin receptor
cm	centimeter
CNF	cytotoxic necrotizing factor
CPT2	carnitine O-palmitoyltransferase 2
DAMP	danger-associated molecular patterns
ddH_2O	distilled water
DDX3	DEAD box helicase 3
DEG	differentially expressed gene
DIAPH1	diaphanous homolog 1
DMSO	dimethyl sulfoxide
DNA	deoxyribonucleic acid
DR	differential region
e.g.	for example
EDTA	ethylenediaminetetraacetic acid
ERK	extracellular signal-regulated kinase
ETS	E26 transformation-specific
F	forward
FA	fatty acid
FADS2	fatty acid desaturase 2
FASN	fatty acid synthase
FC	fold change
FDR	false discovery rate
FKHRL1	forkhead homolog (rhabdomyosarcoma) like 1
FNBP1	formin binding protein 1
mA	mili ampere
MAP3K4	mitogen-activated protein kinase kinase kinase 4
MAPK	mitogen-activated protein kinase
MCP-1	macrophage chemotactic factor 1
MD-2	myeloid differentiation factor 2
MDa	megadalton
me	methylation
mg	miligram
$MgCl_2$	magnesium chloride
min	minute
MKK	mitogen activated protein kinase (MAPK) kinase
ml	mililiter
mM	milimolar
MOI	multiplicity-of-infection
mRNA	messenger-RNA
MRTF	myocardin related transcription factor
MTB	Mycobacterium tuberculosis
MX2	myxovirus resistance 2
Myd88	myeloid differentiation primary response 88
nal	nalidixic acid
NF-κB	nuclear factor kappa-light-chain-enhancer of activated B cells
NFY	nuclear transcription factor Y
ng	nanogram
NGS	next-generation sequencing
NLR	nucleotide-binding oligomerization domain (NOD)-like receptor
nM	nanomolar
NR	nuclear receptor
NR1D1	nuclear receptor subfamily 1 group D member 1
OD	optical density
OPHN1	oligophrenin-1
PAGE	polyacrylamide gel electrophoresis
PAMP	pathogen-associated molecular patterns
PBS	phosphate buffer saline
PBS-T	PBS with Tween-20
PCA	principal component analysis
ph	phosporylation
PI	phosphoinositide
PKN	protein kinase N
PPARA	peroxisome proliferator-activated receptor alpha
PRG	primary response gene
PRR	pattern recognition receptor
PTGS2	prostaglandin-endoperoxide synthase 2
PTM	Post-translational modification
PVDF	polyvinylidenfluoride
pYV	plasmid Yersinia virulence
qPCR	quantitative polymerase chain reaction
R	reverse
Rac	Ras-related C3 botulinum toxin substrate
RARG	retinoic acid receptor gamma

FOXO1	forkhead box O1
FZD4	frizzled class receptor 4
g	gram
G	guanine
g	relative centrifugal force
Gabpa	GA binding protein transcription factor subunit alpha
GAP	GTPase activating protein
GBP	guanylate binding protein
GDI	GDP dissociation inhibitor
GDP	guanosine diphosphate
GEF	guanine nucleotide exchange factor
GILZ	glucocorticoid-induced leucine zipper
GM-CSF	granulocyte-macrophage colony-stimulating factor
GO	gene ontology
GPCR	G protein-coupled receptor
GSDM	gasdermin
GSK3	glycogen synthase kinase 3
GTP	guanosine-5'-triphosphate
H	histone
h	hour
HBP	d-β-d-heptose 1-phosphate
HP1	heterochromatin protein 1
HPI	high pathogenicity island
HRP	horse radish peroxidase
IDH1	isocitrate dehydrogenase 1
IDO1	indoleamine 2,3-dioxygenase 1
IFN	interferon
IFNAR	interferon (IFN) alpha receptor
IKK	inhibitor of nuclear factor kappaB (IkB) kinase
IKZF4	ikaros family zinc-finger 4
IL	interleukin
IQGAP1	IQ motif containing GTPase activating protein 1
IRF	interferon regulatory factor
ISRE	interferon-sensitive response element
JAK	janus kinase
JNK	c-Jun NH2-terminal kinase
K	lysine
K^+	potassium
kana	kanamycin
kb	kilobase
kDa	kilodalton
KEGG	Kyoto Encyclopedia of Genes and Genomes
KLF2	krueppel-like factor 2
KRAB	kruppel-associated box
L	liter
LAMP1	lysosomal associated membrane protein 1
LB	lysogeny broth (Luria-Bertani)
LCR	low calcium response
LDTF	lineage determining transcription factor (TF)
LRR	leucine rich repeat
M	molar
M cells	microfold cells
RHD	rel homology domain
Rho	Ras homologous
RhoBTB	Rho related BTB domain containing
RIPK1	receptor-interacting serine/threonine-protein kinase 1
RLR	retinoic acid-inducible gene (RIG)-I-like receptor
RNA	ribonucleic acid
ROCK2	Rho associated coiled-coil containing protein kinase 2
ROS	reactive oxygen species
rpm	revolutions per minute
RSK	ribosomal S6 kinase
RT	room temperature
s	second
S	serine
SD	standard deviation
SDS	sodium dodecylsulfate
seq	sequencing
SH3RF1	SH3 domain containing ring finger 1
SP-1	specificity protein 1
SPEN	spen family transcriptional repressor
spp.	species
SRF	serum response factor
SRG	secondary response gene
SRTF	stimulus regulated transcription factor
STAT	signal transducer and activator of transcription
T	thymine
t-RNA	transfer RNA
T3SS	type three secretion system
TAD	topologically associated domain
TAE	Tris-acetate EDTA
TAK1	transforming growth factor beta-activated kinase 1
TBS	tris buffered saline
TBS-T	TBS with Tween-20
TCA	trichloroacetic acid
TF	transcription factor
TGF-β	transforming growth factor beta
TLR	Toll-like receptor
TNF	tumor necrosis factor
Trif	Toll/IL-1R homology (TIR)-domain-containing adapter-inducing interferon-beta
TSS	transcirption start site
U	Uracil
UV	ultraviolet
V	volt
WB	Western blot
YadA	Yersinia adhesin A
Yop	Yersinia Outer Protein
YpkA	Yersinia protein kinase A
YY1	ying yang 1
ZNF	zinc-finger gene
µg	microgram
µl	microliter
µm	micrometer
µM	micromolar

8 References

[1] A. McNally, N. R. Thomson, S. Reuter, and B. W. Wren, "'Add, stir and reduce': Yersinia spp. as model bacteria for pathogen evolution", Nature Reviews Microbiology **14**, 177–190 (2016).

[2] A. Łyskowski, J. C. Leo, and A. Goldman, "Structure and Biology of Trimeric Autotransporter Adhesins", in *Bacterial Adhesion: Chemistry, Biology and Physics*, edited by D. Linke and A. Goldman (Springer Netherlands, Dordrecht, 2011), pp. 143–158.

[3] R. D. Perry and J. D. Fetherston, "Yersinia pestis - Etiologic agent of plague", Clinical Microbiology Reviews **10**, 35–66 (1997).

[4] A. Chlebicz and K. Śliżewska, "Campylobacteriosis, Salmonellosis, Yersiniosis, and Listeriosis as Zoonotic Foodborne Diseases: A Review", International Journal of Environmental Research and Public Health **15**, 1–28 (2018).

[5] G. I. Viboud and J. B. Bliska, " YERSINIA OUTER PROTEINS: Role in Modulation of Host Cell Signaling Responses and Pathogenesis ", Annual Review of Microbiology **59**, 69–89 (2005).

[6] E. Carniel, I. Autenrieth, G. Cornelis, H. Fukushima, F. Guinet, R. Isberg, J. Pham, M. Prentice, M. Simonet, M. Skurnik, and G. Wauters, "Y. enterocolitica and Y. pseudotuberculosis", in *The Prokaryotes: Volume 6: Proteobacteria: Gamma Subclass*, edited by M. Dworkin, S. Falkow, E. Rosenberg, K.-H. Schleifer, and E. Stackebrandt (Springer New York, New York, NY, 2006), pp. 270–398.

[7] E. Carniel, "Plasmids and Pathogenicity Islands of Yersinia", in *Pathogenicity Islands and the Evolution of Pathogenic Microbes: Volume I*, edited by J. Hacker and J. B. Kaper (Springer Berlin Heidelberg, Berlin, Heidelberg, 2002), pp. 89–108.

[8] B. W. Wren, "The Yersiniae — a model genus to study the rapid evolution of bacterial pathogens", Nature Reviews Microbiology **1**, 55–64 (2003).

[9] Y. Sabina, A. Rahman, R. C. Ray, and D. Montet, " Yersinia enterocolitica : Mode of Transmission, Molecular Insights of Virulence, and Pathogenesis of Infection ", Journal of Pathogens **2011**, 1–10 (2011).

[10] J. Heesemann, "Chromosomal-encoded siderophores are required for mouse virulence of enteropathogenic Yersinia species", FEMS Microbiology Letters **48**, 229–233 (1987).

[11] A. Rakin, D. Garzetti, H. Bouabe, and L. D. Sprague, "Chapter 73 - Yersinia enterocolitica", in *Molecular Medical Microbiology (Second Edition)*, edited by Y.-W. Tang, M. Sussman, D. Liu, I. Poxton, and J. Schwartzman, Second Edition (Academic Press, Boston, 2015), pp. 1319 –1344.

[12] M. Fredriksson-Ahomaa, A. Stolle, and H. Korkeala, "Molecular epidemiology of Yersinia enterocolitica infections", FEMS Immunology and Medical Microbiology **47**, 315–329 (2006).

[13] L. Navarro, N. M. Alto, and J. E. Dixon, "Functions of the Yersinia effector proteins in inhibiting host immune responses", Current Opinion in Microbiology **8**, 21–27 (2005).

[14] G. R. Cornelis, "Yersinia type III secretion: Send in the effectors", Journal of Cell Biology **158**, 401–408 (2002).

[15] R. S. Dewoody, P. M. Merritt, and M. M. Marketon, "Regulation of the Yersinia type III secretion system: Traffic control", Frontiers in Cellular and Infection Microbiology **4**, 1–13 (2013).

[16] M. Aepfelbacher and M. Wolters, "Acting on Actin: Rac and Rho Played by Yersinia", in *The Actin Cytoskeleton and Bacterial Infection*, edited by H. G. Mannherz (Springer International Publishing, Cham, 2017), pp. 201–220.

[17] J. Eitel and P. Dersch, "The YadA Protein of Yersinia pseudotuberculosis Mediates High-Efficiency Uptake into Human Cells under Environmental Conditions in Which Invasin Is Repressed", Infection and Immunity **70**, 4880–4891 (2002).

[18] S. Wagner, I. Grin, S. Malmsheimer, N. Singh, C. E. Torres-Vargas, and S. Westerhausen, "Bacterial type III secretion systems: A complex device for the delivery of bacterial effector proteins into eukaryotic host cells", FEMS Microbiology Letters **365**, 1–13 (2018).

[19] T. Nauth, F. Huschka, M. Schweizer, J. B. Bosse, A. Diepold, A. V. Failla, A. Steffen, T. Stradal, M. Wolters, and M. Aepfelbacher, "Visualization of translocons in Yersinia type III protein secretion machines during host cell infection", PLoS Pathogens **14**, 1–29 (2018).

[20]V. T. Lee, D. M. Anderson, and O. Schneewind, "Targeting of Yersinia Yop proteins into the cytosol of HeLa cells: One- step translocation of YopE across bacterial and eukaryotic membranes is dependent on SycE chaperone", Molecular Microbiology **28**, 593–601 (1998).

[21]K. Guan and J. E. Dixon, "Protein tyrosine phosphatase activity of an essential virulence determinant in Yersinia", Science **249**, 553–556 (1990).

[22]B. Grabowski, M. A. Schmidt, and C. Rüter, "Immunomodulatory Yersinia outer proteins (Yops)–useful tools for bacteria and humans alike", Virulence **8**, 1124–1147 (2017).

[23]M Fällman, K Andersson, S Håkansson, K. E. Magnusson, O Stendahl, and H Wolf-Watz, "Yersinia pseudotuberculosis inhibits Fc receptor-mediated phagocytosis in J774 cells.", Infection and Immunity **63**, 3117–3124 (1995).

[24]K. Ruckdeschel, A. Roggenkamp, S. Schubert, and J. Heesemann, "Differential contribution of Yersinia enterocolitica virulence factors to evasion of microbicidal action of neutrophils", Infection and Immunity **64**, 724–733 (1996).

[25]N. Sauvonnet, I. Lambermont, P. Van Der Bruggen, and G. R. Cornelis, "YopH prevents monocyte chemoattractant protein 1 expression in macrophages and T-cell proliferation through inactivation of the phosphatidylinositol 3-kinase pathway", Molecular Microbiology **45**, 805–815 (2002).

[26]H. G. Rolán, E. A. Durand, and J. Mecsas, "Identifying Yersinia YopH-targeted signal transduction pathways that impair neutrophil responses during in vivo murine infection", Cell Host and Microbe **14**, 306–317 (2013).

[27]K. Ruckdeschel, J. Machold, A. Roggenkamp, S. Schubert, J. Pierre, R. Zumbihl, J.-P. Liautard, J. Heesemann, and B. Rouot, " Yersinia enterocolitica Promotes Deactivation of Macrophage Mitogen-activated Protein Kinases Extracellular Signal-regulated Kinase-1/2, p38, and c-Jun NH 2 -terminal Kinase ", Journal of Biological Chemistry **272**, 15920–15927 (1997).

[28]J. B. Bliska and D. S. Black, "Inhibition of the Fc receptor-mediated oxidative burst in macrophages by the Yersinia pseudotuberculosis tyrosine phosphatase", Infection and Immunity **63**, 681–685 (1995).

[29]K. Andersson, K. E. Magnusson, M. Majeed, O. Stendahl, and M. Fällman, "Yersinia pseudotuberculosis-induced calcium signaling in neutrophils is blocked by the virulence effector YopH", Infection and Immunity **67**, 2567–2574 (1999).

[30]C. Gerke, S. Falkow, and Y. H. Chien, "The adaptor molecules LAT and SLP-76 are specifically targeted by Yersinia to inhibit T cell activation", Journal of Experimental Medicine **201**, 361–371 (2005).

[31]Y. Tony, J. Mecsas, J. I. Healy, S. Falkow, and Y. H. Chien, "Suppression of T and B lymphocyte activation by a Yersinia pseudotuberculosis virulence factor, YopH", Journal of Experimental Medicine **190**, 1343–1350 (1999).

[32]L. K. Logsdon and J. Mecsas, "Requirement of the Yersinia pseudotuberculosis effectors YopH and YopE in colonization and persistence in intestinal and lymph tissues", Infection and Immunity **71**, 4595–4607 (2003).

[33]M. N. Dave, J. E. Silva, R. J. Eliçabe, M. B. Jeréz, V. P. Filippa, C. V. Gorlino, S. Autenrieth, I. B. Autenrieth, and M. S. Di Genaro, "Yersinia enterocolitica YopH-Deficient Strain Activates Neutrophil Recruitment to Peyer's Patches and Promotes Clearance of the Virulent Strain", Infection and Immunity **84**, 3172–3181 (2016).

[34]R. Rosqvist, Forsberg, M. Rimpiläinen, T. Bergman, and H. Wolf-Watz, "The cytotoxic protein YopE of Yersinia obstructs the primary host defence", Molecular Microbiology **4**, 657–667 (1990).

[35]M. Aili, E. L. Isaksson, S. E. Carlsson, H. Wolf-Watz, R. Rosqvist, and M. S. Francis, "Regulation of Yersinia Yop-effector delivery by translocated YopE", International Journal of Medical Microbiology **298**, 183–192 (2008).

[36]W. Songsungthong, M. C. Higgins, H. G. Rolán, J. L. Murphy, and J. Mecsas, "ROS-inhibitory activity of YopE is required for full virulence of Yersinia in mice", Cellular Microbiology **12**, 988–1001 (2010).

[37]G. I. Viboud, E. Mejía, and J. B. Bliska, "Comparison of YopE and YopT activities in counteracting host signalling responses to Yersinia pseudotuberculosis infection", Cellular Microbiology **8**, 1504–1515 (2006).

[38]L. K. Chung, Y. H. Park, Y. Zheng, I. E. Brodsky, P. Hearing, D. L. Kastner, J. J. Chae, and J. B. Bliska, "The Yersinia Virulence Factor YopM Hijacks Host Kinases to Inhibit Type III Effector-Triggered Activation of the Pyrin Inflammasome", Cell Host and Microbe **20**, 296 –306 (2016).

[39]D. Ratner, M. P. A. Orning, M. K. Proulx, D. Wang, M. A. Gavrilin, M. D. Wewers, E. S. Alnemri, P. F. Johnson, B. Lee, J. Mecsas, N. Kayagaki, J. D. Goguen, and E. Lien, "The Yersinia pestis Effector YopM Inhibits Pyrin Inflammasome Activation", PLoS Pathogens **12**, 1–17 (2016).

[40]P. Schotte, G. Denecker, A. Van Den Broeke, P. Vandenabeele, G. R. Cornelis, and R. Beyaert, "Targeting Rac1 by the Yersinia effector protein YopE inhibits caspase-1-mediated maturation and release of interleukin-1β", Journal of Biological Chemistry **279**, 25134–25142 (2004).

[41] D. S. Black and J. B. Bliska, "The RhoGAP activity of the Yersinia pseudotuberculosis cytotoxin YopE is required for antiphagocytic function and virulence", Molecular Microbiology **39**, 822–822 (2001).

[42] E. E. Galyov, S. Håkansson, Å. Forsberg, and H. Wolf-Watz, "A secreted protein kinase of Yersinia pseudotuberculosis is an indispensable virulence determinant", Nature **361**, 730–732 (1993).

[43] S. Håkansson, E. E. Galyov, R. Rosqvist, and H. Wolf-Watz, "The Yersinia YpkA Ser/Thr kinase is translocated and subsequently targeted to the inner surface of the HeLa cell plasma membrane", Molecular Microbiology **20**, 593–603 (1996).

[44] S. J. Juris, A. E. Rudolph, D. Huddler, K. Orth, and J. E. Dixon, "A distinctive role for the Yersinia protein kinase: Actin binding, kinase activation, and cytoskeleton disruption", Proceedings of the National Academy of Sciences of the United States of America **97**, 9431–9436 (2000).

[45] C. Trasak, G. Zenner, A. Vogel, G. Yüksekdag, R. Rost, I. Haase, M. Fischer, L. Israel, A. Imhof, S. Linder, M. Schleicher, and M. Aepfelbacher, "Yersinia protein kinase YopO is activated by a novel G-actin binding process", Journal of Biological Chemistry **282**, 2268–2277 (2007).

[46] E. Groves, K. Rittinger, M. Amstutz, S. Berry, D. W. Holden, G. R. Cornelis, and E. Caron, "Sequestering of Rac by the Yersinia effector YopO blocks Fcγ receptor-mediated phagocytosis", Journal of Biological Chemistry **285**, 4087–4098 (2010).

[47] K. Pha, M. E. Wright, T. M. Barr, R. A. Eigenheer, and L. Navarro, "Regulation of yersinia protein kinase A (YpkA) Kinase activity by Multisite autophosphorylation and identification of an n-terminal substrate-binding domain in YpkA", Journal of Biological Chemistry **289**, 26167–26177 (2014).

[48] W. L. Lee, J. M. Grimes, and R. C. Robinson, "Yersinia effector YopO uses actin as bait to phosphorylate proteins that regulate actin polymerization", Nature Structural and Molecular Biology **22**, 248–255 (2015).

[49] L. Navarro, A. Koller, R. Nordfelth, H. Wolf-Watz, S. Taylor, and J. E. Dixon, "Identification of a Molecular Target for the Yersinia Protein Kinase A", Molecular Cell **26**, 465–477 (2007).

[50] J. M. Dukuzumuremyi, R. Rosqvist, B. Hallberg, B. Åkerström, H. Wolf-Watz, and K. Schesser, "The Yersinia protein kinase A is a host factor inducible RhoA/Rac-binding virulence factor", Journal of Biological Chemistry **275**, 35281–35290 (2000).

[51] G. Prehna, M. I. Ivanov, J. B. Bliska, and C. E. Stebbins, "Yersinia Virulence Depends on Mimicry of Host Rho-Family Nucleotide Dissociation Inhibitors", Cell **126**, 869–880 (2006).

[52] D. J. Wiley, R. Nordfeldth, J. Rosenzweig, C. J. DaFonseca, R. Gustin, H. Wolf-Watz, and K. Schesser, "The Ser/Thr kinase activity of the Yersinia protein kinase A (YpkA) is necessary for full virulence in the mouse, mollifying phagocytes, and disrupting the eukaryotic cytoskeleton", Microbial Pathogenesis **40**, 234–243 (2006).

[53] K. Trülzsch, T. Sporleder, E. I. Igwe, H. Rüssmann, and J. Heesemann, "Contribution of the major secreted Yops of Yersinia enterocolitica O:8 to pathogenicity in the mouse infection model", Infection and Immunity **72**, 5227–5234 (2004).

[54] M. Iriarte and G. R. Cornelis, "YopT, a new Yersinia Yop effector protein, affects the cytoskeleton of host cells", Molecular Microbiology **29**, 915–929 (1998).

[55] I. Sorg, U. M. Goehring, K. Aktories, and G. Schmidt, "Recombinant Yersinia YopT leads to uncoupling of RhoA-effector Interaction", Infection and Immunity **69**, 7535–7543 (2001).

[56] R. Zumbihl, M. Aepfelbacher, A. Andor, C. A. Jacobi, K. Ruckdeschel, B. Rouot, and J. Heesemann, "The cytotoxin YopT of Yersinia enterocolitica induces modification and cellular redistribution of the small GTP-binding protein RhoA", Journal of Biological Chemistry **274**, 29289–29293 (1999).

[57] N. Grosdent, I. Maridonneau-Parini, M. P. Sory, and G. R. Cornelis, "Role of Yops and adhesins in resistance of Yersinia enterocolitica to phagocytosis", Infection and Immunity **70**, 4165–4176 (2002).

[58] F. Shao, P. M. Merritt, Z. Bao, R. W. Innes, and J. E. Dixon, "A Yersinia effector and a Pseudomonas avirulence protein define a family of cysteine proteases functioning in bacterial pathogenesis", Cell **109**, 575–588 (2002).

[59] F. Shao, P. O. Vacratsis, Z. Bao, K. E. Bowerst, C. A. Fierke, and J. E. Dixon, "Biochemical characterization of the Yersinia YopT protease: Cleavage site and recognition elements in Rho GTPases", Proceedings of the National Academy of Sciences of the United States of America **100**, 904–909 (2003).

[60] M. Aepfelbacher, C. Trasak, G. Wilharm, A. Wiedemann, K. Trülzsch, K. Krauss, P. Gierschik, and J. Heesemann, "Characterization of YopT effects on Rho GTPases in Yersinia enterocolitica-infected cells", Journal of Biological Chemistry **278**, 33217–33223 (2003).

[61] A. G. Evdokimov, D. E. Anderson, K. M. Routzahn, and D. S. Waugh, "Unusual molecular architecture of the Yersinia pestis cytotoxin YopM: A leucine-rich repeat protein with the shortest repeating unit", Journal of Molecular Biology **312**, 807–821 (2001).

[62]R. Benabdillah, L. J. Mota, S. Lützelschwab, E. Demoinet, and G. R. Cornelis, "Identification of a nuclear targeting signal in YopM from Yersinia spp.", Microbial Pathogenesis **36**, 247–261 (2004).

[63]A. Boland, S. Havaux, and G. R. Cornelis, "Heterogeneity of the Yersinia YopM protein", Microbial Pathogenesis **25**, 343–348 (1998).

[64]B. S. Reisner and S. C. Straley, "Yersinia pestis YopM: Thrombin binding and overexpression", Infection and Immunity **60**, 5242–5252 (1992).

[65]E. Skrzypek, C. Cowan, and S. C. Straley, "Targeting of the Yersinia pestis YopM protein into HeLa cells and intracellular trafficking to the nucleus", Molecular Microbiology **30**, 1051–1065 (1998).

[66]C. McDonald, P. O. Vacratsis, J. B. Bliska, and J. E. Dixon, "The Yersinia virulence factor YopM forms a novel protein complex with two cellular kinases", Journal of Biological Chemistry **278**, 18514–18523 (2003).

[67]M. Hentschke, L. Berneking, C. B. Campos, F. Buck, K. Ruckdeschel, and M. Aepfelbacher, "Yersinia virulence factor YopM induces sustained RSK activation by interfering with dephosphorylation", PLoS ONE **5**, 1–12 (2010).

[68]C. N. Larock and B. T. Cookson, "The yersinia virulence effector YopM binds caspase-1 to arrest inflammasome assembly and processing", Cell Host and Microbe **12**, 799–805 (2012).

[69]L. K. Chung, N. H. Philip, V. A. Schmidt, A. Koller, T. Strowig, R. A. Flavell, I. E. Brodsky, and J. B. Bliska, "IQGAP1 is important for activation of caspase-1 in macrophages and is targeted by Yersinia pestis type III effector YopM", mBio **5**, 1–11 (2014).

[70]L. Berneking, M. Schnapp, A. Rumm, C. Trasak, K. Ruckdeschel, M. Alawi, A. Grundhoff, A. G. Kikhney, F. Koch-Nolte, F. Buck, M. Perbandt, C. Betzel, D. I. Svergun, M. Hentschke, and M. Aepfelbacher, "Immunosuppressive Yersinia Effector YopM Binds DEAD Box Helicase DDX3 to Control Ribosomal S6 Kinase in the Nucleus of Host Cells", PLoS Pathogens **12**, 1–35 (2016).

[71]D. Ratner, M. P. A. Orning, K. K. Starheim, R. Marty-Roix, M. K. Proulx, J. D. Goguen, and E. Lien, "Manipulation of interleukin-1β and interleukin-18 production by Yersinia pestis effectors YopJ and YopM and redundant impact on virulence", Journal of Biological Chemistry **291**, 9894–9905 (2016).

[72]Y. H. Park, E. F. Remmers, W. Lee, A. K. Ombrello, L. K. Chung, Z. Shilei, D. L. Stone, M. I. Ivanov, N. A. Loeven, K. S. Barron, P. Hoffmann, M. Nehrebecky, Y. Z. Akkaya-Ulum, E. Sag, B. Balci-Peynircioglu, I. Aksentijevich, A. Gül, C. N. Rotimi, H. Chen, J. B. Bliska, S. Ozen, D. L. Kastner, D. Shriner, and J. J. Chae, "Ancient familial Mediterranean fever mutations in human pyrin and resistance to Yersinia pestis", Nature Immunology, 857–867 (2020).

[73]K. Orth, Z. Xu, M. B. Mudgett, Z. Q. Bao, L. E. Palmer, J. B. Bliska, W. F. Mangel, B. Staskawicz, and J. E. Dixon, "Disruption of signaling by yersinia effector YopJ, a ubiquitin-like protein protease", Science **290**, 1594–1597 (2000).

[74]H. Zhou, D. M. Monack, N. Kayagaki, I. Wertz, J. Yin, B. Wolf, and V. M. Dixit, "Yersinia virulence factor YopJ acts as a deubiquitinase to inhibit NF-κB activation", Journal of Experimental Medicine **202**, 1327–1332 (2005).

[75]C. R. Sweet, J. Conlon, D. T. Golenbock, J. Goguen, and N. Silverman, "YopJ targets TRAF proteins to inhibit TLR-mediated NF-κB, MAPK and IRF3 signal transduction", Cellular Microbiology **9**, 2700–2715 (2007).

[76]R. Mittal, S. Y. Peak-Chew, and H. T. McMahon, "Acetylation of MEK2 and IκB (IKK) activation loop residues by YopJ inhibits signaling", Proceedings of the National Academy of Sciences of the United States of America **103**, 18574–18579 (2006).

[77]S. Mukherjee, G. Keitany, Y. Li, Y. Wang, H. L. Ball, E. J. Goldsmith, and K. Orth, "Yersinia YopJ Acetylates and Inhibits Kinase Activation by Blocking Phosphorylation", Science **312**, 1211–1214 (2006).

[78]R. Mittal, S. Y. Peak-Chew, R. S. Sade, Y. Vallis, and H. T. McMahon, "The acetyltransferase activity of the bacterial toxin YopJ of Yersinia is activated by eukaryotic host cell inositol hexakisphosphate", Journal of Biological Chemistry **285**, 19927–19934 (2010).

[79]U. Meinzer, F. Barreau, S. Esmiol-Welterlin, C. Jung, C. Villard, T. Léger, S. Ben-Mkaddem, D. Berrebi, M. Dussaillant, Z. Alnabhani, M. Roy, S. Bonacorsi, H. Wolf-Watz, J. Perroy, V. Ollendorff, and J. P. Hugot, "Yersinia pseudotuberculosis effector YopJ subverts the Nod2/RICK/TAK1 pathway and activates caspase-1 to induce intestinal barrier dysfunction", Cell Host and Microbe **11**, 337–351 (2012).

[80]N. Paquette, J. Conlon, C. Sweet, F. Rus, L. Wilson, A. Pereira, C. V. Rosadini, N. Goutagny, A. N. Weber, W. S. Lane, S. A. Shaffer, S. Maniatis, K. A. Fitzgerald, L. Stuart, and N. Silverman, "Serine/threonine acetylation of TGFβ-activated kinase (TAK1) by Yersinia pestis YopJ inhibits innate immune signaling", Proceedings of the National Academy of Sciences of the United States of America **109**, 12710–12715 (2012).

[81]K. A. Schubert, Y. Xu, F. Shao, and V. Auerbuch, "The Yersinia Type III Secretion System as a Tool for Studying Cytosolic Innate Immune Surveillance", Annual Review of Microbiology **74**, 221–245 (2020).

[82]P. Orning, D. Weng, K. Starheim, D. Ratner, Z. Best, B. Lee, A. Brooks, S. Xia, H. Wu, M. A. Kelliher, S. B. Berger, P. J. Gough, J. Bertin, M. M. Proulx, J. D. Goguen, N. Kayagaki, K. A. Fitzgerald, and E. Lien, "Pathogen blockade of TAK1 triggers caspase-8–dependent cleavage of gasdermin D and cell death", Science **362**, 1064–1069 (2018).

[83]I. E. Brodsky and R. Medzhitov, "Reduced secretion of YopJ by Yersinia limits in vivo cell death but enhances bacterial virulence", PLoS Pathogens **4**, 1–14 (2008).

[84]N. H. Philip and I. E. Brodsky, "Cell death programs in Yersinia immunity and pathogenesis.", Frontiers in cellular and infection microbiology **2**, 149 (2012).

[85]N. H. Philip, C. P. Dillon, A. G. Snyder, P. Fitzgerald, M. A. Wynosky-Dolfi, E. E. Zwack, B. Hu, L. Fitzgerald, E. A. Mauldin, A. M. Copenhaver, S. Shin, L. Wei, M. Parker, J. Zhang, A. Oberst, D. R. Green, and I. E. Brodsky, "Caspase-8 mediates caspase-1 processing and innate immune defense in response to bacterial blockade of NF- B and MAPK signaling", Proceedings of the National Academy of Sciences **111**, 7385–7390 (2014).

[86]L. W. Peterson, N. H. Philip, A. DeLaney, M. A. Wynosky-Dolfi, K. Asklof, F. Gray, R. Choa, E. Bjanes, E. L. Buza, B. Hu, C. P. Dillon, D. R. Green, S. B. Berger, P. J. Gough, J. Bertin, and I. E. Brodsky, "RIPK1-dependent apoptosis bypasses pathogen blockade of innate signaling to promote immune defense", Journal of Experimental Medicine **214**, 3171–3182 (2017).

[87]E. E. Zwack, A. G. Snyder, M. A. Wynosky-Dolfi, G. Ruthel, N. H. Philip, M. M. Marketon, M. S. Francis, J. B. Bliska, and I. E. Brodsky, "Inflammasome activation in response to the yersinia type III secretion system requires hyperinjection of translocon proteins YopB and YopD", mBio **6**, 1–11 (2015).

[88]E. E. Zwack, E. M. Feeley, A. R. Burton, B. Hu, M. Yamamoto, T.-D. Kanneganti, J. B. Bliska, J. Coers, and I. E. Brodsky, "Guanylate Binding Proteins Regulate Inflammasome Activation in Response to Hyperinjected Yersinia Translocon Components", Infection and Immunity **85**, 10. 1128/IAI.00778-16 (2017).

[89]I. E. Brodsky, N. W. Palm, S. Sadanand, M. B. Ryndak, F. S. Sutterwala, R. A. Flavell, J. B. Bliska, and R. Medzhitov, "A Yersinia Effector Protein Promotes Virulence by Preventing Inflammasome Recognition of the Type III Secretion System", Cell Host and Microbe **7**, 376 –387 (2010).

[90]K. Dach, J. Zovko, M. Hogardt, I. Koch, K. Van Erp, J. Heesemann, and R. Hoffmann, "Bacterial toxins induce sustained mRNA expression of the silencing transcription factor klf2 via inactivation of RhoA and rhophilin 1", Infection and Immunity **77**, 5583–5592 (2009).

[91]M. Köberle, D. Göppel, T. Grandl, P. Gaentzsch, B. Manncke, S. Berchtold, S. Müller, B. Lüscher, M. L. Asselin-Labat, M. Pallardy, I. Sorg, S. Langer, H. Barth, R. Zumbihl, I. B. Autenrieth, and E. Bohn, "Yersinia enterocolitica YopT and Clostridium difficile Toxin B Induce Expression of GILZ in Epithelial Cells", PLoS ONE **7**, 1–17 (2012).

[92]G. I. Viboud, S. S. K. So, M. B. Ryndak, and J. B. Bliska, "Proinflammatory signalling stimulated by the type III translocation factor YopB is counteracted by multiple effectors in epithelial cells infected with Yersinia pseudotuberculosis", Molecular Microbiology **47**, 1305–1315 (2003).

[93]R. Schulte, G. A. Grassl, S. Preger, S. Fessele, C. A. Jacobi, M. Schaller, P. J. Nelson, and I. B. Autenrieth, " Yersinia enterocolitica invasin protein triggers IL-8 production in epithelial cells via activation of Rel p65-p65 homodimers ", The FASEB Journal **14**, 1471–1484 (2000).

[94]G. A. Grassl, M. Kracht, A. Wiedemann, E. Hoffmann, M. Aepfelbacher, C. von Eichel-Streiber, E. Bohn, and I. B. Autenrieth, "Activation of NF-κB and IL-8 by Yersinia enterocolitica invasin protein is conferred by engagement of Rac1 and MAP kinase cascades", Cellular Microbiology **5**, 957–971 (2003).

[95]Y. Schmid, G. A. Grassl, O. T. Bühler, M. Skurnik, I. B. Autenrieth, and E. Bohn, "Yersinia enterocolitica adhesin A induces production of interleukin-8 in epithelial cells", Infection and Immunity **72**, 6780–6789 (2004).

[96]K. Ruckdeschel, S. Harb, A. Roggenkamp, M. Hornef, R. Zumbihl, S. Köhler, J. Heesemann, and B. Rouot, "Yersinia enterocolitica impairs activation of transcription factor NF- κB: Involvement in the induction of programmed cell death and in the suppression of the macrophage tumor necrosis factor α production", Journal of Experimental Medicine **187**, 1069–1079 (1998).

[97]L. E. Palmer, S. Hobble, J. E. Galán, and J. B. Bliska, "YopJ of Yersinia pseudotuberculosis is required for the inhibition of macrophage TNF-α production and downregulation of the MAP kinases p38 and JNK", Molecular Microbiology **27**, 953–965 (1998).

[98]V. Auerbuch, D. T. Golenbock, and R. R. Isberg, "Innate immune recognition of Yersinia pseudotuberculosis type III secretion", PLoS Pathogens **5**, 1–16 (2009).

[99]N. Sauvonnet, B. Pradet-Balade, J. A. Garcia-Sanz, and G. R. Cornelis, "Regulation of mRNA Expression in Macrophages afterYersinia enterocolitica Infection: ROLE OF DIFFERENT Yop EFFECTORS", Journal of Biological Chemistry **277**, 25133–25142 (2002).

[100]R. Hoffmann, K. van Erp, K. Trülzsch, and J. Heesemann, "Transcriptional responses of murine macrophages to infection with Yersinia enterocolitica", Cellular Microbiology **6**, 377–390 (2004).

[101]Y. Zhang, A. T. Ting, K. B. Marcu, and J. B. Bliska, " Inhibition of MAPK and NF-κB Pathways Is Necessary for Rapid Apoptosis in Macrophages Infected with Yersinia ", The Journal of Immunology **174**, 7939–7949 (2005).

[102]I. Koch, K. Dach, J. Heesemann, and R. Hoffmann, "Yersinia enterocolitica inactivates NK cells", International Journal of Medical Microbiology **303**, 433–442 (2013).

[103]E. Bohn, S. Müller, J. Lauber, R. Geffers, N. Speer, C. Spieth, J. Krejci, B. Manncke, J. Buer, A. Zell, and I. B. Autenrieth, "Gene expression patterns of epithelial cells modulated by pathogenicity factors of Yersinia enterocolitica", Cellular Microbiology **6**, 129–141 (2004).

[104]Y. V. B. K. Subrahmanyam, S. Yamaga, Y. Prashar, H. H. Lee, N. P. Hoe, Y. Kluger, M. Gerstein, J. D. Goguen, P. E. Newburger, and S. M. Weissman, "RNA expression patterns change dramatically in human neutrophils exposed to bacteria", Blood **97**, 2457–2468 (2001).

[105]A. M. Nuss, M. Beckstette, M. Pimenova, C. Schmühl, W. Opitz, F. Pisano, A. K. Heroven, and P. Dersch, "Tissue dual RNA-seq allows fast discovery of infection-specific functions and riboregulators shaping host-pathogen transcriptomes", Proceedings of the National Academy of Sciences of the United States of America **114**, E791–E800 (2017).

[106]W. Heine, M. Beckstette, A. K. Heroven, S. Thiemann, U. Heise, A. M. Nuss, F. Pisano, T. Strowig, and P. Dersch, "Loss of CNFY toxin-induced inflammation drives Yersinia pseudotuberculosis into persistency", PLOS Pathogens **14**, 1–32 (2018).

[107]L. B. Ivashkiv, "Epigenetic regulation of macrophage polarization and function", Trends in Immunology **34**, 216–223 (2013).

[108]F. Ginhoux, J. L. Schultze, P. J. Murray, J. Ochando, and S. K. Biswas, "New insights into the multidimensional concept of macrophage ontogeny, activation and function", Nature Immunology **17**, 34–40 (2016).

[109]C. C. Bain and A. Schridde, "Origin, differentiation, and function of intestinal macrophages", Frontiers in Immunology **9**, 1–15 (2018).

[110]C. K. Glass and G. Natoli, "Molecular control of activation and priming in macrophages", Nature Immunology **17**, 26–33 (2015).

[111]D. G. Ryan and L. A. O'Neill, "Krebs Cycle Reborn in Macrophage Immunometabolism", Annual Review of Immunology **38**, 289–313 (2020).

[112]O. Takeuchi and S. Akira, "Pattern Recognition Receptors and Inflammation", Cell **140**, 805–820 (2010).

[113]G. P. Amarante-Mendes, S. Adjemian, L. M. Branco, L. C. Zanetti, R. Weinlich, and K. R. Bortoluci, "Pattern recognition receptors and the host cell death molecular machinery", Frontiers in Immunology **9**, 1–19 (2018).

[114]J. Moretti and J. M. Blander, "Insights into phagocytosis-coupled activation of Pattern Recognition Receptors and Inflammasomes", Current Opinion in Immunology **26**, 100–110 (2014).

[115]V. A. Rathinam, Y. Zhao, and F. Shao, "Innate immunity to intracellular LPS", Nature Immunology **20**, 527–533 (2019).

[116]S. Pandey, T. Kawai, and S. Akira, "Microbial sensing by toll-like receptors and intracellular nucleic acid sensors", Cold Spring Harbor Perspectives in Biology **7**, 1–18 (2015).

[117]L. Escoubet-Lozach, C. Benner, M. U. Kaikkonen, J. Lozach, S. Heinz, N. J. Spann, A. Crotti, J. Stender, S. Ghisletti, D. Reichart, C. S. Cheng, R. Luna, C. Ludka, R. Sasik, I. Garcia-Bassets, A. Hoffmann, S. Subramaniam, G. Hardiman, M. G. Rosenfeld, and C. K. Glass, "Mechanisms Establishing TLR4-Responsive Activation States of Inflammatory Response Genes", PLOS Genetics **7**, 1–14 (2011).

[118]V. R. Ramirez-Carrozi, D. Braas, D. M. Bhatt, C. S. Cheng, C. Hong, K. R. Doty, J. C. Black, A. Hoffmann, M. Carey, and S. T. Smale, "A Unifying Model for the Selective Regulation of Inducible Transcription By CpG Islands and Nucleosome Remodeling Cheng4," Cell **138**, 114–128 (2009).

[119]N. Serrat, C. Sebastian, S. Pereira-Lopes, L. Valverde-Estrella, J. Lloberas, and A. Celada, "The Response of Secondary Genes to Lipopolysaccharides in Macrophages Depends on Histone Deacetylase and Phosphorylation of C/EBPβ", The Journal of Immunology **192**, 418–426 (2014).

[120]S. Henikoff and J. M. Greally, "Epigenetics, cellular memory and gene regulation", Current Biology **26**, R644–R648 (2016).

[121]J. M. Greally, "A user's guide to the ambiguous word 'epigenetics'", Nature Reviews Molecular Cell Biology **19**, 207–208 (2018).

[122]T. Kouzarides, "Chromatin Modifications and Their Function", Cell **128**, 693–705 (2007).

[123]K. E. Gardner, C. D. Allis, and B. D. Strahl, "OPERating ON chromatin, a colorful language where context matters", **409**, 36–46 (2011).

[124]H. Bierne, M. Hamon, and P. Cossart, "Epigenetics and Bacterial Infections", Cold Spring Harbor Perspectives in Medicine **2**, 10.1101/cshperspect.a010272 (2012).

[125]Z. Wang, C. Zang, J. A. Rosenfeld, D. E. Schones, A. Barski, S. Cuddapah, K. Cui, T. Y. Roh, W. Peng, M. Q. Zhang, and K. Zhao, "Combinatorial patterns of histone acetylations and methylations in the human genome", Nature Genetics **40**, 897–903 (2008).

[126]P. J. Wittkopp and G. Kalay, "Cis-regulatory elements: Molecular mechanisms and evolutionary processes underlying divergence", Nature Reviews Genetics **13**, 59–69 (2012).

[127]S. Schoenfelder and P. Fraser, "Long-range enhancer–promoter contacts in gene expression control", Nature Reviews Genetics, 437–455 (2019).

[128]A. Barski, S. Cuddapah, K. Cui, T. Y. Roh, D. E. Schones, Z. Wang, G. Wei, I. Chepelev, and K. Zhao, "High-Resolution Profiling of Histone Methylations in the Human Genome", Cell **129**, 823–837 (2007).

[129]M. Connor, L. Arbibe, and M. Hamon, "Customizing Host Chromatin: A Bacterial Tale", in *Bacteria and Intracellularity* (American Society of Microbiology, 2019), pp. 227–245.

[130]S. Saeed, J. Quintin, H. H. D. Kerstens, N. A. Rao, A. Aghajanirefah, F. Matarese, S.-c. Cheng, J. Ratter, K. Berentsen, M. A. V. D. Ent, N. Sharifi, E. M. Janssen-megens, M. T. Huurne, A. Mandoli, T. van Schaik, A. Ng, F. Burden, K. Downes, M. Frontini, V. Kumar, E. J. Giamarellos-Bourboulis, W. H. Ouwehand, J. W. M. van der Meer, L. A. Joosten, C. Wijmenga, J. H. A. Martens, R. J. Xavier, C. Logie, M. G. Netea, and H. G. Stunnenberg, "Epigenetic programming of monocyte-to-macrophage differentiation and trained innate immunity", Science **345**, 1–26 (2015).

[131]B. Novakovic, E. Habibi, S. Y. Wang, R. J. Arts, R. Davar, W. Megchelenbrink, B. Kim, T. Kuznetsova, M. Kox, J. Zwaag, F. Matarese, S. J. van Heeringen, E. M. Janssen-Megens, N. Sharifi, C. Wang, F. Keramati, V. Schoonenberg, P. Flicek, L. Clarke, P. Pickkers, S. Heath, I. Gut, M. G. Netea, J. H. Martens, C. Logie, and H. G. Stunnenberg, "β-Glucan Reverses the Epigenetic State of LPS-Induced Immunological Tolerance", Cell **167**, 1354–1368.e14 (2016).

[132]Y. Lavin, D. Winter, R. Blecher-Gonen, E. David, H. Keren-Shaul, M. Merad, S. Jung, and I. Amit, "Tissue-resident macrophage enhancer landscapes are shaped by the local microenvironment", Cell **159**, 1312–1326 (2014).

[133]S. Ghisletti, I. Barozzi, F. Mietton, S. Polletti, F. De Santa, E. Venturini, L. Gregory, L. Lonie, A. Chew, C. L. Wei, J. Ragoussis, and G. Natoli, "Identification and Characterization of Enhancers Controlling the Inflammatory Gene Expression Program in Macrophages", Immunity **32**, 317–328 (2010).

[134]A. Mancino, A. Termanini, I. Barozzi, S. Ghisletti, R. Ostuni, E. Prosperini, K. Ozato, and G. Natoli, "A dual cis-regulatory code links IRF8 to constitutive and inducible gene expression in macrophages", Genes and Development **29**, 394–408 (2015).

[135]S. T. Smale and G. Natoli, "Transcriptional Control of Inflammatory Responses", Cold Spring Harbor Perspectives in Biology **6**, 10.1101/cshperspect.a016261 (2014).

[136]J. Gatchalian, J. Liao, M. B. Maxwell, and D. C. Hargreaves, "Control of Stimulus-Dependent Responses in Macrophages by SWI/SNF Chromatin Remodeling Complexes", Trends in Immunology **41**, 126–140 (2020).

[137]R. Ostuni, V. Piccolo, I. Barozzi, S. Polletti, A. Termanini, S. Bonifacio, A. Curina, E. Prosperini, S. Ghisletti, and G. Natoli, "Latent enhancers activated by stimulation in differentiated cells", Cell **152**, 157–171 (2013).

[138]K. Kang, S. H. Park, J. Chen, Y. Qiao, E. Giannopoulou, K. Berg, A. Hanidu, J. Li, G. Nabozny, K. Kang, K. H. Park-Min, and L. B. Ivashkiv, "Interferon-γ Represses M2 Gene Expression in Human Macrophages by Disassembling Enhancers Bound by the Transcription Factor MAF", Immunity **47**, 235–250.e4 (2017).

[139]K. Kang, M. Bachu, S. H. Park, K. Kang, S. Bae, K. H. Park-Min, and L. B. Ivashkiv, "IFN-γ selectively suppresses a subset of TLR4-activated genes and enhancers to potentiate macrophage activation", Nature Communications **10**, 10.1038/s41467-019-11147-3 (2019).

[140]S. Ho Park, K. Kang, E. Giannopoulou, Y. Qiao, K. Kang, G. Kim, K.-H. Park-Min, and L. B. Ivashkiv, "Type I IFNs and TNF cooperatively reprogram the macrophage epigenome to promote inflammatory activation HHS Public Access", Nature Immunology **18**, 1104–1116 (2017).

[141]M. G. Netea, J. Domínguez-Andrés, L. B. Barreiro, T. Chavakis, M. Divangahi, E. Fuchs, L. A. Joosten, J. W. van der Meer, M. M. Mhlanga, W. J. Mulder, N. P. Riksen, A. Schlitzer, J. L. Schultze, C. Stabell Benn, J. C. Sun, R. J. Xavier, and E. Latz, "Defining trained immunity and its role in health and disease", Nature Reviews Immunology, 375–388 (2020).

[142]H. Bierne and R. Pourpre, "Bacterial factors targeting the nucleus: The growing family of nucleomodulins", Toxins **12**, 10.3390/toxins12040220 (2020).

[143]J. Heesemann and R. Laufs, "Construction of a mobilizable Yersinia enterocolitica virulence plasmid", Journal of Bacteriology **155**, 761–767 (1983).
[144]M. Schnapp, "Characterization of novel interaction partners of the Yersinia enterocolitica effector protein YopM and their role in macrophage cytokine expression", (2016).
[145]P. Kopp, R. Lammers, M. Aepfelbacher, G. Woehlke, T. Rudel, N. Machuy, W. Steffen, and S. Linder, "The Kinesin KIF1C and Microtubule Plus Ends Regulate Podosome Dynamics in Macrophages", Molecular Biology of the Cell **17**, 2811–2823 (2006).
[146]A. R. Quinlan and I. M. Hall, "BEDTools: A flexible suite of utilities for comparing genomic features", Bioinformatics **26**, 841–842 (2010).
[147]H. Li and R. Durbin, "Fast and accurate short read alignment with Burrows-Wheeler transform", Bioinformatics **25**, 1754–1760 (2009).
[148]A. T. Lun and G. K. Smyth, "Csaw: A Bioconductor package for differential binding analysis of ChIP-seq data using sliding windows", Nucleic Acids Research **44**, e45 (2015).
[149]D. W. Huang, B. T. Sherman, and R. A. Lempicki, "Bioinformatics enrichment tools: Paths toward the comprehensive functional analysis of large gene lists", Nucleic Acids Research **37**, 1–13 (2009).
[150]D. W. Huang, B. T. Sherman, and R. A. Lempicki, "Systematic and integrative analysis of large gene lists using DAVID bioinformatics resources", Nature Protocols **4**, 44–57 (2009).
[151]F. Ramírez, F. Dündar, S. Diehl, B. A. Grüning, and T. Manke, "DeepTools: A flexible platform for exploring deep-sequencing data", Nucleic Acids Research **42**, 187–191 (2014).
[152]M. I. Love, W. Huber, and S. Anders, "Moderated estimation of fold change and dispersion for RNA-seq data with DESeq2", Genome Biology **15**, 1–21 (2014).
[153]L. Shen, N. Y. Shao, X. Liu, I. Maze, J. Feng, and E. J. Nestler, "diffReps: Detecting Differential Chromatin Modification Sites from ChIP-seq Data with Biological Replicates", PLoS ONE **8**, 1–13 (2013).
[154]M. Lerdrup, J. V. Johansen, S. Agrawal-Singh, and K. Hansen, "An interactive environment for agile analysis and visualization of ChIP-sequencing data", Nature Structural and Molecular Biology **23**, 349–357 (2016).
[155]Y. Liao, G. K. Smyth, and W. Shi, "FeatureCounts: An efficient general purpose program for assigning sequence reads to genomic features", Bioinformatics **30**, 923–930 (2014).
[156]T. Barrett, S. E. Wilhite, P. Ledoux, C. Evangelista, I. F. Kim, M. Tomashevsky, K. A. Marshall, K. H. Phillippy, P. M. Sherman, M. Holko, A. Yefanov, H. Lee, N. Zhang, C. L. Robertson, N. Serova, S. Davis, and A. Soboleva, "NCBI GEO: Archive for functional genomics data sets - Update", Nucleic Acids Research **41**, 991–995 (2013).
[157]H. Wickham, *ggplot2: Elegant Graphics for Data Analysis* (Springer-Verlag New York, 2016).
[158]S. Heinz, C. Benner, N. Spann, E. Bertolino, Y. C. Lin, P. Laslo, J. X. Cheng, C. Murre, H. Singh, and C. K. Glass, "Simple combinations of lineage-determining transcription factors prime cis-regulatory elements required for macrophage and B cell identities", Molecular Cell **38**, 576–589 (2010).
[159]H. Thorvaldsdóttir, J. T. Robinson, and J. P. Mesirov, "Integrative Genomics Viewer (IGV): High-performance genomics data visualization and exploration", Briefings in Bioinformatics **14**, 178–192 (2013).
[160]Y. Zhang, T. Liu, C. A. Meyer, J. Eeckhoute, D. S. Johnson, B. E. Bernstein, C. Nussbaum, R. M. Myers, M. Brown, W. Li, and X. S. Shirley, "Model-based analysis of ChIP-Seq (MACS)", Genome Biology **9**, 10.1186/gb-2008-9-9-r137 (2008).
[161]B. Braschi, P. Denny, K. Gray, T. Jones, R. Seal, S. Tweedie, B. Yates, and E. Bruford, "Genenames.org: The HGNC and VGNC resources in 2019", Nucleic Acids Research **47**, D786–D792 (2019).
[162]J. Ye, G. Coulouris, I. Zaretskaya, I. Cutcutache, S. Rozen, and T. L. Madden, "Primer-BLAST: a tool to design target-specific primers for polymerase chain reaction.", BMC bioinformatics **13**, 134 (2012).
[163]L. Wang, S. Wang, and W. Li, "RSeQC: Quality control of RNA-seq experiments", Bioinformatics **28**, 2184–2185 (2012).
[164]RStudio Team, *RStudio: Integrated Development Environment for R*, RStudio, PBC. (Boston, MA, 2020).
[165]H. Li, B. Handsaker, A. Wysoker, T. Fennell, J. Ruan, N. Homer, G. Marth, G. Abecasis, and R. Durbin, "The Sequence Alignment/Map format and SAMtools", Bioinformatics **25**, 2078–2079 (2009).
[166]C. Zang, D. E. Schones, C. Zeng, K. Cui, K. Zhao, and W. Peng, "A clustering approach for identification of enriched domains from histone modification ChIP-Seq data", Bioinformatics **25**, 1952–1958 (2009).

[167]A. Dobin, C. A. Davis, F. Schlesinger, J. Drenkow, C. Zaleski, S. Jha, P. Batut, M. Chaisson, and T. R. Gingeras, "STAR: Ultrafast universal RNA-seq aligner", Bioinformatics **29**, 15–21 (2013).

[168]M. Haeussler, A. S. Zweig, C. Tyner, M. L. Speir, K. R. Rosenbloom, B. J. Raney, C. M. Lee, B. T. Lee, A. S. Hinrichs, J. N. Gonzalez, D. Gibson, M. Diekhans, H. Clawson, J. Casper, G. P. Barber, D. Haussler, R. M. Kuhn, and W. J. Kent, "The UCSC Genome Browser database: 2019 update", Nucleic Acids Research **47**, D853–D858 (2019).

[169]M. E. Ritchie, B. Phipson, D. Wu, Y. Hu, C. W. Law, W. Shi, and G. K. Smyth, "Limma powers differential expression analyses for RNA-sequencing and microarray studies", Nucleic Acids Research **43**, e47 (2015).

[170]N. D. Heintzman, R. K. Stuart, G. Hon, Y. Fu, C. W. Ching, R. D. Hawkins, L. O. Barrera, S. Van Calcar, C. Qu, K. A. Ching, W. Wang, Z. Weng, R. D. Green, G. E. Crawford, and B. Ren, "Distinct and predictive chromatin signatures of transcriptional promoters and enhancers in the human genome", Nature Genetics **39**, 311–318 (2007).

[171]A. Rada-Iglesias, R. Bajpai, T. Swigut, S. A. Brugmann, R. A. Flynn, and J. Wysocka, "A unique chromatin signature uncovers early developmental enhancers in humans", Nature **470**, 279–283 (2011).

[172]T. Günther, J. M. Theiss, N. Fischer, and A. Grundhoff, "Investigation of viral and host chromatin by ChIP-PCR or ChIP-Seq analysis", Current Protocols in Microbiology **2016**, 1E.10.1–1E.10.21 (2016).

[173]H. M. Amemiya, A. Kundaje, and A. P. Boyle, "The ENCODE Blacklist: Identification of Problematic Regions of the Genome", Scientific Reports **9**, 1–5 (2019).

[174]M. D. Robinson and A. Oshlack, "A scaling normalization method for differential expression analysis of RNA-seq data", Genome Biology **11**, 10.1186/gb-2010-11-3-r25 (2010).

[175]X. R. Bustelo, V. Sauzeau, and I. M. Berenjeno, "GTP-binding proteins of the Rho/Rac family: regulation, effectors and functions in vivo", BioEssays **29**, 356–370 (2007).

[176]H. Bagci, N. Sriskandarajah, A. Robert, J. Boulais, I. E. Elkholi, V. Tran, Z. Y. Lin, M. P. Thibault, N. Dubé, D. Faubert, D. R. Hipfner, A. C. Gingras, and J. F. Côté, "Mapping the proximity interaction network of the Rho-family GTPases reveals signalling pathways and regulatory mechanisms", Nature Cell Biology **22**, 120–134 (2020).

[177]F. Paul, H. Zauber, L. von Berg, O. Rocks, O. Daumke, and M. Selbach, "Quantitative GTPase Affinity Purification Identifies Rho Family Protein Interaction Partners", Molecular & Cellular Proteomics **16**, 73–85 (2017).

[178]P. M. Müller, J. Rademacher, R. D. Bagshaw, C. Wortmann, C. Barth, J. van Unen, K. M. Alp, G. Giudice, R. L. Eccles, L. E. Heinrich, P. Pascual-Vargas, M. Sanchez-Castro, L. Brandenburg, G. Mbamalu, M. Tucholska, L. Spatt, M. T. Czajkowski, R. W. Welke, S. Zhang, V. Nguyen, T. Rrustemi, P. Trnka, K. Freitag, B. Larsen, O. Popp, P. Mertins, A. C. Gingras, F. P. Roth, K. Colwill, C. Bakal, O. Pertz, T. Pawson, E. Petsalaki, and O. Rocks, "Systems analysis of RhoGEF and RhoGAP regulatory proteins reveals spatially organized RAC1 signalling from integrin adhesions", Nature Cell Biology **22**, 498–511 (2020).

[179]K. Wennerberg and C. J. Der, "Rho-family GTPases: It's not only Rac and Rho (and i like it)", Journal of Cell Science **117**, 1301–1312 (2004).

[180]H. Senoo, Y. Kamimura, R. Kimura, A. Nakajima, S. Sawai, H. Sesaki, and M. Iijima, "Phosphorylated Rho-GDP directly activates mTORC2 kinase towards AKT through dimerization with Ras-GTP to regulate cell migration", Nature cell biology **21**, 867—878 (2019).

[181]W. M. Schneider, M. D. Chevillotte, and C. M. Rice, "Interferon-Stimulated Genes: A Complex Web of Host Defenses", Annual Review of Immunology **32**, 513–545 (2014).

[182]E. S. Malsin, S. Kim, A. P. Lam, and C. J. Gottardi, "Macrophages as a Source and Recipient of Wnt Signals", Frontiers in immunology **10**, 1813 (2019).

[183]L. A. O'Neill, R. J. Kishton, and J. Rathmell, "A guide to immunometabolism for immunologists", Nature Reviews Immunology **16**, 553–565 (2016).

[184]M. Cassandri, A. Smirnov, F. Novelli, C. Pitolli, M. Agostini, M. Malewicz, G. Melino, and G. Raschellà, "Zinc-finger proteins in health and disease", Cell Death Discovery **3**, 10 . 1038 / cddiscovery.2017.71 (2017).

[185]M. J. Vogel, L. Guelen, E. De Wit, D. Peric-Hupkes, M. Lodén, W. Talhout, M. Feenstra, B. Abbas, A. K. Classen, and B. Van Steensel, "Human heterochromatin proteins form large domains containing KRAB-ZNF genes", Genome Research **16**, 1493–1504 (2006).

[186]A. Lupo, E. Cesaro, G. Montano, D. Zurlo, P. Izzo, and P. Costanzo, "KRAB-Zinc Finger Proteins: A Repressor Family Displaying Multiple Biological Functions", Current genomics **14**, 268—278 (2013).

[187]H. Hu, Y.-R. Miao, L.-H. Jia, Q.-Y. Yu, Q. Zhang, and A.-Y. Guo, "AnimalTFDB 3.0: a comprehensive resource for annotation and prediction of animal transcription factors", Nucleic Acids Research **47**, D33–D38 (2018).

[188]C. M. Leopold Wager, E. Arnett, and L. S. Schlesinger, "Macrophage nuclear receptors: Emerging key players in infectious diseases", PLoS Pathogens **15**, 1–23 (2019).

[189]P. Mlcochova, K. A. Sutherland, S. A. Watters, C. Bertoli, R. A. Bruin, J. Rehwinkel, S. J. Neil, G. M. Lenzi, B. Kim, A. Khwaja, M. C. Gage, C. Georgiou, A. Chittka, S. Yona, M. Noursadeghi, G. J. Towers, and R. K. Gupta, " A G1-like state allows HIV -1 to bypass SAMHD 1 restriction in macrophages ", The EMBO Journal **36**, 604–616 (2017).

[190]P. Mlcochova, H. Winstone, L. Zuliani-Alvarez, and R. K. Gupta, "TLR4-Mediated Pathway Triggers Interferon-Independent G0 Arrest and Antiviral SAMHD1 Activity in Macrophages", Cell Reports **30**, 3972–3980.e5 (2020).

[191]N. Navasa, I. Martin-Ruiz, E. Atondo, J. D. Sutherland, M. Angel Pascual-Itoiz, A. Carreras-González, H. Izadi, J. Tomás-Cortázar, F. Ayaz, N. Martin-Martin, I. M. Torres, R. Barrio, A. Carracedo, E. R. Olivera, M. Rincón, and J. Anguita, "Ikaros mediates the DNA methylation-independent silencing of MCJ/DNAJC15 gene expression in macrophages", Scientific Reports **5**, 1–9 (2015).

[192]K.-S. Oh, R. A. Gottschalk, N. W. Lounsbury, J. Sun, M. G. Dorrington, S. Baek, G. Sun, Z. Wang, K. S. Krauss, J. D. Milner, B. Dutta, G. L. Hager, M.-H. Sung, and I. D. C. Fraser, "Dual Roles for Ikaros in Regulation of Macrophage Chromatin State and Inflammatory Gene Expression", The Journal of Immunology **201**, 757–771 (2018).

[193]M. A. Zarnegar and E. V. Rothenberg, "Ikaros represses and activates PU.1 cell-type-specifically through the multifunctional Sfpi1 URE and a myeloid specific enhancer", Oncogene **31**, 4647–4654 (2012).

[194]F. Penas, G. A. Mirkin, M. Vera, Á. Cevey, C. D. González, M. I. Gómez, M. E. Sales, and N. B. Goren, "Treatment in vitro with PPARα and PPARγ ligands drives M1-to-M2 polarization of macrophages from T. cruzi-infected mice", Biochimica et Biophysica Acta - Molecular Basis of Disease **1852**, 893–904 (2015).

[195]H. Miao, J. Ou, X. Zhang, Y. Chen, B. Xue, H. Shi, L. Gan, L. Yu, and H. Liang, "Macrophage CGI-58 deficiency promotes IL-1β transcription by activating the SOCS3-FOXO1 pathway", Clinical Science **128**, 493–506 (2015).

[196]W. Fan, H. Morinaga, J. J. Kim, E. Bae, N. J. Spann, S. Heinz, C. K. Glass, and J. M. Olefsky, "FoxO1 regulates Tlr4 inflammatory pathway signalling in macrophages", EMBO Journal **29**, 4223–4236 (2010).

[197]S. Chung, R. Ranjan, Y. G. Lee, G. Y. Park, M. Karpurapu, J. Deng, L. Xiao, J. Y. Kim, T. G. Unterman, and J. W. Christman, "Distinct role of FoxO1 in M-CSF- and GM-CSF-differentiated macrophages contributes LPS-mediated IL-10: implication in hyperglycemia", Journal of Leukocyte Biology **97**, 327–339 (2015).

[198]A. Verger and M. Duterque-Coquillaud, "When Ets transcription factors meet their partners", BioEssays **24**, 362–370 (2002).

[199]R. G. Hodge and A. J. Ridley, "Regulating Rho GTPases and their regulators", Nature Reviews Molecular Cell Biology **17**, 496–510 (2016).

[200]D. Szklarczyk, A. L. Gable, D. Lyon, A. Junge, S. Wyder, J. Huerta-Cepas, M. Simonovic, N. T. Doncheva, J. H. Morris, P. Bork, L. J. Jensen, and C. v. Mering, "STRING v11: protein–protein association networks with increased coverage, supporting functional discovery in genome-wide experimental datasets", Nucleic Acids Research **47**, D607–D613 (2018).

[201]M. C. McNeill, J. Wray, G. B. Sala-Newby, C. C. Hindmarch, S. A. Smith, R. Ebrahimighaei, A. C. Newby, and M. Bond, "Nuclear actin regulates cell proliferation and migration via inhibition of SRF and TEAD", Biochimica et Biophysica Acta (BBA) - Molecular Cell Research **1867**, 118691 (2020).

[202]E. Toska, H. A. Campbell, J. Shandilya, S. J. Goodfellow, P. Shore, K. F. Medler, and S. G. E. Roberts, "Repression of Transcription by WT1-BASP1 Requires the Myristoylation of BASP1 and the PIP2-Dependent Recruitment of Histone Deacetylase", Cell Reports **2**, 462–469 (2012).

[203]A. G. O'Sullivan, E. P. Mulvaney, P. B. Hyland, and B. T. Kinsella, "Protein kinase C-related kinase 1 and 2 play an essential role in thromboxane-mediated neoplastic responses in prostate cancer", Oncotarget **6**, 26437–26456 (2015).

[204]A. G. O'Sullivan, E. P. Mulvaney, and B. T. Kinsella, "Regulation of protein kinase C-related kinase (PRK) signalling by the TPα and TPβ isoforms of the human thromboxane A2 receptor: Implications for thromboxane- and androgen- dependent neoplastic and epigenetic responses in prostate cancer", Biochimica et Biophysica Acta (BBA) - Molecular Basis of Disease **1863**, 838 –856 (2017).

[205]R. A. Mathias, A. J. Guise, and I. M. Cristea, "Post-translational Modifications Regulate Class IIa Histone Deacetylase (HDAC) Function in Health and Disease", Molecular & Cellular Proteomics **14**, 456–470 (2015).

[206]"ROCK2, but not ROCK1 interacts with phosphorylated STAT3 and co-occupies TH17/TFH gene promoters in TH17-activated human T cells", Scientific Reports **9**, 16636 (2018).

[207]J. M. Weiss, W. Chen, M. S. Nyuydzefe, A. Trzeciak, R. Flynn, J. R. Tonra, S. Marusic, B. R. Blazar, S. D. Waksal, and A. Zanin-Zhorov, "ROCK2 signaling is required to induce a subset of T follicular helper cells through opposing effects on STATs in autoimmune settings", Science Signaling **9**, ra73–ra73 (2016).

[208]A. Zanin-Zhorov, J. M. Weiss, M. S. Nyuydzefe, W. Chen, J. U. Scher, R. Mo, D. Depoil, N. Rao, B. Liu, J. Wei, S. Lucas, M. Koslow, M. Roche, O. Schueller, S. Weiss, M. V. Poyurovsky, J. Tonra, K. L. Hippen, M. L. Dustin, B. R. Blazar, C.-j. Liu, and S. D. Waksal, "Selective oral ROCK2 inhibitor down-regulates IL-21 and IL-17 secretion in human T cells via STAT3-dependent mechanism", Proceedings of the National Academy of Sciences **111**, 16814–16819 (2014).

[209]T. Tanaka, D. Nishimura, R.-C. Wu, M. Amano, T. Iso, L. Kedes, H. Nishida, K. Kaibuchi, and Y. Hamamori, "Nuclear Rho kinase, ROCK2, targets p300 acetyltransferase", The Journal of biological chemistry **281**, 15320—15329 (2006).

[210]E. Ricker, Y. Chinenov, T. Pannellini, D. Flores-Castro, C. Ye, S. Gupta, M. Manni, J. K. Liao, and A. B. Pernis, "Serine-threonine kinase ROCK2 regulates germinal center B cell positioning and cholesterol biosynthesis", The Journal of clinical investigation **130**, 3654—3670 (2020).

[211]R. B. Haga and A. J. Ridley, "Rho GTPases: Regulation and roles in cancer cell biology", Small GTPases **7**, 207–221 (2016).

[212]P. Aspenström, A. Ruusala, and D. Pacholsky, "Taking Rho GTPases to the next level: The cellular functions of atypical Rho GTPases", Experimental Cell Research **313**, 3673 –3679 (2007).

[213]V. Tajadura-Ortega, R. Garg, R. Allen, C. Owczarek, M. Bright, S. Kean, A. Mohd-Noor, A. Grigoriadis, T. Elston, K. Hahn, and A. Ridley, "An RNAi screen of Rho signalling networks identifies RhoH as a regulator of Rac1 in prostate cancer cell migration", BMC Biology **16**, 10.1186/s12915-018-0489-4 (2018).

[214]A. L. Stiegler and T. J. Boggon, "The pseudoGTPase group of pseudoenzymes", The FEBS Journal **287**, 4232–4245 (2020).

[215]P. Chardin, "Function and regulation of Rnd proteins", Nature reviews. Molecular cell biology **7**, 54—62 (2006).

[216]M. S. Rao, T. R. Van Vleet, R. Ciurlionis, W. R. Buck, S. W. Mittelstadt, E. A. Blomme, and M. J. Liguori, "Comparison of RNA-Seq and microarray gene expression platforms for the toxicogenomic evaluation of liver from short-term rat toxicity studies", Frontiers in Genetics **10**, 1–16 (2019).

[217]K. Schroder, K. M. Irvine, M. S. Taylor, N. J. Bokil, K. A. Le Cao, K. A. Masterman, L. I. Labzin, C. A. Semple, R. Kapetanovic, L. Fairbairn, A. Akalin, G. J. Faulkner, J. K. Baillie, M. Gongora, C. O. Daub, H. Kawaji, G. J. McLachlan, N. Goldman, S. M. Grimmond, P. Carninci, H. Suzuki, Y. Hayashizaki, B. Lenhard, D. A. Hume, and M. J. Sweet, "Conservation and divergence in Toll-like receptor 4-regulated gene expression in primary human versus mouse macrophages", Proceedings of the National Academy of Sciences of the United States of America **109**, E944–E953 (2012).

[218]J. Sarhan, B. C. Liu, H. I. Muendlein, P. Li, R. Nilson, A. Y. Tang, A. Rongvaux, S. C. Bunnell, F. Shao, D. R. Green, and A. Poltorak, "Caspase-8 induces cleavage of gasdermin D to elicit pyroptosis during Yersinia infection", Proceedings of the National Academy of Sciences of the United States of America **115**, E10888–E10897 (2018).

[219]K Ruckdeschel, A Roggenkamp, V Lafont, P Mangeat, J Heesemann, and B Rouot, "Interaction of Yersinia enterocolitica with macrophages leads to macrophage cell death through apoptosis.", Infection and Immunity **65**, 4813–4821 (1997).

[220]G. Trinchieri, "Type I interferon: Friend or foe?", Journal of Experimental Medicine **207**, 2053–2063 (2010).

[221]S. P. John, J. Sun, R. J. Carlson, B. Cao, C. J. Bradfield, J. Song, M. Smelkinson, and I. D. Fraser, "IFIT1 Exerts Opposing Regulatory Effects on the Inflammatory and Interferon Gene Programs in LPS-Activated Human Macrophages", Cell Reports **25**, 95–106.e6 (2018).

[222]H. Hu and S. C. Sun, "Ubiquitin signaling in immune responses", Cell Research **26**, 457–483 (2016).

[223]E. Fiskin, T. Bionda, I. Dikic, and C. Behrends, "Global Analysis of Host and Bacterial Ubiquitinome in Response to Salmonella Typhimurium Infection", Molecular Cell **62**, 967–981 (2016).

[224]E. Platanitis and T. Decker, "Regulatory networks involving STATs, IRFs, and NFκB in inflammation", Frontiers in Immunology **9**, 1–16 (2018).

[225]Y. Chinenov, M. Coppo, R. Gupte, M. A. Sacta, and I. Rogatsky, "Glucocorticoid receptor coordinates transcription factor-dominated regulatory network in macrophages", BMC Genomics **15**, 10.1186/1471-2164-15-656 (2014).

[226]A. C. Groner, S. Meylan, A. Ciuffi, N. Zangger, G. Ambrosini, N. Dénervaud, P. Bucher, and D. Trono, "KRAB-zinc finger proteins and KAP1 can mediate long-range transcriptional repression through heterochromatin spreading", PLoS Genetics **6**, 1–14 (2010).

[227] P. Jha and H. Das, "KLF2 in regulation of NF-κB-mediated immune cell function and inflammation", International Journal of Molecular Sciences **18**, 2383 (2017).

[228] B. Pourcet, M. Zecchin, L. Ferri, J. Beauchamp, S. Sitaula, C. Billon, S. Delhaye, J. Vanhoutte, A. Mayeuf-Louchart, Q. Thorel, J. T. Haas, J. Eeckhoute, D. Dombrowicz, C. Duhem, A. Boulinguiez, S. Lancel, Y. Sebti, T. P. Burris, B. Staels, and H. M. Duez, "Nuclear Receptor Subfamily 1 Group D Member 1 Regulates Circadian Activity of NLRP3 Inflammasome to Reduce the Severity of Fulminant Hepatitis in Mice", Gastroenterology **154**, 1449 –1464.e20 (2018).

[229] H. Liu, Y. Zhu, Y. Gao, D. Qi, L. Zhao, L. Zhao, C. Liu, T. Tao, C. Zhou, X. Sun, F. Guo, and J. Xiao, "NR1D1 modulates synovial inflammation and bone destruction in rheumatoid arthritis", Cell Death and Disease **11**, 10.1038/s41419-020-2314-6 (2020).

[230] M. H. Orzalli and J. C. Kagan, "Apoptosis and Necroptosis as Host Defense Strategies to Prevent Viral Infection", Trends in Cell Biology **27**, Special Issue: Cell Communication, 800 –809 (2017).

[231] E. Araldi, M. Fernández-Fuertes, A. Canfrán-Duque, W. Tang, G. W. Cline, J. Madrigal-Matute, J. S. Pober, M. A. Lasunción, D. Wu, C. Fernández-Hernando, and Y. Suárez, "Lanosterol Modulates TLR4-Mediated Innate Immune Responses in Macrophages", Cell Reports **19**, 2743–2755 (2017).

[232] Y. Oishi, N. J. Spann, V. M. Link, E. D. Muse, T. Strid, C. Edillor, M. J. Kolar, T. Matsuzaka, S. Hayakawa, J. Tao, M. U. Kaikkonen, A. F. Carlin, M. T. Lam, I. Manabe, H. Shimano, A. Saghatelian, and C. K. Glass, "SREBP1 Contributes to Resolution of Pro-inflammatory TLR4 Signaling by Reprogramming Fatty Acid Metabolism", Cell Metabolism **25**, 412–427 (2017).

[233] Y. Qiao, E. G. Giannopoulou, C. H. Chan, S.-H. Park, S. Gong, J. Chen, X. Hu, O. Elemento, and L. B. Ivashkiv, "Synergistic activation of inflammatory cytokine genes by interferon-γ-induced chromatin remodeling and toll-like receptor signaling", Immunity **39**, 454—469 (2013).

[234] M. U. Kaikkonen, N. Spann, S. Heinz, C. E. Romanoski, A Karmel, J. D. Stender, H. B. Chun, D. F. Tough, R. K. Prinjha, C. Benner, and C. K. Glass, "Remodeling of the Enhancer Landscape during Macrophage Activation Is Coupled to Enhancer Transcription", Molecular Cell **51**, 310–325 (2013).

[235] F. De Santa, V. Narang, Z. H. Yap, B. K. Tusi, T. Burgold, L. Austenaa, G. Bucci, M. Caganova, S. Notarbartolo, S. Casola, G. Testa, W. K. Sung, C. L. Wei, and G. Natoli, "Jmjd3 contributes to the control of gene expression in LPS-activated macrophages", EMBO Journal **28**, 3341–3352 (2009).

[236] Y. Qiao, K. Kang, E. Giannopoulou, C. Fang, and L. B. Ivashkiv, "IFN-γ Induces Histone 3 Lysine 27 Trimethylation in a Small Subset of Promoters to Stably Silence Gene Expression in Human Macrophages", Cell Reports **16**, 3121–3129 (2016).

[237] A. Sing, D. Rost, N. Tvardovskaia, A. Roggenkamp, A. Wiedemann, C. J. Kirschning, M. Aepfelbacher, and J. Heesemann, "Yersinia V-antigen exploits toll-like receptor 2 and CD14 for interleukin 10-mediated immunosuppression", Journal of Experimental Medicine **196**, 1017–1024 (2002).

[238] D. M. Underhill and H. S. Goodridge, "Information processing during phagocytosis", Nature Reviews Immunology **12**, 492–502 (2017).

[239] M. Rolando, S. Sanulli, C. Rusniok, L. Gomez-Valero, C. Bertholet, T. Sahr, R. Margueron, and C. Buchrieser, "Legionella pneumophila effector RomA uniquely modifies host chromatin to repress gene expression and promote intracellular bacterial replication", Cell Host and Microbe **13**, 395–405 (2013).

[240] A. Pacis, L. Tailleux, A. M. Morin, J. Lambourne, J. L. MacIsaac, V. Yotova, A. Dumaine, A. Danckært, F. Luca, J. C. Grenier, K. D. Hansen, B. Gicquel, M. Yu, A. Pai, C. He, J. Tung, T. Pastinen, M. S. Kobor, R. Pique-Regi, Y. Gilad, and L. B. Barreiro, "Bacterial infection remodels the DNA methylation landscape of human dendritic cells", Genome Research **25**, 1801–1811 (2015).

[241] A. Pacis, F. Mailhot-Léonard, L. Tailleux, H. E. Randolph, V. Yotova, A. Dumaine, J. C. Grenier, and L. B. Barreiro, "Gene activation precedes DNA demethylation in response to infection in human dendritic cells", Proceedings of the National Academy of Sciences of the United States of America **116**, 6938–6943 (2019).

[242] D. Cizmeci, E. L. Dempster, O. L. Champion, S. Wagley, O. E. Akman, J. L. Prior, O. S. Soyer, J. Mill, and R. W. Titball, "Mapping epigenetic changes to the host cell genome induced by Burkholderia pseudomallei reveals pathogen-specific and pathogen-generic signatures of infection", Scientific Reports **6**, 1–9 (2016).

[243] S. H. Sinclair, S. Yegnasubramanian, and J. S. Dumler, "Global DNA methylation changes and differential gene expression in Anaplasma phagocytophilum-infected human neutrophils", Clinical Epigenetics **7**, 1–17 (2015).

[244] D. T. Graves and T. N. Milovanova, "Mucosal Immunity and the FOXO1 Transcription Factors", Frontiers in Immunology **10**, 2530 (2019).

[245]A. Kelly, S. Gunaltay, C. P. McEntee, E. E. Shuttleworth, C. Smedley, S. A. Houston, T. M. Fenton, S. Levison, E. R. Mann, and M. A. Travis, "Human monocytes and macrophages regulate immune tolerance via integrin αvβ8–mediated TGFβ activation", Journal of Experimental Medicine **215**, 2725–2736 (2018).

[246]J. J. Worthington, J. E. Klementowicz, and M. A. Travis, "TGFβ: a sleeping giant awoken by integrins", Trends in Biochemical Sciences **36**, 47 –54 (2011).

[247]K. Alasoo, F. O. Martinez, C. Hale, S. Gordon, F. Powrie, G. Dougan, S. Mukhopadhyay, and D. J. Gaffney, "Transcriptional profiling of macrophages derived from monocytes and iPS cells identifies a conserved response to LPS and novel alternative transcription", Scientific Reports **5**, 1–12 (2015).

[248]G. M. Bokoch, "Regulation of innate immunity by Rho GTPases", Trends in Cell Biology **15**, 163 –171 (2005).

[249]L. Tong and V. Tergaonkar, "Rho protein GTPases and their interactions with NFκB: crossroads of inflammation and matrix biology", Bioscience Reports **34**, e00115, 10.1042/BSR20140021 (2014).

[250]M. J. Marinissen, M. Chiariello, and J. S. Gutkind, "Regulation of gene expression by the small GTPase Rho through the ERK6 (p38γ) MAP kinase pathway", Genes and Development **15**, 535–553 (2001).

[251]C. Esnault, A. Stewart, F. Gualdrini, P. East, S. Horswell, N. Matthews, and R. Treisman, "Rho-actin signaling to the MRTF coactivators dominates the immediate transcriptional response to serum in fibroblasts", Genes and Development **28**, 943–958 (2014).

[252]E. Vergadi, E. Ieronymaki, K. Lyroni, K. Vaporidi, and C. Tsatsanis, "Akt Signaling Pathway in Macrophage Activation and M1/M2 Polarization", The Journal of Immunology **198**, 1006–1014 (2017).

[253]L. Dortet, C. Lombardi, F. Cretin, A. Dessen, and A. Filloux, "Pore-forming activity of the Pseudomonas aeruginosa type III secretion system translocon alters the host epigenome", Nature Microbiology **3**, 378–386 (2018).

[254]S. E. Doyle, R. M. O'Connell, G. A. Miranda, S. A. Vaidya, E. K. Chow, P. T. Liu, S. Suzuki, N. Suzuki, R. L. Modlin, W. C. Yeh, T. F. Lane, and G. Cheng, "Toll-like Receptors Induce a Phagocytic Gene Program through p38", Journal of Experimental Medicine **199**, 81–90 (2004).

9 Acknowledgements

I would like to thank everyone who has helped me during the past years to accomplish my PhD thesis.

I would like to thank my supervisor, Prof. Martin Aepfelbacher, for guiding my research work and providing invaluable support.

Furthermore, I would like to thank to my PhD committee members, Prof. Klaus Ruckdeschel and Prof. Adam Grundhoff, for constructive feedback and ideas during my committee meetings.

I would like to acknowledge Dr. Thomas Günther for very important help in teaching ChIP-seq protocol steps. In addition, many thanks go to Dr. Daniela Indenbirken for NGS library preparation.

I thank to Jiabin Huang for help with the data analysis and useful answers to numerous questions.

Many thanks to the organisers of the EPILOG, Prof. Nicole Fischer and Prof. Adam Grundhoff, who provided important training for the participants and organised monthly seminars. I greatly appreciate all the feedback and discussions from all the EPILOG members.

I would like to thank to all the members of AG Aepfelbacher for the help during my thesis, especially to Marie and Laura for help with RNA-seq and epigenetic matters.

Finally, i would like to thank to all my friends and family, who took a fantastic care of me outside my PhD and gave me a lot of support and distractions.

10 Lebenslauf

Lebenslauf wurde aus datenschutzrechtlichen Gründen entfernt.

11 Eidesstattliche Versicherung

Ich versichere ausdrücklich, dass ich die Arbeit selbständig und ohne fremde Hilfe verfasst, andere als die von mir angegebenen Quellen und Hilfsmittel nicht benutzt und die aus den benutzten Werken wörtlich oder inhaltlich entnommenen Stellen einzeln nach Ausgabe (Auflage und Jahr des Erscheinens), Band und Seite des benutzten Werkes kenntlich gemacht habe.

Ferner versichere ich, dass ich die Dissertation bisher nicht einem Fachvertreter an einer anderen Hochschule zur Überprüfung vorgelegt oder mich anderweitig um Zulassung zur Promotion beworben habe.

Ich erkläre mich einverstanden, dass meine Dissertation vom Dekanat der Medizinischen Fakultät mit einer gängigen Software zur Erkennung von Plagiaten überprüft werden kann.

Unterschrift: .....